

**University of Szeged**

**Faculty of Pharmacy**

**Institute of Pharmaceutical Technology and Regulatory Affairs**

Head: *Dr. habil. Ildikó Csóka PhD*

**PhD Thesis**

**DEVELOPMENT AND CHARACTERIZATION OF LORATADINE NANOSYSTEMS FOR  
INTRANASAL DELIVERY USING QUALITY BY DESIGN APPROACH**

By

*Areen Alshweiat*

Pharmacist

Supervisors:

*Dr. habil. Rita Ambrus PhD*

and

*Dr. habil. Ildikó Csóka PhD*

**SZEGED**

**2020**

## PUBLICATIONS RELATED TO THE SUBJECT OF THE THESIS

1. **A. Alshweiat**, G. Katona, I. Csóka, R. Ambrus. *Design and characterization of loratadine nanosuspension prepared by ultrasonic-assisted precipitation*, Eur. J. Pharm. Sci. 122 (2018) 94–104. doi:10.1016/j.ejps.2018.06.010.

**IF: 3.532 (2018), Q1**

2. **A. Alshweiat**, R. Ambrus, I. Csóka. *QbD based control strategy of loratadine nanosuspensions and dry nanoparticles stabilized by soluplus®*, Farmacia. 67 (2019) 729–735. doi:10.31925/farmacia.2019.4.23.

**IF: 1.527 (2018), Q2**

3. **A. Alshweiat**, R. Ambrus, I. Csóka. *Intranasal nanoparticulate systems as alternative route of drug delivery*, Curr. Med. Chem. 26 (2019) 6459–6492. doi:10.2174/0929867326666190827151741.

**IF: 3.894 (2018), Q1**

4. **A. Alshweiat**, I. Csóka, F. Tömösi, T. Janáky, A. Kovács, R. Gáspár, A. Sztojkov-Ivanov, E. Ducza, Á. Márki, P. Szabó-Révész, R. Ambrus. *Nasal delivery of nanosuspension-based mucoadhesive formulation with improved bioavailability of loratadine: preparation, characterization, and in vivo evaluation*. Int. J. Pharm. 579 (2020) 119166. doi:10.1016/j.ijpharm.2020.119166.

**IF: 4.213 (2018), Q1**

## OTHER PUBLICATIONS

1. R. Ambrus, **A. Alshweiat**, I. Csóka, G. Ovari, A. Esmail, N. Radacsi, *3D-printed electrospinning setup for the preparation of loratadine nanofibers with enhanced physicochemical properties*, Int. J. Pharm. 567 (2019) 118455. doi:10.1016/j.ijpharm.2019.118455.

**IF: 4.213 (2019), Q1**

## **ABBREVIATIONS**

<b>AUC</b>	Area under the curve
<b>API</b>	Active pharmaceutical ingredient
<b>BCS</b>	Biopharmaceutical Classification System
<b>Cd</b>	Drug concentration
<b>CQA</b>	Critical quality attribute
<b>CMP</b>	Critical material parameter
<b>CNS</b>	Central nervous system
<b>CPP</b>	Critical process parameter
<b>DE</b>	Dissolution efficiency
<b>DLN</b>	Dried loratadine nanoparticle
<b>DSC</b>	Differential scanning calorimetry
<b>EMA</b>	European Medicines Agency
<b>F68</b>	Pluronic F68
<b>FDA</b>	U.S. Food and Drug Administration
<b>FTIR</b>	Fourier-transform infrared spectroscopy
<b>HA</b>	Sodium hyaluronate
<b>HPMC</b>	Hydroxypropyl methylcellulose
<b>ICH</b>	International Council on Harmonization
<b>IN</b>	Intranasal
<b>J</b>	Flux
<b>Kp</b>	Permeability coefficient
<b>LNS</b>	Loratadine nanosuspension
<b>LOR</b>	Loratadine
<b>M</b>	Mucin
<b>MDT</b>	Mean dissolution time
<b>MPS</b>	Mean particle size
<b>NF</b>	Nasal formulation
<b>PDI</b>	Polydispersity index
<b>PM</b>	Physical mixture
<b>PVP</b>	Polyvinylpyrrolidone
<b>QbD</b>	Quality by design
<b>QTPP</b>	Quality target product profile

<b>RA</b>	Risk assessment
<b>REF</b>	Reference
<b>RD</b>	Relative dissolution
<b>SEM</b>	Scanning electron microscopy
<b>SLS</b>	Sodium lauryl sulfate
<b>TRE</b>	Trehalose
<b>XRPD</b>	X-ray powder diffraction
<b>ZP</b>	Zeta potential

# CONTENTS

1.	INTRODUCTION .....	1
2.	AIMS .....	2
3.	LITERATURE BACKGROUND .....	3
3.1	Strategies to enhance the solubility of the poorly water-soluble drugs.....	3
3.2	Actualities of nanosuspension preparations .....	3
3.2.1	<i>Methods of preparation of nanosuspensions .....</i>	<i>4</i>
3.2.2	<i>Potential benefits of nanosuspensions .....</i>	<i>6</i>
3.2.3	<i>Solvent-antisolvent precipitation-the commonly used bottom-up method 7</i>	
3.3	Intranasal delivery as an alternative route of administration .....	8
3.4	Innovation in nanosized-based intranasal delivery .....	10
3.5	Formulation aspects of intranasal delivery.....	11
3.5.1	<i>Factors related to the properties of the nanoparticles .....</i>	<i>11</i>
3.5.2	<i>Factors related to the properties of the active agent .....</i>	<i>12</i>
3.5.3	<i>Factors related to the properties of the formulation .....</i>	<i>12</i>
3.5.4	<i>Dosage forms of the nasal delivery.....</i>	<i>12</i>
3.5.5	<i>Factors related to the physiology of the nasal cavity .....</i>	<i>12</i>
3.5.6	<i>Additives of nasal formulations .....</i>	<i>13</i>
3.5.7	<i>Nasal drug delivery devices .....</i>	<i>13</i>
3.5.8	<i>Patient expectations of intranasal delivery.....</i>	<i>14</i>
3.6	Quality by Design (QbD) .....	15
4.	MATERIALS .....	17
5.	METHODS .....	18
5.1	Determination of QbD elements for producing LOR nanosuspension .....	18
5.2	Preparation of LOR nanosuspensions .....	18
5.2.1	<i>Preparation of loratadine nanosuspensions (LNSs) .....</i>	<i>18</i>
5.2.2	<i>Preparation of nanosuspensions related physical mixtures .....</i>	<i>19</i>
5.3	Preparation of loratadine nasal formulations (NFs) .....	19
5.4	Micrometric characterization of nanosuspensions and dry nanoparticles.....	19
5.5	Structural analysis of the dry nanoparticles .....	20
5.6	Saturation solubility of the dry nanoparticles .....	20
5.7	Drug content and dissolution behaviours of the dry nanoparticles .....	21
5.8	Characterization of the nanosuspension-based nasal formulations (NFs) ....	22

5.8.1	<i>pH and drug loading of the nasal formulations</i> .....	22
5.8.2	<i>Rheological measurements of NFs</i> .....	22
5.8.3	<i>In vitro studies of the selected NF</i> .....	22
5.8.4	<i>In vivo studies of the selected NF</i> .....	23
5.8.5	<i>Stability assessment of the selected NF</i> .....	25
6	RESULTS .....	26
6.1	QbD and Knowledge space of LNS-based product .....	26
6.2	Selection of process parameters for the development of LNS .....	31
6.3	Effects of material parameters on particle size and stability of LNS .....	31
6.4	Effects of freeze-drying on particle size and stability.....	34
6.5	Characterization of LOR dry nanoparticles .....	34
6.5.1	<i>Morphology of DLNs</i> .....	34
6.5.2	<i>Differential scanning calorimetry of DLNs</i> .....	35
6.5.3	<i>Structural analysis of DLNs</i> .....	36
6.5.4	<i>Fourier transform infrared spectroscopy of DLNs</i> .....	37
6.5.5	<i>Effect of drying process on drug-excipients interactions</i> .....	37
6.5.6	<i>Solubility and in vitro release from DLNs</i> .....	39
6.5.7	<i>In vitro dissolution kinetics</i> .....	40
6.6	Nanosuspension-based nasal formulations .....	41
6.6.1	<i>Characterization of the nanoparticles in the nasal formulations</i> .....	42
6.6.2	<i>Characterization of the nasal formulations</i> .....	43
6.6.3	<i>Rheological properties of NFs</i> .....	43
6.6.4	<i>Mucoadhesion of the nasal formulations</i> .....	44
6.6.5	<i>Effects of nanosizing on the dissolution, diffusion, and permeability</i> ....	45
6.6.6	<i>In vivo studies of the selected NF</i> .....	47
6.6.7	<i>Stability of the selected NF</i> .....	48
7.	CONCLUSIONS .....	49
8.	NOVELTY AND PRACTICAL ASPECTS .....	50
	REFERENCES .....	51

# 1. INTRODUCTION

Dosage forms design is associated with a great challenge to match the pharmacological/therapeutical expectations of the clinical practice with the attributes of the active pharmaceutical ingredients (API) and the biopharmaceutical environment of the targeted administration route. Poor aqueous solubility is one of the major challenges concerning the APIs in this complex development process within the task of pharmaceutical technology. Therefore, special interest can be seen on these Class II and IV drugs of the BCS (Lipinski, 2002, 1997).

Solubility enhancement and using alternative routes of administration are the main leading strategies to make these drugs available for the patients in several cases (Kansara et al., 2015; Peterson et al., 2019). The combination of the mentioned strategies is advised for drugs that have both weaknesses, namely (1) suffer from poor water solubility and (2) are extensively metabolized by the first-pass metabolism (Bartos et al., 2018).

As a potential solution for the first challenge is nanosizing (nanotechnology) as the nanoscale-sized particles of an API exhibit higher solubility and dissolution rate compared to their large counterparts. It can be seen through the evaluating the new delivery pathways, that intranasal delivery has recently received a high interest as an alternative route of administration, as a promising route of administration for local, systemic, brain, and vaccine therapy. Moreover, combining these two strategies, one can lead to an innovative product, namely an intranasal nanosystem based formulation making the API available for both systemic use and brain targeting (Alshweiat et al., 2019a).

Loratadine (LOR) is the most frequently prescribed antihistamine drug for the treatment of various allergic conditions. Moreover, LOR has been introduced as a safe and effective emergency therapy for the management of bone pain in particular cases (Moore and Haroz, 2017). This API exhibits poor and variable bioavailability. Therefore, the delivery of LOR in a new dosage form based on a nanosized system could be advantageous to improve the bioavailability and introduce a new preparation of LOR of high patient acceptance.

From regulatory aspects, nanosystems form a distinctive group regarding their acceptance; relevant guidelines and relevant chapters of the European Medicines Agency (EMA) and U.S. Food and Drug Administration (FDA) must be applied during all manufacturing stages from material selection and formulation to the final production. Furthermore, the FDA has emphasized the application of the Quality by Design (QbD) methodology, which can be remarkably useful for the novel, high-risk dosage forms, and administration routes for careful planning and development even at the early phase of the research (FDA, 2019a). The adaptation of this method for the early development phase has also been published (Csóka et al., 2018).

## 2. AIMS

The main aim of this study was to develop a nanosystem-based intranasal formulation of LOR. Based on the literature background of the nasal delivery, nanosuspension was selected to prepare the pre-dispersion for the nasal formulation. The applicability of a nanosuspension in a nasal formulation is a new approach in pharmaceutical technology, therefore few data for such systems are available up till now. QbD approach was implemented to set the critical process and material parameters that impact the preparation of nanosuspensions. A nasal formulation containing the nanosuspension of the poor water-soluble LOR was developed as liquid formulations based on using a mucoadhesive agent. The nasal delivery of nanosystem-based LOR is a novel strategy that could improve the bioavailability of LOR and introduce a new dosage form with high patient acceptance.

Experimentally, the influential parameters were studied and optimized to develop the LOR nanosuspension as a pre-dispersion. For the final product, the concentrations of the drug and the mucoadhesive agent were investigated to finally evaluate the *in vitro* and *in vivo* characteristics of the prepared nanosuspension-based nasal formulation.

The main steps in the experiments were the following:

- Application of the extended QbD for research and development approach of nanosuspension as pre-dispersions containing LOR as H1 antihistamine agent.
- Selection of the pre-dispersion of LOR to formulate a nasal product.
- Evaluation of the pre-dispersions (nanosuspensions), and the dry nanoparticles by applying the related tests.
- Performing *in vitro* and *in vivo* comparison studies of the nasal formulation.
- Study the stability of the nasal formulation.



## **3. LITERATURE BACKGROUND**

### **3.1 Strategies to enhance the solubility of the poorly water-soluble drugs**

The progress in combinatorial chemistry research and high-throughput screening has led to introducing a vast number of poorly water-soluble drugs in the pharmaceutical pipeline. The non-parenteral administration of the poor water-soluble API is associated with poor and variable bioavailability, whereas the parenteral delivery requires the use of high amounts of solubilizing excipients thus safety margins are compromised (Fahr and Liu, 2007).

Different techniques and formulation strategies have been utilized to improve the solubility and the dissolution rate of poorly water-soluble drugs such as complexation with cyclodextrin derivatives (Davis and Brewster, 2004; Loftsson et al., 2004; McEwen, 2000), solid dispersions (Baghel et al., 2016; Leuner and Dressman, 2000), micellar solubilization (Rangel-Yagui et al., 2005), microemulsions (He et al., 2010; Talegaonkar et al., 2008), and salt formation (Serajuddin, 2007).

In addition to the conventional methods, tackling the solubility problems has become one of the main applications of nanotechnology in drug delivery. The most commonly used nanotechnology-based strategies in the development of delivery systems are divided generally into nanocrystals systems (nanosuspensions) (Agrawal and Patel, 2011), and nanostructured systems. The structured nanosystems of improved solubility and biopharmaceutical efficacy for poorly-water soluble drugs are nanoemulsions (Gorain et al., 2014), dendrimers (Milhem et al., 2000), self-emulsifying drug delivery system (Gursoy and Benita, 2004; Rahman et al., 2013), micelles (Satturwar et al., 2007), liposomes (Fenske et al., 2008; Prabhu et al., 2011), solid lipid nanoparticles (Venishetty et al., 2012), polymeric nanoparticles (Zhang et al., 2010), and carbon nanotubes (Wong et al., 2013). These nanosystems provide controlled and targeted drug delivery.

The selection of the specific approach depends on the drug's physicochemical properties such as intrinsic solubility and melting point, route of administration, as well as therapeutic requirements.

### **3.2 Actualities of nanosuspension preparations**

Nanosuspension is an essential division of the nanotechnology geared mainly for pharmaceutical applications. EMA precisely defines nanomaterial as a natural or manufactured material containing particles, in an unbound state or as an aggregate or an agglomerate, where 50 % or more of the particles in the number size distribution, one or more external dimensions is in a size range 1-100 nm, or material has a specific surface area greater than  $60 \text{ m}^2 \text{ cm}^{-3}$  (EMA, 2006). On the other hand, the FDA has not set regulatory definitions for nanotechnology and nanomaterials but considers the engineering definition as materials that have at least one dimension in a size range of 1-100 nm (FDA, 2014).

Nanosuspensions are carrier-free dispersions of submicron drug particles stabilized by a minimum amount of ionic or steric stabilizer(s). Drugs in nanosuspension can exist in crystalline or amorphous forms (Müller et al., 1999; Müller and Peters, 1998; Sigfridsson et al., 2007).

### **3.2.1 Methods of preparation of nanosuspensions**

The first generation of nanosuspension was nanocrystal and was chiefly produced by top-down and bottom-up techniques. The top-down method requires energy input to disintegrate the drug particles to the submicron level, such as milling. On the other hand, the bottom-up method depends on the assembling of the particles from the molecular state, as in precipitation (Junghanns and Müller, 2008). SmartCrystals<sup>®</sup> represents the second generation of nanocrystals. They have been created by the combination of the bottom-up and top-down methods. Consequently, new techniques have been introduced such as NanoEdge™ or H69 technologies that depend on microprecipitation followed by high-pressure homogenization (HPH) (Kipp et al., 2003; Müller and Möschwitzer, 2005), H42 that connects spray drying and HPH, and H96 technologies used freeze-drying and HPH (Möschwitzer and Andreas, 2006; Salazar et al., 2013). Combination technology has also been developed. It combines wet bead milling and HPH (Rolf, 2006). These new technologies can maximize particle reduction and overcome the limitations of the standard processes (Möschwitzer and Müller, 2006). The other new technology is NanoEdge™. This technology uses precipitation step with subsequent annealing step by applying high shear or thermal energy (Kipp et al., 2003). **Fig.1** illustrates examples of the most commonly used methods for the preparation of nanosuspensions.

Since the nanosuspension drug delivery system was firstly developed in 1994, nanosuspension has attracted attention as a formulation solution for poorly soluble drugs. Consequently, many nanosuspension products have been authorized and marketed. **Table 1** lists examples of marketed pharmaceutical nanosuspensions products for different routes as different dosage forms. However, up-to-date, there is no nanosuspension-based nasal dosage form in the market.

**Table 1:** Examples of marketed pharmaceutical nanosuspension-based products (Junghanns and Müller, 2008; Soares et al., 2018; Zhong et al., 2018).

API	Trade name	Nanosuspension technology	Route of administration	Dosage form	Indication
Aprepitant	Emend®	Media milling	Oral	Capsule	Nausea and vomiting
Fenofibrate	Tricor®	Media milling	Oral	Tablet	Hypercholesterolemia
Fenofibrate	Triglid	HPH	Oral	Tablet	Hypercholesterolemia
Griseofulvin	Gris-PEG®	Coprecipitation	Oral	Tablet	Fungal infections
Megestrol acetate	Megace ES®	Media milling	Oral	Liquid nanosuspension	Appetite stimulant
Nabilone	Cesamet®	Coprecipitation	Oral	Capsule	Nausea and vomiting
Sirolimus	Rapamune®	Media milling	Oral	Tablet	Immunosuppressant
Paliperidone palmitate	Invega Sustenna®	HPH	Parenteral	Liquid nanosuspension	Schizophrenia
Paliperidone palmitate	Invega Trinza®	Media milling	Parenteral	Liquid nanosuspension	Schizophrenia
Aripiprazole Lauroxil	Aristada®	Media milling	Parenteral	Liquid nanosuspension	Schizophrenia
Naproxen sodium	Naprelan®	Media milling	Oral	Tablet	Inflammation
Morphine sulfate	Avinza®	Media milling	Oral	Capsule	Chronic pain
Methylphenidate hydrochloride	Ritalin LA®	Media milling	Oral	Capsule	Nausea and vomiting
Aripiprazole	Abilify Maintena®	Media milling	Parenteral	Liquid nanosuspension	Schizophrenia
Dantrolene sodium	Ryanodex®	Media milling	Parenteral	Liquid nanosuspension	Malignant hyperthermia

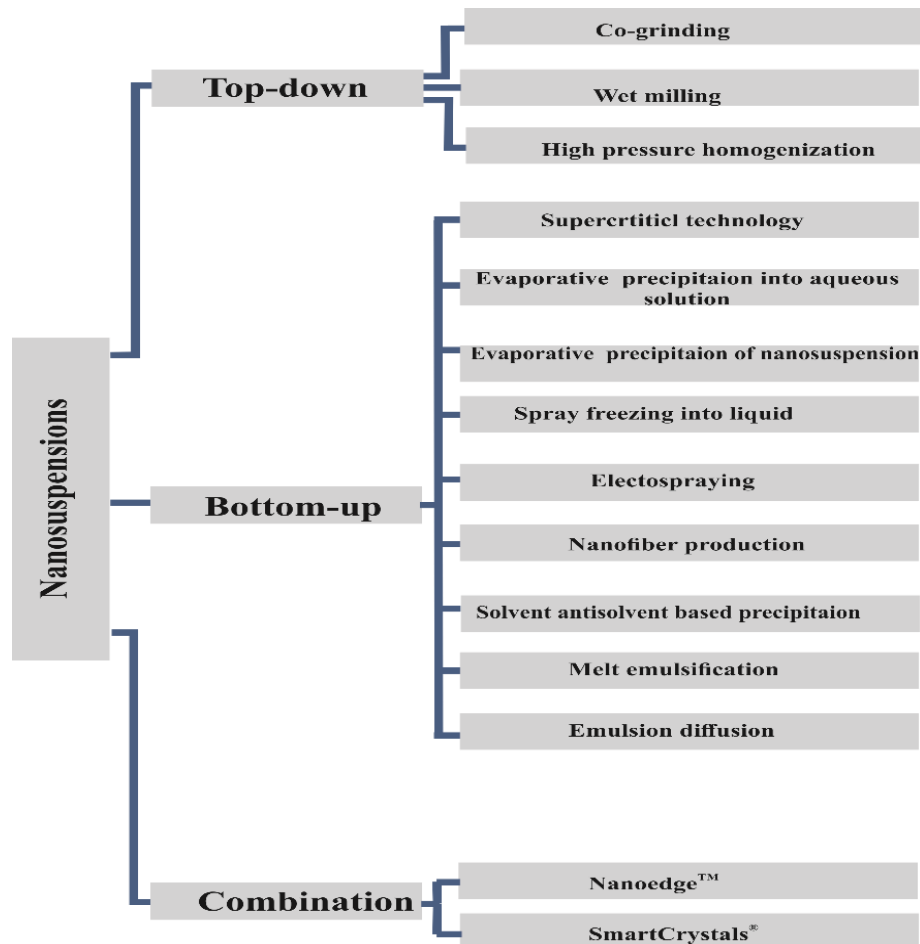


**Figure 1:** The most common methods for the preparation of nanosuspensions.

### 3.2.2 *Potential benefits of nanosuspensions*

The nanosuspensions offer many benefits that are milestones for this method. The followings represent the main advantages of the application of nanosuspensions:

a. Enhancement of dissolution rate and saturation solubility

Size reduction of the particles is accompanied by a dramatic increase of the solute surface area, thus dissolution rate according to the Noyes-Whitney model. Ostwald–Freundlich equation relates the saturation solubility to the dissolution pressure and radii of the particles. Accordingly, an increase of dissolution rate and saturation solubility are postulated by particle size reduction into the nanoscale (Noyes and Whitney, 1897; Wu and Nancollas, 1998).

b. Development of various dosage forms

Nanosuspensions can be further processed through granulating, layering, and developing of dry powder. Consequently, nanosuspension permits the production of different dosage forms with enhanced physicochemical properties. Tablets (Nekkanti et al., 2009), intravenous (Ben Zirar et al., 2008; Ganta et al., 2009; Gao et al., 2010; Muller and Keck, 2004; Liu et al., 2010), pulmonary (Kraft et al., 2004; Shrewsbury et al., 2009; Yang et al., 2008), and nasal (Bhavna et al., 2014; Saindane et al., 2013) nanosuspension-based dosage forms have extensively been reported in the literature.

c. Enhancement of mucoadhesive properties

Nanosized particles possess a higher adhesion to the mucosal tissue than their large counterparts (Ponchel et al., 1997).

d. Enhancement of stability

Nanosuspension can protect the drug particles from the external environment and minimize the hydrolysis. On the other hand, the preservation of the crystalline structure promotes drug stability (Möschwitzer et al., 2004; Pu et al., 2009).

e. Cost-effectiveness

Nanosuspensions require a low amount of additives as a stabilizer, hence high drug loading can be achieved. The production processes are generally simple, adaptable, and scalable, thus facilitates large-scale production for the market (Gao et al., 2013).

On the other hand, particle size reduction is associated with agglomeration due to the high Gibbs free energy, whereas Ostwald ripening involves the dissolving of small particles followed by the deposition of the larger particles. Therefore, using surfactants or polymers is crucial to stabilize the nanocrystals (George and Ghosh, 2013; Kumar and Burgess, 2014; Lindfors et al., 2007; Tuomela et al., 2016).

### 3.2.3 Solvent-antisolvent precipitation - the commonly used bottom-up method

Antisolvent precipitation is an effective bottom-up method for nanosuspension preparation. This method depends on changing the solubility of the drug in a water-miscible organic solvent by the addition of antisolvent that contains the stabilizers. Thus, drug particles covered by the stabilizer(s) as a consequence of the change of supersaturation are generated. This method is simple, cost-effective, and easy for scaling-up (Patravale et al., 2004; Rogers et al., 2004; Viçosa et al., 2012).

Several factors affect the prepared nanosuspensions, such as solvent type, solvent: antisolvent ratio, stabilizer type, stabilizer concentration, drug amount, and drug: stabilizer(s) ratio (Hecq et al., 2005). Mostly, precipitation is assisted by ultrasonication for further particle size reduction and nucleation control (Anil et al., 2016; Bartos et al., 2015b). Moreover, drying procedures such as spray drying and freeze-drying are usually applied to produce stable dry nanoparticle and nanocrystals (Beirowski et al., 2011; Chaubal and Popescu, 2008; Van Eerdenbrugh et al., 2008; Wu et al., 2011).

In a multivariate production process, all the parameters of the different operations should be cautiously selected, and their effects on the final product must be assessed. In the case of preparing nanosuspension by precipitation ultrasonication, all the parameters related to these processes, in addition to the drying procedure, must be evaluated (**Table 2**) (Alshweiat et al., 2018).

**Table 2:** The effects of different material and process parameters on the quality of attributes for the precipitation ultrasonication method (Alshweiat et al., 2019b).

Parameter	Justification
Drug amount in the solvent phase	An increase in drug concentration decreases the particle size due to increased saturation. This effect lasts until an optimum concentration above which particle size increases as drug concentration increases.
Stabilizer type	The proper type depends mainly on the affinity between the drug particles and the specific part of the stabilizer.
Stabilizer concentration	A sufficient amount is required to cover the nascent surface to prevent aggregation and agglomeration. However, a high concentration may form a viscous solution that can reduce solvent diffusion and affect ultrasonic wave transmission.
Solvent: antisolvent ratio	Particle size decreases by decreasing the solvent: antisolvent ratio due to increasing the degree of supersaturation. This reduction in particle size attains a constant value above a critical ratio.
Antisolvent temperature	A decrease in temperature generally reduces particle size and narrows particle size distribution.
Sonication power	Particle size usually increases with the increase of ultrasonic power input due to the increased erosion effect on the surface of large crystals and crystal agglomerates. However, if the energy exceeds a critical value, it increases the kinetic energy of particles and increases agglomeration.
Sonication time	The optimal time length can support particle size reduction. The time effect is linked to the sonication power.
Drying method	Drying conditions have a critical impact on nanoparticle re-dispersibility. Optimal excipient type and quantities are required to ensure maximum stabilization. The drying rate also has significant effects on particle size.

### 3.3 Intranasal delivery as an alternative route of administration

Poor aqueous solubility and dissolution rate and first-pass metabolism are the main limitations for oral administration. These factors inevitably produce poor and variable drug bioavailability. The parenteral administration (IV, IM, SC, and IP) offers high bioavailability. However, it is not a preferred route of administration due to factors related to safety and the patient's acceptance. Moreover, drug characteristics such as solubility and toxicity, have a crucial role in the preparation of parenteral dosage forms. Accordingly, other alternative routes of administration have been introduced, such as transdermal (Tanner and Marks, 2008), buccal (Patel et al., 2012), pulmonary (Patton, 2004), and intranasal delivery (Alshweiat et al., 2019a).

Intranasal delivery (IN) has been introduced for systemic and brain drug delivery in addition to vaccination (Djupesland, 2013; Kushwaha et al., 2011; Li et al., 2013; Meredith et al., 2015; Vyas et al., 2005; Zaman et al., 2013). The advantages of IN delivery are related to the high surface area, high vascularization and permeation, and avoidance of the first-pass metabolism. For brain delivery, the IN route provides a direct nose to the brain pathway and circumvent the blood-brain barrier. Moreover, the IN route displays an efficient way for vaccine delivery (**Fig.2**).

These factors introduced the nasal cavity as a suitable route for drugs that suffer from extensive first-pass metabolism, poor solubility, and are degraded in the gastrointestinal tract. Therefore, the IN delivery is attractive for vaccines and peptides that are administered parentally so far. IN is a non-invasive, nonsterile, and easily applied method. These aspects will increase patient acceptance and compliance (Costantino et al., 2007; Menzel et al., 2017).

Several limitations can adversely affect the application and absorption of IN administered dosage form such as mucociliary clearance, limited volume of nasal administration (max. 200  $\mu$ L), and presence of enzymes and efflux transporters. Moreover, the narrow nasal valve represents a potential hurdle for convenient drug delivery. On the other hand, pathological changes and environmental are also considered factors that affect the intranasal blood supply, hence the systemic absorption (Gizurarson, 2015).

Intranasal products with systemic effects are commercially available for certain drugs like zolmitriptan, sumatriptan, and fentanyl as well as peptides such as calcitonin, desmopressin, and nafarelin (Abboud et al., 1994; Dodick et al., 2005; El-Nemr et al., 2002; Gawel et al., 2005; Munjal et al., 2016; Nave et al., 2013; Nozaki et al., 2016; Winner et al., 2006). Other drugs have been nasally introduced for the treatment of urgent conditions such as migraine, seizures, opioid overdose, and pain breakthroughs in cancer. (Afridi et al., 2013; Corrigan et al., 2015; Graudins et al., 2015; Kapoor et al., 2014; Pavis et al., 2002; Steenblik et al., 2012).

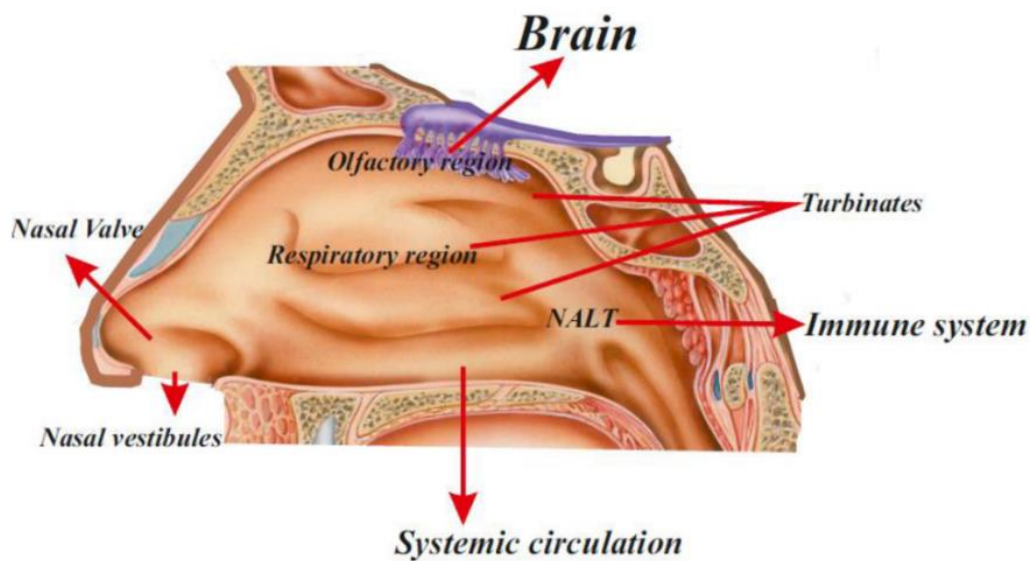


**Figure 2:** The delivery purposes of the intranasal route of administration (Alshweiat et al., 2019a).

In certain pathological conditions, nasal drug delivery is preferred over oral delivery, such as in the case of antihistamine for the treatment of allergic rhinitis. Allergic rhinitis is an inflammatory disease induced by allergen exposure and IgE-mediated inflammation that affects the upper respiratory tract and produces traditional symptoms of sneezing, itching, rhinorrhea, nasal congestion, and ocular symptoms of allergic conjunctivitis (Randall and Hawkins, 2018). It represents a global health problem affecting 10% to more than 40% of the population worldwide and highly recognized to have significant impacts on the quality of life, emotional well-being, sleep, social activity, and productivity. Therefore, allergic rhinitis is associated with a considerable economic burden (Blaiss et al., 2018; Rosenwasser, 2002).

Intranasal antihistamine effects have been noted on many mediators, including histamines, leukotrienes, cytokines, chemokines, mast cells, eosinophils, and neutrophils at clinically relevant concentrations. However, much higher concentrations (than routine dosing) of oral antihistamines are required to obtain any anti-inflammatory effects (Horak and Zieglmayer, 2009; Kaliner et al., 2011). The recommendations for using nasal antihistamines are based on the following; antihistamines are considered the first-line therapy for allergic and non-allergic rhinitis, they offer rapid onset of action, they are equal or superior to the oral antihistamines for the treatment of the seasonal rhinitis, they offer significant effects on nasal congestions, and they can achieve higher concentration to the target tissue (Berger et al., 2003; LaForce et al., 2004). Several studies have reported the efficacy of nasal antihistamines, compared to intranasal corticosteroids. Despite the superior effects of nasal

corticosteroids over the nasal antihistamines, both categories show an equal effect in reducing all symptoms of allergic rhinitis. Moreover, in short term studies, intranasal antihistamines showed a faster onset of action than intranasal corticosteroids (Kaliner et al., 2009; Meltzer et al., 1994).

### 3.4 Innovation in nanosized-based intranasal delivery

Innovations in nasal delivery have been raised by the applying nanotechnology to this route. Nanotechnology could address the limitations that are related to the physicochemical properties of the active agents as well as restrictions of the nasal delivery (**Table 3**) (Alshweiat et al., 2019a).

**Table 3:** Nanotechnology solutions for intranasal delivery limitations (Alshweiat et al., 2019a).

Limitation	Nanotechnology effects
Poor drug solubility	High ratio of surface area to volume. Providing interactions between the groups of the polymer and drug molecule by electrostatic and hydrogen bonding. Production of a microenvironment with specific low polarity inside the nanoparticles than in the aqueous bulk phase. (Chen et al., 2011; Devarakonda et al., 2004; Milhem et al., 2000; Pistoris et al., 1999; Shrestha et al., 2014).
Mucociliary clearance and short residence time	Localization of the formulation for a longer time. Enhancement of contact time inside the nasal cavity. (Cui et al., 2006; Issa et al., 2005; Pawar et al., 2010).
Poor penetration for large and hydrophilic molecules	Ability to open up tight junctions. Possibility of high endocytosis. Ability to change mucosal membrane properties. (Bernocchi et al., 2016; Gao et al., 2006)
Enzymatic activity	Encapsulation of liable molecules. (Kato et al., 1992).
P-glycoprotein efflux transporter	Efficiency for bypassing and inhibition of P-glycoprotein. Chavanpatil et al., 2007; Shah et al., 2013).

Recently, nanosuspensions have been introduced as competent solubility enhancement techniques, and newly have been emerged as a delivery system. Nanosuspension-based formulation with the nasal route has been proved for many purposes. The chief key is the selection of the proper dosage form that supports the localization of drugs at the nasal cavity for adequate time for drug absorption without being inhaled into the lungs. Therefore, nanoparticles must be incorporated into mucoadhesive formulations that maintain the nanosizing effects and prevent the inhalation of the particles (Alshweiat et al., 2019a).

The knowledge of applying nanosuspension into nasal delivery has been reported in many studies. Saindane et al. (Saindane et al., 2013) incorporated a carvedilol-containing nanosuspension into *in situ* gel, Hao et al. (Hao et al., 2016) prepared resveratrol-based nanosuspension, and Gieszinger et al. (Gieszinger et al., 2017) formulated nanosized-based lamotrigine for brain delivery. Moreover,



meloxicam nanosuspensions have been produced for systemic delivery as a powder (Kürti et al., 2013) and sodium hyaluronate-based sprays (Bartos et al., 2015a).

LOR is a class II agent according to the BCS, characterized by poor water solubility ( $3.03 \mu\text{g mL}^{-1}$ ) and high permeability ( $\log P= 5$ ). It is a weak base with a reported pKa value of 5.25 at 25 °C, responsible for its pH-dependent solubility and consequent variability in bioavailability (Ambrus et al., 2019; Dagenais et al., 2009; Han et al., 2004). Up-to-date, the nasal dosage form is not available on the market. Therefore, it could be advantageous to develop a nasal formulation based on nanosuspension of LOR to produce this agent in a new and novel dosage form.

### **3.5 Formulation aspects of intranasal delivery**

Various aspects must be considered for the development and production of nasal formulations. For nanosystem-based formulations, the properties of the nanoparticles play a crucial role in nasal delivery from regulatory and industrial points of view. Moreover, customer voice must be included to develop nasal systems with high patient acceptance.

#### ***3.5.1 Factors related to the properties of the nanoparticles***

The nanosized particles maintain distinctive physicochemical properties compared to their conventional counterparts. These properties are responsible for the nanoparticles' promising characteristics. The physicochemical characteristics of nanoparticles with significant effects on the nasal administration are size, shape, chemical composition, physicochemical stability, crystal structure/polymorphism, surface area, surface charge, and surface energy.

Particle size is a critical evaluation parameter to assess the desired properties of nanoparticles due to its consequences on surface area and viscosity, and thus drug dissolution, release, absorption, and stability (Anantachaisilp et al., 2010). Due to their small size, nanoparticles are usually used as a drug carrier via passive transport, active transport, and endocytosis (Lockman et al., 2004; Shin et al., 2015). However, the mechanism by which nanoparticles enhance drug transport is not fully described.

The surface charge also plays an essential role in the interactions of nanoparticles with biological systems. For example, positively charged nanoparticles have been designed to improve nasal adhesion with the nasal mucosa via the electrostatic interaction with the sialic groups of mucin (Alpar et al., 2005).

The shape of nanoparticles affects their stability, absorption, and cellular uptake. However, these effects are connected to the particle size and surface charge (Gratton et al., 2008).

### ***3.5.2 Factors related to the properties of the active agent***

Physicochemical characteristics of the used drug profoundly affect its absorption and bioavailability following the nasal administration.

- a. Solubility and Dissolution Rate
- b. Lipophilicity
- c. Partition Coefficient and pKa
- d. Chemical form
- e. Polymorphism
- f. Molecular Weight

### ***3.5.3 Factors related to the properties of the formulation***

The properties of the nasal formulation have significant effects on the drug's permeation and bioavailability, as well as satisfying application.

- a. Chemical reaction (pH)
- b. Osmolarity
- c. Viscosity

### ***3.5.4 Dosage forms of the nasal delivery***

The selection of dosage form depends upon the drug being used, proposed indication, patient population, and marketing preferences.

- a. Liquid dosage form

The most simple and convenient systems developed for nasal delivery are solutions and suspensions.

- b. Gel dosage form

Gels increase the contact time between the drug and the nasal mucosa due to their high viscosity. They also reduce the post-nasal drip and leakage of the formulation and reduce the irritation inside the nasal cavity.

- c. Powder dosage form

Powders generally exhibit high stability. However, irritation is the major drawback of using powders in the nasal cavity.

### ***3.5.5 Factors related to the physiology of the nasal cavity***

- a. Mucociliary clearance
- b. Enzymatic activity
- c. Nasal blood flow
- d. Pathological conditions

### **3.5.6 Additives of nasal formulations**

Various additives are required to promote the efficiency, safety, and acceptance of the nasal formulation.

#### **a. Permeation enhancers**

Permeation-enhancers are mainly studied to develop formulations for hydrophilic drugs of poor nasal membrane permeability. These agents enable the paracellular transport of hydrophilic and large molecules across the mucosal surface by opening tight junctions. The most used enhancing excipients are cyclodextrins and chitosan derivatives. These agents are biocompatible and induce the enhancing effects without causing damage to nasal mucosa (Illum, 2012; Rassa et al., 2018).

#### **b. Solubility enhancers**

Solubility enhancers are functional excipients used to enhance the solubility of the poorly water-soluble drugs hence absorption and bioavailability such as cyclodextrins, dendrimers (Ghadiri et al., 2019), and surfactants (Balakrishnan et al., 2004).

#### **c. Mucoadhesive agents**

Increase the contact time between the active agent and the nasal mucosa, thereby contributing to drug absorption. Many mucoadhesive agents have been used in nasal preparations such as carbomers, chitosan, alginate, Poloxamers, and sodium hyaluronate (Chaturvedi et al., 2011).

#### **d. Viscosity enhancing agents**

Viscosity enhancement is essential to localize the drug inside the nasal cavity. Moreover, entrapment of the drug in a viscous gel matrix can protect the drug from enzymatic degradation (Buwalda et al., 2017; Warnken et al., 2016).

#### **e. Others**

Other excipients are required to improve the efficiency and safety of the nasal formulations such as buffers, osmolarity control agents, preservatives.

The excipients must be compatible with the constituents of the formulations, used in small quantities, and of low toxicity.

### **3.5.7 Nasal drug delivery devices**

The selection of the suitable delivery system depends on the dosage form, physicochemical properties of the drug, properties of the nasal formulation, the intended use, dosing accuracy, and marketing issues (Ali et al., 2010).

For liquid dosage forms, the following devices are the most commonly used for nasal delivery.

- Drops
- Unit-dose containers

- Instillation and rhinyle catheter
- Squeezed bottle
- Airless and preservative-free sprays
- Compressed air nebulizers
- Metered-dose inhalers (MDIs)

For powders, the following devices are commonly used.

- Insufflators
- Mono-dose powder inhaler
- Multi-dose dry powder systems
- Metered-dose aerosols

The site of deposition and the deposition area depend on several parameters that are related to the delivery device such as mode of administration, geometry, and particle size of the formulation and velocity of the delivered particles. The traditional devices and pressurized metered-dose aerosols provide the dose of medication primarily to the anterior segment of the nasal passage. However, targeted delivery is highly required to deliver the active agent into the respiratory, trigeminal, and olfactory regions for systemic and brain targeting (Xi et al., 2016).

New technologies have been introduced to overcome the inconveniences of the traditional nasal devices, improve systemic drug absorption, or to enable drug delivery to the brain through the olfactory area. Therefore, these emerging technologies, such as the bidirectional technology Optinose<sup>®</sup> (Djupestrand, 2013), Controlled Particle Dispersion (CPD)<sup>®</sup> (Kurve) (Giroux et al., 2005), and Pressurized Olfactory Device (POD) (Hoekman and Ho, 2011) can widen and specify the intranasal delivery for efficient outcomes.

Design parameters, such as the nosepiece shape, the flow rate, the particle size profile, and release angle can be adapted to optimize delivery to target sites beyond the nasal valve, avoid lung deposition, and to assure that particles are deeply deposited without exiting the contralateral nostril (Djupestrand, 2013).

### **3.5.8 Patient expectations of intranasal delivery**

Patients -as users of the medicinal products- have an increasing role in therapeutic success. Identifying what is expected or is critical for patients and reflecting on these aspects during research and development is the first step to achieve patient acceptance and the required therapeutic outcome. This field has been ignored for many years, but as the effects of customers' preferences increase, it should be considered more as part of R&D thinking (Hellings et al., 2012; Yanez et al., 2016).

Patient requirements have extended the need for safe and efficient drug delivery to other concerns such as the comfort of both formulation and applicator device in the nasal cavity, the ease of application, confidence in the delivered amount, and a warning about the remaining dose (dose counting). All these factors can enhance patients' satisfaction and, therefore, their adherence. To improve efficiency and productivity, manufacturers must understand the best tools, methods, and analysis. They have to define their goals based on the patients' opinions before proceeding into the production stage. Integrating the voice of the customer can help to assess the patients' convenience for their product and induce manufacturers to develop patient-friendly products. These considerations have not been kept in the theoretical framework of companies, but have transferred to the regulatory agencies that seriously consider patients' preferences and their assessments of using formulations and delivery devices (Alshweiat et al., 2019a).

### **3.6 Quality by Design (QbD)**

QbD is a holistic, scientific, and risk-based approach of development, focusing on the understanding of the product and manufacturing process, starting with predefined objectives and controlling the used material and process to ensure the quality of pharmaceutical products (Yu, 2008). According to QbD, objectives, materials, methods, delivery systems, and expected outcomes should be identified clearly to end up with a product that can compromise between patients' demands and industrial expectation alongside with the regulatory guidelines of the EMA or FDA (EMA, 2001; FDA, 1998; 2002). In 2005, the FDA enforced the submission of QbD with new drug application requests. This proactive design offers the rewards of transferring the chemistry manufacturing control of the new abbreviated drug into the pharmaceutical quality assessment, thus saving the time of development and submission, saving the time of regulatory authorities' approval, and defining the probability of out of specification and out of tolerance (Sangshetti et al., 2014). Three relevant documents were published as the International Council on Harmonization (ICH) guidelines describing the pharmaceutical development-Q8, risk management-Q9, and quality system-Q10. The adoption of these guidelines provides immense potential for careful planning during formulation and development, even at the early stage of the research. Implementation of the QbD begins with determining the quality target product profile (QTTP) that describes information related to anticipated indications, route of administration, dosage form, and safety. This entails the identification of the critical attributes of the drug product that must be achieved to ensure the desired quality, considering the safety and efficacy of the drug product. The next step involves the identification of the relevant critical quality attributes (CQAs) that influence the QTTP in addition to the critical process parameters (CPPs) and critical material parameters (CMPs)

of high impacts on the CQAs. The selection of the CQAs, CPPs should be based on previous scientific experience and knowledge from relevant literature sources.

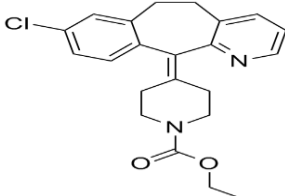
Risk assessment (RA) is a principal part of QbD-based development. It assists in organizing the information to take the risk decision, thus saving time, cost, and efforts. The stage where RA must be applied throughout the research process is varied. Besides, it can be redefined and repeated (EMA, 2015). Pallagi *et al.* (Pallagi et al., 2015) point out the importance of the risk assessment in the development of intranasal meloxicam nanosuspension at the early production stage.

## 4. MATERIALS

### a. Active agent

Loratadine (LOR) was purchased from Teva (Budapest, Hungary). LOR shows a poor water solubility of  $3.03 \mu\text{g mL}^{-1}$  and high permeability ( $\log P$  5.5). It is a weak basic agent with  $pK_a$  5.25 at  $25^\circ\text{C}$  (**Table 4**). Therefore, LOR shows poor and variable bioavailability.

**Table 4:** The properties of the active agent

Chemical structure	
Molecular weight	382.888 $\text{g mol}^{-1}$ .
Melting point	134-136 $^\circ\text{C}$ .
Physical Description	Solid-white crystal.
Application	H1 antihistamine, used for the treatment of different allergic conditions.

### b. Excipients

Different types of stabilizers have been used to prepare the nanosuspensions. On the other hand, a mucoadhesive agent was used to formulate the nanosuspension into nasal formulations (**Table 5**).

**Table 5:** Properties and purchase data for the excipients used to prepare the loratadine nasal formulation.

Excipient	Characterization	Role	Purchase data
Polyvinylpyrrolidone K-25 (PVP K25)	Linear hydrophilic polymer.	Steric stabilizer	ISP Customer Service GmbH (Cologne, Germany)
Soluplus <sup>®</sup>	Polyvinyl caprolactam–polyvinyl acetate–polyethylene glycol. It acts as a stabilizer and a solubilizing agent in the formulations of poorly water-soluble drugs.	Steric stabilizer	BASF (Ludwigshafen, Germany)
Poloxamer 188 (F68)	Nonionic triblock copolymer composed of a central hydrophobic chain of polyoxypropylene (poly(propylene oxide)) flanked by two hydrophilic chains of polyoxyethylene (poly(ethylene oxide)).	Steric stabilizer	BASF (Ludwigshafen, Germany)
Tween 80	Polyoxyethylene sorbitan monooleate is a non-ionic surfactant.	Steric stabilizer	Fluka Chemika (Buchs, Switzerland)
Sodium lauryl sulphate (SLS)	Anionic surfactant.	Anionic stabilizer	FreeHand Ltd. (Pecs, Hungary)
Hydroxypropylmethylcellulos (HPMC)	Semisynthetic cellulose derivative.	Steric stabilizer	Colorcon (Budapest, Hungary)
Sodium hyaluronate	Linear polysaccharide polymer. It is biocompatible, biodegradable, and non-immunological material.	Mucoadhesive agent	Gedeon Richter Plc. (Budapest, Hungary)
Trehalose dihydrate (TRE)	Sugar, consisting of two units of glucose, used to stabilize molecules during both freezing and drying.	Cryoprotectant	Sigma-Aldrich (New York, USA)

## 5. METHODS

### 5.1 Determination of QbD elements for producing LOR nanosuspension

QTPP, CQAs, CMPs, CPPs were determined for producing loratadine nanosuspension (LNS), based on prior knowledge, previous studies, preliminary experiments, and data from relevant literature. Particle size, polydispersity, and zeta potential were selected as CQAs for the nanosuspension. For the freeze-dried nanoparticles (DLNS), particle size, polydispersity index, solubility, and dissolution properties were determined as CQAs. The RA was performed with Lean QbD Software<sup>®</sup> (2014QbD Works LLC., Fremont, USA). According to this software, the connections between CQAs and CPPs were evaluated and rated on a three-level scale. This scale reflects the impact of their interaction on the product as high (H), medium (M), or low (L). The dynamism of this interdependence rating is presented in tables generated by the software. This was followed by the probability rating step, in which CPPs were estimated and categorized on a 10-point scale. Further, Pareto charts were generated by the software, presenting the numeric data and the ranking of CQAs and CPPs (Pallagi et al. 2015).

### 5.2 Preparation of LOR nanosuspensions

#### 5.2.1 Preparation of loratadine nanosuspensions (LNSs)

LNSs were prepared using the precipitation-ultrasonication method. LOR was dissolved in ethanol according to its solubility, while the stabilizer(s) was (were) dissolved in water. For the mixtures of stabilizers, one was added to the solvent phase, while the other one was added to the antisolvent phase (**Fig.3**). Both solutions were filtered through a 0.45 µm filter (FilterBio PES Syringe Filter, Labex Ltd., Budapest, Hungary). The fresh-made LOR solution was rapidly introduced into the cool antisolvent under sonication using a UP 200 s Ultrasonic processor (HielscherUltrasonics GmbH, Germany) and different conditions in terms of energy power, sonication time and sonication temperature. The temperature of sonication was controlled (Julabo F32, JULABO GmbH, Germany). The prepared nanosuspensions were stirred at room temperature for 24 h to remove the organic solvent.

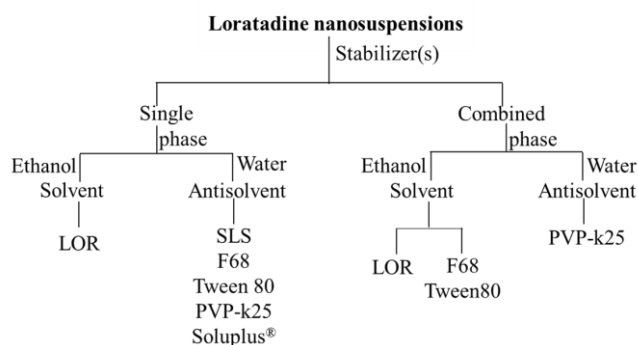


**Figure 3:** Schematic illustration of the contents of the solvent and antisolvent phases of LNSs.



### 5.2.2 Preparation of nanosuspensions related physical mixtures

Physical mixtures (PMs) corresponding to the composition of the nanosuspensions were prepared as reference samples by blending LOR with the suitable excipients in a Turbula mixer (Turbula System Schatz; Willy A. Bachofen AG Maschinenfabrik, Basel, Switzerland) using 60 rpm for 10 min.

### 5.3 Preparation of loratadine nasal formulations (NFs)

The intranasal formulations (NFs) were prepared from the nanosuspensions (pre-dispersions). These pre-dispersions were prepared by using 1 mL of the solvent phase contained 200 mg of LOR in ethanol and 40 mL of 0.2% w/v F68 as the antisolvent under the specified process conditions of 30 min sonication time, 4 °C sonication temperature, and 50% sonication amplitude. The pre-dispersions were stirred for 24 h to remove ethanol. Afterward, HA was added to prepare the nasal formulation. The final concentrations of the formulations were controlled by dilution with 0.2%, w/v F68. NFs were stored in a refrigerator at 4 °C for 24 h to ensure the complete solvation of the polymer. For comparison, reference samples (REF) were prepared. **Table 6** shows the final concentrations of LOR and HA in the prepared nasal formulations and corresponding reference samples that contained the same amount of LOR and HA in 0.2%, w/v F68. However, the LOR in the reference samples was added without any processing. The REF samples were prepared by mixing raw LOR powder with HA and 0.2% F68 solution, using ULTRA-TURRAX® homogenizer at 5000 rpm for 10 min (GmbH, Germany).

**Table 6:** Concentrations of LOR and HA ( $\text{mg mL}^{-1}$ ) in the HA-based nasal formulation and reference samples (Alshweait et al., 2020).

Sample	LOR ( $\text{mg mL}^{-1}$ )	HA ( $\text{mg mL}^{-1}$ )
NF1	1	1
NF2	1	5
NF3	2.5	1
NF4	2.5	5
REF1	1	1
REF2	1	5
REF3	2.5	1
REF4	2.5	5

### 5.4 Micrometric characterization of nanosuspensions and dry nanoparticles

Selected LNSs were dried to obtain solid products to study the physicochemical and investigate the biocompatibility. The LNSs were dried by vacuum oven at 25 °C for 24 h and freeze-drying in a Scanvac, CoolSafe 100-9 Pro type apparatus (LaboGeneApS, Lyngø, Denmark). In freeze-drying, the nanosuspensions were lyophilized with 5% w/v trehalose (TRE) to -40°C.

Scanning electron microscopy (SEM) (Hitachi S4700, Hitachi Scientific Ltd., Tokyo, Japan) was used to characterize the morphology of the LOR, PMs, and dry nanoparticles. The samples were coated with gold-palladium using a sputter coater (Bio-Rad SC 502, VG Microtech, Uckfield, UK) under an electric potential of 10.0 kV at 10 mA for 10 min. The air pressure was set to 1.3–13.0 mPa.

The mean particle size (MPS), zeta potential (ZP), and polydispersity index (PDI) of LNSs were measured by laser diffraction using a Malvern Nano ZS zetasizer (Malvern Instrument, UK), using water as the dispersant and setting the refractive index to 1.62. 12 parallel measurements were carried out.

### 5.5 Structural analysis of the dry nanoparticles

The structures of LOR, raw material, and dry nanoparticles were characterized using a BRUKER D8 Advance X-ray powder diffractometer (Bruker AXS GmbH, Karlsruhe, Germany) with Cu K  $\lambda_1$  radiation ( $\lambda = 1.5406 \text{ \AA}$ ) and a VÅNTEC-1 detector. Powder samples were scanned at 40 kV and 40 mA, with an angular range of  $3^\circ$  to  $40^\circ 2\theta$ , at a step time of 0.1s and a step size of  $0.01^\circ$ . Eva software was used to separate the crystal and related amorphous peaks. Thus, the software calculated the values of the integrated intensities of the amorphous and crystalline contribution and the crystalline-only contribution. The crystallinity index values ( $X_c$ ) of the samples were calculated based on the following equation:

$$X_c = \frac{A_{crystalline}}{A_{crystalline} + A_{amorphous}} * 100 \quad (1)$$

Thermal analysis of the samples was carried out using a differential scanning calorimeter (Mettler Toledo DSC 821 $^\circ$ , Mettler Inc., Schwerzenbach, Switzerland). About 3–5 mg of powder was accurately weighed into DSC sample pans, which were hermetically sealed and lid pierced. An empty pan was used as a reference in an inert atmosphere under constant argon purge. The samples were analyzed in the temperature range of 25–300  $^\circ\text{C}$  at a heating rate of 5 $^\circ\text{C min}^{-1}$ .

FT-IR spectra of raw materials and the prepared samples were obtained by Fourier-transform infrared spectroscopy (Thermo Nicolet AVATAR 330, USA) equipped with the GRAMS/AI ver. 7 program. Samples were grounded and compressed into pastilles with 150 mg dry KBr. The pastilles were scanned 128 times at a resolution of 4  $\text{cm}^{-1}$  in the wavenumber region 4000–400  $\text{cm}^{-1}$ .

### 5.6 Saturation solubility of the dry nanoparticles

Saturation solubility of the samples was investigated by adding excess amounts of the sample into 5 mL of water, PBS (pH 7.4), or PBS (pH 5.6) at 25 $^\circ\text{C}$ . Next, the suspensions were filtered, and the drug concentrations in the filtrate were measured by UV spectroscopy at  $\lambda_{\text{max}}$  248 nm.

## 5.7 Drug content and dissolution behaviours of the dry nanoparticles

The LOR content of the sample was determined by dissolving 10 mg of the dry nanoparticles in 50 mL of 0.1N HCl. After stirring the solution with a magnetic stirrer (400 rpm) at room temperature for 24 h, it was filtered and analyzed. The concentration was measured spectrophotometrically at 248 nm. The modified paddle method (USP dissolution apparatus, type II Pharma Test, Hainburg, Germany) was used to characterize the dissolution rates of LOR, PMs, and DLNs. 1.11 mg of pure LOR or DLN equivalent to 1.11 mg of LOR in 100 mL PBS, pH 7.4 was used. The paddles were rotated at 100 rpm at 37°C. 5 mL aliquots were taken at 5, 10, 15, 30, 60, 90, and 120 min and were filtered. Concentrations of LOR were measured spectrophotometrically (Unicam UV/VIS Spectrophotometer, Cambridge, UK) at  $\lambda_{\max}$  248 nm. The calibration curve was taken in the concentration range of 2–20  $\mu\text{g mL}^{-1}$ . The calibration curve was linear throughout the whole range tested and was described by the equation  $A = 0.0388 \text{ conc.}$  ( $R^2 = 0.9997$ ) (Alshweiat et al., 2018).

Dissolution efficiency (DE) of the samples was determined by calculating the percentage of the ratio of the area up to time  $t$  divided by the area that described 100% dissolution at the same time (Khan, 1975).

$$\%DE = \frac{\int_0^t y X dt}{y_{100} X t} \times 100\% \quad (2)$$

Relative dissolution (RD) concerning the raw LOR at 60 minutes was calculated using the following formula:

$$RD \ 60 \ min = \frac{\% \ DE \ 60 \ min}{\% \ DE \ 60 \ min \ LOR} \quad (3)$$

The trapezoidal method was used to calculate the area under the curve (AUC). AUC is the sum of all trapezia:

$$AUC = \sum_{i=1}^{i=n} \frac{(t_1 - t_{i-1})(y_{i-1} + y_i)}{2} \quad (4)$$

Where  $t_i$  represents the time point, and  $y_i$  is the percentage of sample dissolved at time  $t_i$ . Mean dissolution time (MDT) was calculated as follows (Costa, P., & Lobo, 2001):

$$MDT = \frac{\sum_{i=1}^n t_{mid} \Delta M}{\sum_{i=1}^n \Delta M} \quad (5)$$

Where  $i$  is the dissolution sample number,  $n$  is the number of dissolution times,  $t_{mid}$  is the time at the midpoint between times  $t_i$  and  $t_{i-1}$ , and  $\Delta M$  is the amount of LOR dissolved (mg) between times  $t_i$  and  $t_{i-1}$ .

## 5.8 Characterization of the nanosuspension-based nasal formulations (NFs)

### 5.8.1 pH and drug loading of the nasal formulations

The pH of the nasal formulations was measured by transferring 1 mL of the formulation into a 10 mL volumetric flask. The solution was diluted with distilled water. The pH of the resulting solution was determined using a digital pH meter (Inolab, pH 7116, Xylem Analytics Germany GmbH, Germany).

The drug loading of the nasal formulation was measured by dissolving 300 mg of the formulation 50 mL of 0.1N HCl, pH 1.2. The mixture was stirred for 24 h at  $37 \pm 0.5$  °C. The mixture was filtered, and the drug content determined by using a UV–visible spectrophotometer (Unicam UV/VIS) at  $\lambda_{\text{max}}$  248 nm. Accordingly, the percent of drug loading was calculated from the ratio of practical and theoretical drug amount.

### 5.8.2 Rheological measurements of NFs

Rheological measurements were performed at 37 °C with a Rheostress 1 Haake instrument (Karlsruhe, Germany). A cone-plate device was used where the cone angle was 1°, the thickness of the sample was 0.052 mm, and the diameter of the device was 6 cm. The flow curves of the samples were plotted under the shear rate range of 0.01 to 100 s<sup>-1</sup>.

Rheology is one of the accepted methods to characterize mucoadhesive behaviours (Hassan and Gallo, 1990). Rheological synergism between mucin and the observed systems can be considered as an *in vitro* parameter to determine the mucoadhesive behaviour of systems. This viscosity change, called the bioadhesive viscosity component ( $\eta_b$ ), is caused by chemical and physical bonds formed in mucoadhesion. It can be calculated as follows:

$$\eta_b = \eta_t - \eta_m - \eta_p \quad (6)$$

Where  $\eta_t$  is the viscosity of the combination of NF with mucin,  $\eta_m$ , and  $\eta_p$  are the viscosities of the mucin and NF, respectively (Thirawong et al., 2008).

For mucoadhesivity, NFs were stirred with mucin (M) for 3 h before the measurement. The final concentration of M in the samples was 5% w/w. Moreover, the viscosity of the NFs and the combination with mucin were measured.

### 5.8.3 *In vitro* studies of the selected NF

*In vitro* release was carried out in a dialysis bag in artificial nasal fluid (ANF) media contained 8.77 mg mL<sup>-1</sup> NaCl, 2.98 mg mL<sup>-1</sup> KCl, and 0.59 mg mL<sup>-1</sup> CaCl<sub>2</sub> at pH 5.6 (Xie et al., 2019). 300 mg of the NF and corresponding reference were loaded into a dialysis bag and dialyzed against 100 mL of the dissolution medium at  $37 \pm 0.5$  °C and under 100 rpm paddle speed. At predetermined intervals, 5 mL

aliquots were withdrawn and replaced with an equal volume of fresh dissolution medium. The samples were filtered through a 0.45- $\mu\text{m}$  filter and analyzed by a UV spectrometer at  $\lambda_{\text{max}}$  248 nm.

Permeability studies were executed using a vertical Franz diffusion cell system (Logan Instrument Corporation, NJ, USA). 300 mg of NF was placed on the polyvinylidene fluoride synthetic membrane (Durapore1 Membrane Filter, EMD Millipore, Billerica, MA, USA). The membrane was impregnated with isopropyl myristate. The actual diffusion surface was 1.72  $\text{cm}^2$ . Phosphate buffer (PBS, pH 7.4, 37 °C) was used as an acceptor phase (7 mL). The rotation of the stirring bar was set to 300 rpm. At predetermined time points of diffusion, 0.8 mL samples were taken from the acceptor phase by the autosampler (Hanson Microette Autosampling System, Hanson Research, Chatsworth CA, USA) and were replaced with a fresh receiving medium. The amount of LOR diffused was determined spectrophotometrically.

The flux (J) of the drug was calculated from the quantity of LOR that permeated through the membrane, divided by the surface of the membrane insert and the duration [ $\text{mg cm}^{-2} \text{h}^{-1}$ ] using the following equation.

$$J = \frac{m}{At} \quad (7)$$

The permeability coefficient ( $K_p$ ,  $\text{cm h}^{-1}$ ) was determined from J and the initial concentration of the drug in the donor phase ( $C_d$  [ $\text{mg cm}^{-3}$ ]):

$$K_p[\text{cm/h}] = \frac{J}{C_d} \quad (8)$$

#### 5.8.4 *In vivo studies of the selected NF*

##### a. Drug administration using rat's model

The experimental protocols and animal care methods were approved by the National Scientific Ethical Committee on Animal Experimentation (permission number IV/1247/2017). The animals were treated following the European Communities Council Directives (2010/63/EU) and the Hungarian Act for the Protection of Animals in Research (Article 32 of Act XXVIII).

Single-dose *in vivo* studies were designed in male Sprague-Dawley rats weighing 220-250 g. The rats were divided into 4 groups of 4 animals each. Each rat received a dose of 0.5  $\text{mg kg}^{-1}$  of LOR. For the first group, 50–62  $\mu\text{L}$  of the selected NF was administered intranasally to each rat via a 100  $\mu\text{L}$  pipette into the nostrils. For the second group, the rats were nasally given the corresponding REF sample. The rats were anesthetized using 50  $\text{mg kg}^{-1}$  isoflurane for 5 min before the nasal administration.

For oral dosing, the third and fourth groups received the selected NF sample and the corresponding REF sample, respectively. The samples were mixed with distilled water to increase the volume to 1 mL containing 0.5  $\text{mg kg}^{-1}$  of LOR and were administered by gastric lavage.

0.5 mL of blood was collected from the tail vein at 0.5, 1, 2, 3, 4, 8, 12, and 24 h post-dosing. The blood samples were transferred into Eppendorf tubes containing sodium ethylenediaminetetraacetate. The samples were centrifuged at 1,500 g for 10 min at 5 °C. The separated plasma samples were stored at -80 °C until analysis.

#### **b. Plasma Sample preparation**

LOR was isolated from plasma samples by a liquid-liquid extraction procedure. To 100 µL of plasma, 10 µL ACN: H<sub>2</sub>O, (1:1, v/v), 10 µL of 3M NaOH, and 20 µL of d5-Loratadine (d5-LOR) –stable isotope-labelled internal standard (15.0 ng mL<sup>-1</sup>, in ACN:H<sub>2</sub>O, 1:1, v/v)– were added. The mixture was vortexed and shaken for 10 min at room temperature with 1 mL of n-hexane on a horizontal shaker, then centrifuged for 10 min at 3,000 rpm at 4°C to obtain the clear organic layer. 800 µL of the upper organic phase was transferred into a 1.5 mL glass vial, evaporated to dryness under a gentle stream of nitrogen and reconstituted in 100 µL starting eluent (5 mM ammonium acetate (pH = 5):ACN, 6:4, v/v). 20 µL was injected into the LC-MS/MS system for analysis.

#### **c. Preparation of the calibration curve**

The calibration curve for the quantification of LOR was set up in drug-free rat plasma. For the preparation of standard points, 100 µL rat plasma, 10 µL LOR standard solution (0.7–30.0 ng mL<sup>-1</sup>, diluted in ACN:H<sub>2</sub>O, 1:1, v/v), 10 µL 3M NaOH, and 20 µL d5-Loratadine (15.0 ng mL<sup>-1</sup>) were mixed and treated as above.

#### **d. LC - MS/MS Analysis of LOR**

The quantitative analysis of LOR was performed by using a Waters Acquity I-Class UPLC™ system (Waters, Manchester, UK), connected to a Q Exactive™ Plus Orbitrap mass spectrometer (Thermo Fisher Scientific, San Jose, CA, USA) equipped with a heated ESI ion source (HESI-II). Chromatographic separation was performed at 25 °C column temperature, on an ACE CN column (50 mm × 2.1 mm, particle size 3.0 µm) protected by an ACE CN guard column (Advanced Chromatography Technologies, Aberdeen, Scotland) by using 5mM of ammonium-acetate (pH = 5) as Solvent A and acetonitrile as Solvent B. Gradient elution program (started and maintained at 40% B for 1 min, increased linearly to 100% B in half min, kept at 100% B for 1.5 min, dropped back to 40% B in 0.1 min and kept there for 1.9 min for equilibration) with a flow rate of 300 µL min<sup>-1</sup> was applied to elute the analyte.

The mass spectrometer was used in positive mode with the following parameters of the HESI-II source: spray voltage at 3.5 kV, capillary temperature at 253 °C, aux gas heater temperature at 406 °C, sheath gas flow rate at 46, aux gas flow rate at 11, sweep gas flow rate at 2, S-lens RF level at 50.0 (source auto-defaults). Data acquisition was performed in parallel-reaction-monitoring (PRM) mode by monitoring the transitions of m/z 383→337 (LOR) and m/z 388→342 (d5-LOR) as quantifier and m/z

383→267 (LOR) and m/z 388→272 (d5-LOR) as qualifier ions. The collision energy (CE) for specific quantitation was optimized to maximize sensitivity and proved to be 28 eV for LOR and its stable isotope-labelled form, too. A valve placed after the analytical column was programmed to switch flow onto MS only when analytes of interest elute from the column (1.4–2.4 min) to prevent excessive contamination of the ion source and ion optics. Washing procedures of the autosampler before and after injecting samples were programmed to avoid carry-over of analytes.

Data acquisition and processing were carried out using Xcalibur and Quan Browser Software (Thermo Fisher Scientific, San Jose, CA, USA).

#### **e. Statistical analysis**

The statistical analysis was performed with Prism 5.0 software (GraphPad, San Diego, CA). The results are shown as the mean ± SD. The statistical methods included Student's *t*-test (two-group comparison). A probability (P) of less than 0.05 was considered statistically significant (\*P < 0.05).

The calculation of area under the curve (AUC) of the time (min) – concentration (nmol L<sup>-1</sup>) curves of each group of animals were performed with PKSolver add-in of Microsoft Excel (MS Office 2010) using non-compartmental analysis of data after extravascular input (model #101) of LOR (Zhang et al., 2010). The AUC values were calculated using the linear trapezoidal method.

#### **5.8.5 Stability assessment of the selected NF**

Stability studies of the selected NF were carried out by visual inspection. Stable systems were identified to be free of any physical changes such as phase separation, flocculation, or precipitation. Stability was observed at temperatures of 4 °C and 25 °C for 6 weeks. Moreover, the formulations were evaluated for particle size, polydispersity index, zeta potential, and drug content.

## 6. RESULTS

### 6.1 QbD and Knowledge space of LNS-based product

The development of knowledge space could visualize the overall manufacturing process for the selection of CPPs, and the definition of the required CQAs (Csóka et al., 2018). The first step was setting up an Ishikawa (fishbone) diagram, including all the parameters influencing the desired nanosuspension-based product containing LOR for nasal administration. Ishikawa diagram could list the parameters of significant effects on the target product into four groups; 1. material characteristics, 2. production method, 3. investigation method, and 4. therapeutic and regulatory aspects (**Fig.4**).

The characteristics of the API, such as solubility, melting point, and lipophilicity, must be identified to set the targets of the preparation. Moreover, the properties of the excipients such as lipophilicity, viscosity, and their effects on the drug's solubility play a crucial role in the production of stable nanosuspensions (Obeidat and Sallam, 2014; Verma et al., 2009).

The production method critically affects the particle size distribution. Ishikawa could help in defining the CPP and performing the risk assessment alongside the QbD (Kola Srinivas et al., 2016).

The most significant characterization parameters of nanosuspension are particle size and particle size distribution. These parameters determine the physicochemical properties of the nanoparticles, such as solubility, dissolution behaviour, and physical stability. Moreover, the shape of the nanoparticles (nanocrystals) is an important parameter that has consequences on the drug's permeability (Müller et al., 2001). Thermal and structural analysis with DSC, XRPD, and FTIR are essential to determine the polymorphic changes, crystallinity status, the structure of the active agent, effects of the production methods on the structure of the drug, and interactions between the active agent and the excipients (Chogale et al., 2016; Pinna, 2005). Improved solubility and dissolution are the ultimate targets of developing the nanosuspension of the poorly water-soluble drugs, and therefore, these analyses are vital to check the achievement of these aims (Gigliobianco et al., 2018).

For nasal formulations, determination and investigation of the drug release and absorption must be assessed. The preset goals determine the required examinations. Moreover, based on RA, experiments that can evaluate the CQAs must be of higher priority (Pallagi et al., 2015).

The next step was to select the elements of QTPPs, CQAs, CMPs, and CPPs for the aimed nasal product. **Table 7** lists these elements alongside with justification and explanation for the selected factors. For adaptation to the QbD-based development principles, QTPP and the required CQAs were defined.



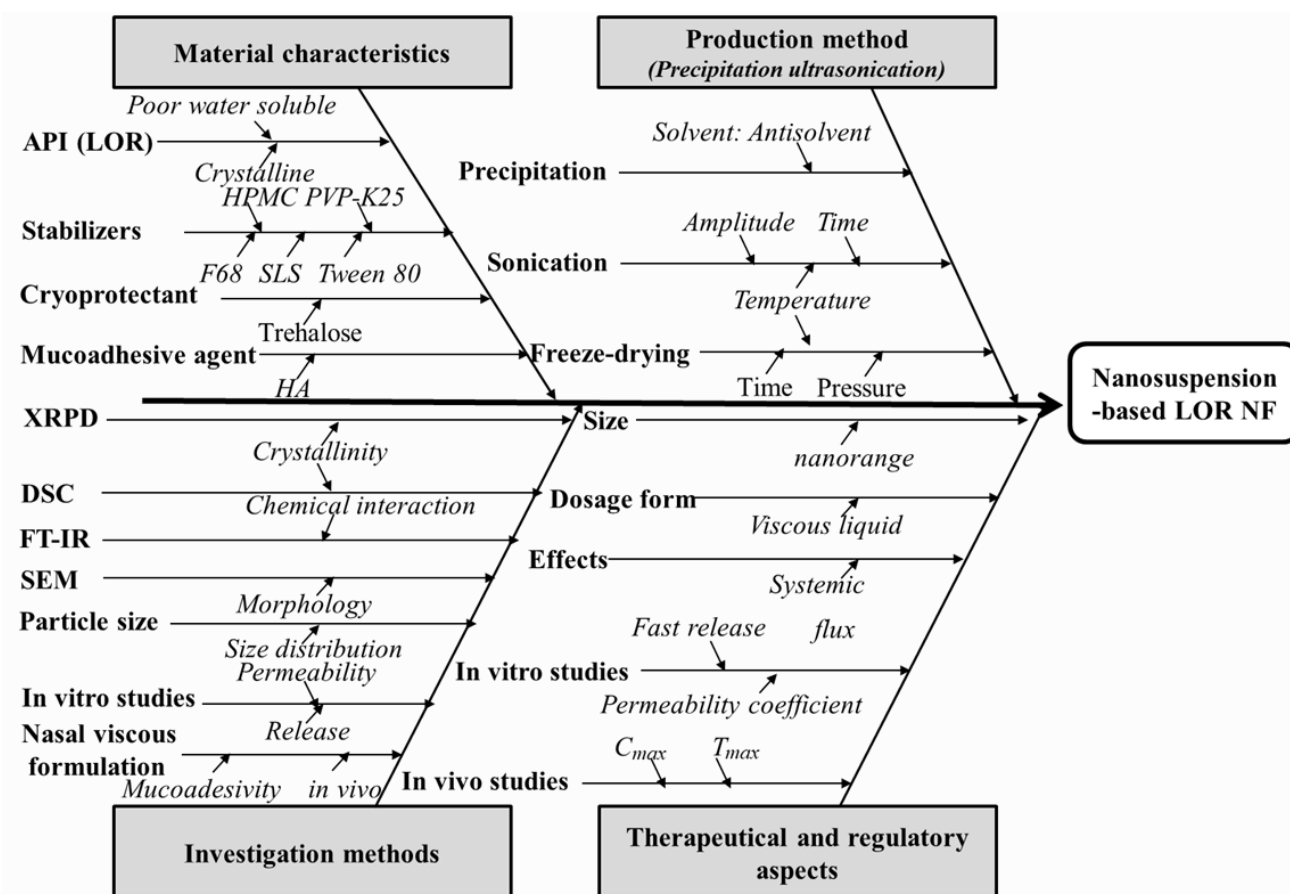


**Figure 4:** Ishikawa diagram illustrating the parameters influencing the quality of the NF containing nanosized LOR.

**Table 7:** QTPP, CQAs, CMP, and CPPs of LOR nanosized-based nasal formulation.

	Target	Justification	Explanation
<i>QTPP</i>			
Therapeutic indication	Histamine H <sub>1</sub> receptor antagonist	LOR is a second-generation H <sub>1</sub> receptor blocker used for the treatment of different allergies without CNS effects.	The therapeutic indication is a suggested QTPP by the ICH Q8.
Target patient population	Adult and children	LOR is administered for a short time until the symptoms clear up or regularly during the seasons of allergy. It is not recommended for children younger than 2-years old. It is pregnancy category B, and it is not recommended during lactation.	The patient target is a suggested QTPP by the ICH Q8 clinical setting.
Route of administration	Nasal	Avoidance of pH-dependent absorption of LOR, highly vascularized, highly absorption, noninvasive, easy to administrate.	The route of administration is a suggested QTPP by the ICH Q8.
Site of activity	Systemic	Absorption through the nasal mucosa into the blood circulation.	The site of activity is critically related to drug quality, efficacy, and being a QTPP requirement.

Dosage form	Nasal formulations viscous contain nanosized LOR	Nanosized particles increase the dissolution and solubility of LOR, enhance the bioadhesive properties, increase the absorption into the systemic circulation.	The dosage form is suggested to be a QTPP part by the ICH Q8.
Dissolution profile	Enhanced dissolution rate	Dissolution affects the bioavailability and pharmacokinetics of the product.	The dissolution profile is critically related to the quality and efficacy of the administered drug. It is suggested to be a QTPP part by the ICH Q8.
Production	Precipitation	Effective, simple, and low cost of production.	Precipitation is a cost-effective process that efficiently leads to particle size reduction to the nano-range.

### CQAs

Excipients	F68, Tween 80, PVP, HPMC, SLS, Soluplus <sup>®</sup> HA Ethanol TRE	Ionic and polymeric stabilizers are used to prevent the aggregation and growth of the nanoparticles. The mucoadhesive polymer (HA) is used to increase the residence time of the formulation in the nasal cavity, and to enhance drug permeation. The organic solvent is used as a solvent to prepare the nanosuspension by the antisolvent precipitation. TRE is used as freeze-drying cryoprotectant.	Critically related to product quality and safety.
Size/ surface area	Nanosize Homogenous product (300-500 nm)	Nanosize dimensions increase the surface area, enhance solubility, dissolution, and diffusion of the LOR through the nasal mucosa.	Critically related to efficacy by its impact on drug dissolution and solubility.
Dosage form	Viscous liquid formulation	Nanoparticles suspended in a mucoadhesive formulation for maximum distribution and absorption.	The dosage form is a suggested QTPP by the ICH Q8.
Dissolution	High drug release (in 15 min)	Dialysis was used to evaluate in vitro dissolution in artificial nasal fluid media.	Critically related to the efficacy and quality, it affects the bioavailability and pharmacokinetics.
Toxicity	Non-toxic, and non-irritative.	Non-toxic and biocompatible agents were used.	Critically related to safety.
Structure (amorphous/crystallinity)	Amorphous. Crystalline.	The amorphous status has a higher dissolution, but lower stability than the crystalline form.	Critically related to efficacy and stability.
Permeability	Effective absorption.	Permeability was evaluated by <i>in vitro</i> diffusion through Franz diffusion cell.	Critically related to the efficacy, affect the administration route, and the bioavailability.
Stability	No visible signs of aggregation or separation.	The viscous formulations should preserve the homogenous distribution of the nanosized particles.	Critically related to efficacy and safety.

### CMPs-CPPs

Composition (Excipients, ratios, additives)	Stabilized, enhanced dissolution rate, and increased mucosal resident of the nasal product.	Amount and type of stabilizer additives. These factors influence water solubility, amorphous, and crystalline structure of the used API. Different drug amounts (50, 75, 100, and 200 mg), stabilizer concentration (0.2, 0.4, and 0.6%, w/v), HA (1 mg mL <sup>-1</sup> and 5 mg mL <sup>-1</sup> ) were tested.	Critically related to efficacy, safety, and quality.
Sonication time	Decreased particle size.	10, 20, and 30 min of sonication periods were tested.	Critically related to efficacy and quality.
Sonication temperature	Affected particle size reduction.	25 and 4 °C temperatures were tested.	Critically related to efficacy and quality.
Sonication power	Decreased particle size	30, 50, and 100% amplitudes were tested.	Critically related to efficacy and quality.
Freeze-drying parameters	Stabilized the particle size.	Freeze drying conditions, including type and concentration of the cryoprotectant, temperature, pressure, and time.	Critically related to efficacy and quality.

RA reveals the interdependence rating between the QTPP and CQAs, and between CQAs and the CPPs-CMPs. The interactions were ranked on the three-level scale of high (H), medium (M), and low (L) (Fig.5).

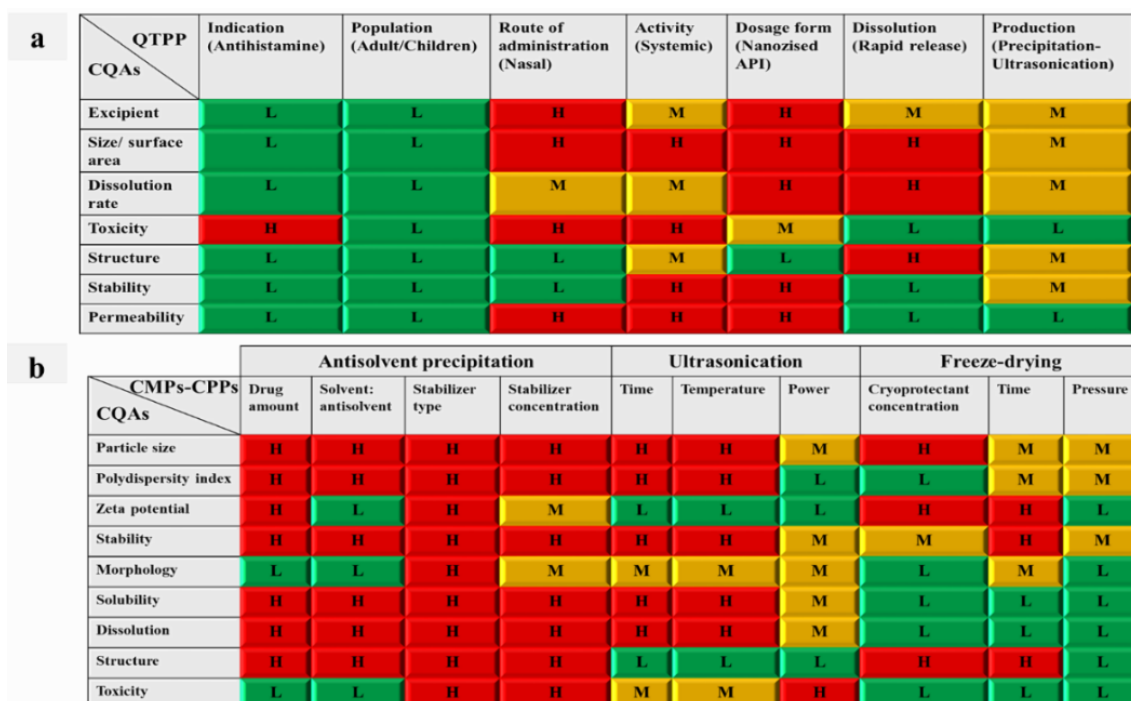


**Figure 5:** Results of RA-based of (a) interdependence rating between QTPP and CQAs, and (b) CQAs and CPPs-CMPs.

Furthermore, the severity scores for each of the critical parameters were selected and presented on a Pareto chart (Fig.6). Pareto charts also give a graphical overview of the hierarchy of CQAs and CPPs as the height of each bar gives information about the significance of the variables.

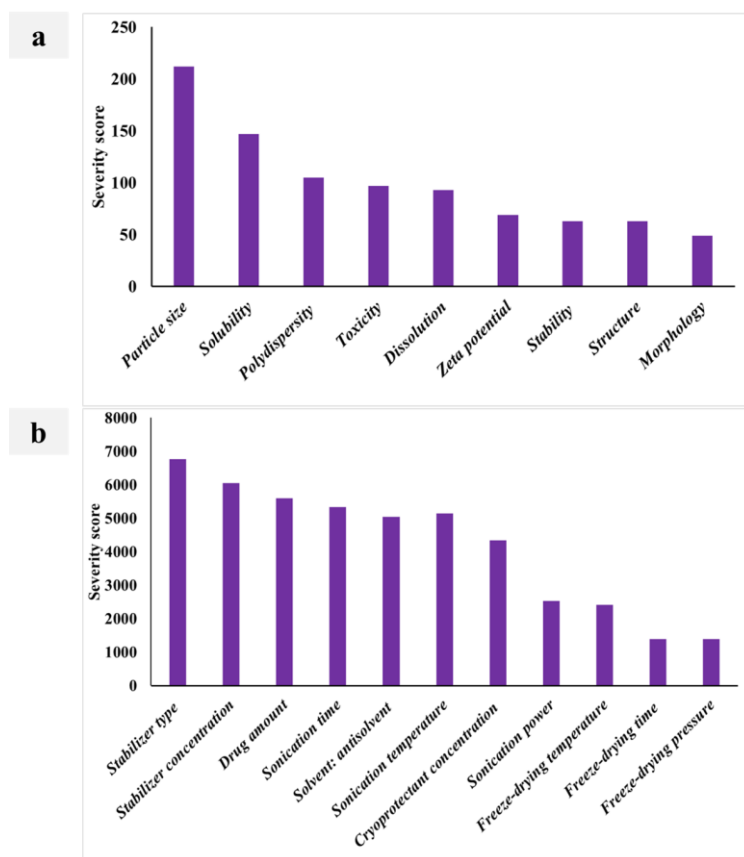


**Figure 6:** Pareto charts of (a) the CQAs and (b) CPPs-CMPs with calculated numeric severity scores.

**Fig.5a** shows the high impacts of size and surface area on the route of administration, site of activity, selection of the dosage form, and dissolution. Dissolution, in turn, was highly affected by the surface area and the structure. Moreover, permeability had significant effects on the route of administration, site of activity, and dosage form. On the other hand, toxicity had significant impacts on the indication, route of administration, and activity. The effects of particle size on dissolution have been documented as small particles have higher dissolution than the large particles (Noyes and Whitney, 1897). Apart from this, excipients have a major role in the safety and efficiency of the nasal administration. Therefore, the selection of suitable non-toxic, and non-irritative excipients, is significant for producing efficient and safe nasal products. The excipients must guarantee the production of nano-sized particles that are stable to increase the surface area and enhance the dissolution rate. Moreover, the effects of the excipients on permeability must be considered.

Accordingly, particle size, polydispersity, solubility, and dissolution were classified as first-line priority CQAs (**Fig.6a**). Therefore, practical research was focused on developing nasal formulations displaying appropriate CQAs (Alshweiat et al., 2018; Alshweiat et al., 2019b).

**Fig.5b** shows that the particle size, polydispersity index, zeta potential, structure, stability, solubility, and dissolution rate were highly influenced by drug concentration, stabilizer type and concentration, and sonication time, power, and temperature. As for freeze-drying, the concentration of the cryoprotectant showed critical impacts on the particle size, zeta potential, and structure, whereas freeze-drying time could highly affect the structure and stability due to its effects on the interactions between LOR and the excipients (stabilizer and cryoprotectant) (Alshweiat et al., 2018). **Fig.6b** illustrates the high severity of stabilizer type, stabilizer concentration, drug content, sonication time, sonication temperature, and solvent: antisolvent ratio as CPPs.

## 6.2 Selection of process parameters for the development of LNS

The QbD suggested the influential effects of CPP on the particle size and its consequences. Therefore, process parameters should be cautiously adjusted to support nanoscale production. In the case of ultrasonic-assisted precipitation, all precipitation and sonication parameters must be defined and selected according to the particle size reduction. For process optimization, the drug amount, and the stabilizer's type and concentration were fixed at 100 mg and 0.2% w/v of F68, respectively. Additionally, various solvent: antisolvent ratios, sonication temperatures, sonication times, and sonication powers were applied at fixed freeze-drying conditions. The optimized CPPs were selected in the light of MPS and PDI (**Fig.7**). Details and results of these experiments are thoroughly discussed in the work of Alshweiat et al. (Alshweiat et al., 2018).

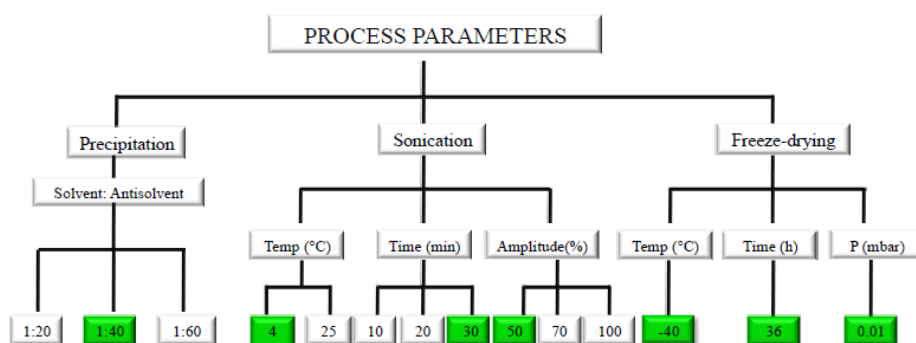


**Figure 7:** Critical process parameters for the preparation of LNSs and dry nanoparticles (DLN) (Alshweiat et al., 2018)

In summary, LNSs suitable for further processing were prepared using the following process parameters; sonication time of 30 min, time, sonication power of 50% amplitude, sonication temperature of 4 °C, and solvent:antisolvent ratio of 1:40.

## 6.3 Effects of material parameters on particle size and stability of LNS

**Table 8** shows the MPS, PDI, and ZP for pure LOR and the prepared LNSs. The mean particle size for unprocessed LOR was approximately 4.6 µm. Moreover, LOR showed aggregations of a size larger

than 120  $\mu\text{m}$  in the aqueous media. Using HPMC or PVP-K25 alone as a single stabilizer was insufficient to stabilize LOR nanoparticles. Adding either of these hydrophilic polymers alone yielded high MPS (4900 and 4212 nm, respectively) with a large particle size distribution as reflected by the PDI values (0.98 and 0.767, respectively) (Alshweiat et al., 2018). This failure to produce stable nanoparticles can be attributed to the weak adsorption of these polymers onto LOR's surface, as well as to the poor dipole-dipole interaction between LOR and the polymers because of a low polar surface area of LOR (Bartzatt, 2017). SLS was also found to be inappropriate to stabilize the nanosuspensions due to insufficient and incomplete adsorption of SLS into the surfaces of LOR (Obeidat and Sallam, 2014). SLS-containing LNSs were characterized by a MPS of 1496.3 nm and a PDI of 0.414. In contrast, Tween 80 and F68 were suitable to produce LNSs when they were used on their own. Combining SLS with F68 or PVP-K25 augmented the latter one's favourable effects on nanosuspension stabilization, while the combination of Tween 80 or F68 with PVP-K25 did not induce any significant changes compared to Tween 80 or F68 alone.

Different concentrations of F68 as a single stabilizer yielded different MPSs with an increasing diameter as concentration increased, due to a higher viscosity of the solutions, which hinders solvent diffusion and affects the transmission of ultrasonic waves.

Drug concentration had a significant effect on particle size reduction. Using a fixed 1:1 ratio of 0.2% w/v of F68 and PVP-K25 as stabilizers, the smallest MPS was obtained with 100 mg of LOR. This can be explained by supersaturation, in which higher drug concentration led to a higher rate of nucleation, resulting in a large number of nuclei and thus a smaller particle size (Lonare and Patel, 2013).

In another related study, QbD suggested process parameters were applied into different material that is not commonly used as a nanosuspensions stabilizers i.e Soluplus<sup>®</sup>. The concept of the QbD and the previously determined RA were followed to link the CPPs with the CQAs.

Polyvinyl caprolactam–polyvinyl acetate–polyethylene glycol (Soluplus<sup>®</sup>) is a graft copolymer with amphiphilic properties. This polymer could act as a stabilizer and also as a solubilizing agent in the formulations of poorly water-soluble drugs. The use of Soluplus<sup>®</sup> as a stabilizer for nanosuspensions has been reported in a few studies with improved solubility and bioavailability (Homayouni et al., 2014; Nagy et al., 2012).

LNSs were prepared with 0.2, 0.4, and 0.6%, w/v of Soluplus<sup>®</sup> (LNS16, LNS17, and LNS18, respectively). The effects of changing the stabilizers type on the previously studied CQAs of MPS, PDI, ZP, were evaluated. Soluplus<sup>®</sup> produced LNS with particle size smaller than the commonly used stabilizers (Alshweiat et al., 2019b). Soluplus<sup>®</sup> interacted with the nonpolar surface area of LOR and covered the newly formed surfaces, providing a steric hindrance to prevent recrystallization from the solution and aggregation of the primary particles. Accordingly, nanoparticles were generated with zeta

potential around -20 mV. Unlike F68, the particle size decreased with increased Soluplus<sup>®</sup> concentration. Higher concentrations of Soluplus<sup>®</sup> could stabilize the NS more effectively due to weak Ostwald ripening as the drug will diffuse slowly from the formed micelles (Yang et al., 2014).

**Table 8:** Mean particle size (MPS), polydispersity index (PDI), and zeta potential (ZP) for LOR and LNSs (Alshweiat et al., 2019b, 2018) (Mean  $\pm$  SD).

Sample	LOR (mg)	Stabilizer type	Stabilizer concentration (%w/v)	MPS (nm)	PDI	ZP (mV)
LOR	100	-	-	4607.5 $\pm$ 41.70	0.71 $\pm$ 0.18	-7.7 $\pm$ 5.28
LNS1	100	PVP-K25	0.2	4900.0 $\pm$ 71.98	0.98 $\pm$ 0.03	-13.4 $\pm$ 4.02
LNS2	100	HPMC	0.2	4212.0 $\pm$ 14.14	0.77 $\pm$ 0.18	-11.9 $\pm$ 4.51
LNS3	100	SLS	0.2	1496.3 $\pm$ 17.45	0.42 $\pm$ 0.11	-54 $\pm$ 7.75
LNS4	100	Tween 80	0.2	414.9 $\pm$ 9.02	0.22 $\pm$ 0.03	-23 $\pm$ 6.51
LNS5	100	F68	0.2	246.5 $\pm$ 1.83	0.13 $\pm$ 0.03	-6.5 $\pm$ 3.98
LNS6	100	F68	0.4	288.3 $\pm$ 37.33	0.10 $\pm$ 0.01	-6.3 $\pm$ 4.45
LNS7	100	F68	0.6	325.4 $\pm$ 28.20	0.20 $\pm$ 0.01	-12.1 $\pm$ 5.91
LNS8	100	PVP-K25+SLS	0.2+0.2	589.3 $\pm$ 12.66	0.23 $\pm$ 0.03	-58.7 $\pm$ 8.54
LNS9	100	F68+SLS	0.2+0.2	557.4 $\pm$ 31.47	0.20 $\pm$ 0.03	-67.2 $\pm$ 8.14
LNS10	50	F68+PVP-K25	0.2+0.2	306.7 $\pm$ 14.97	0.16 $\pm$ 0.11	-27.8 $\pm$ 5.08
LNS11	75	F68+PVP-K25	0.2+0.2	276.5 $\pm$ 2.69	0.11 $\pm$ 0.02	-4.81 $\pm$ 4.11
LNS12	100	F68+PVP-K25	0.2+0.2	253.4 $\pm$ 1.27	0.12 $\pm$ 0.01	- 11.14 $\pm$ 4.89
LNS13	100	F68+PVP-K25	0.2+0.4	265.6 $\pm$ 20.79	0.12 $\pm$ 0.03	- 18.10 $\pm$ 3.85
LNS14	100	F68+PVP-K25	0.2+0.6	307.25 $\pm$ 7.28	0.17 $\pm$ 0.01	-23.6 $\pm$ 5.07
LNS15	100	Tween80+PVP-K25	0.2+0.2	423.4 $\pm$ 15.06	0.20 $\pm$ 0.02	-22.9 $\pm$ 4.39
LNS16	100	Soluplus <sup>®</sup>	0.2	220.4 $\pm$ 5.30	0.25 $\pm$ 0.0	-21.5 $\pm$ 5.59
LNS17	100	Soluplus <sup>®</sup>	0.4	178.7 $\pm$ 6.50	0.12 $\pm$ 0.02	-19.7 $\pm$ 4.85
LNS18	100	Soluplus <sup>®</sup>	0.6	168.3 $\pm$ 6.5	0.16 $\pm$ 0.03	-16.5 $\pm$ 6.59

In conclusion, the selection of the material was based on the ability to produce LOR nanosuspensions of the smallest particle size. Thus, nanosuspensions with 0.6% Soluplus<sup>®</sup>, and 0.2% w/v F68 either as

a single stabilizer or as a mixture with PVP-K25 at 1:1 or 1:2 ratios (LNS5, LNS12, LNS13, and LNS18) were selected to be dried and further analyzed to evaluate the morphology, thermal, structure, solubility, and dissolution characteristics.

#### 6.4 Effects of freeze-drying on particle size and stability

Aggregation of the selected LNSs did not occur for 1 week upon storage at 4°C, and nanoscale size was preserved (**Table 9**). However, MPS increased for all the selected samples compared to the MPS measured on the day of preparation. Therefore, this storage time was enough for the nanosuspension to be transferred into the freeze-dryer and converted into dried nanoparticles.

**Table 9:** Mean particle size (MPS), polydispersity index (PDI), and zeta potential (ZP) for selected LNSs after 7 day of storage at 4°C (Alshweiat et al., 2019b, 2018) (Mean ± SD, n=3).

Sample	MPS (nm)	PDI	ZP (mV)
LNS5	276.1±17.11	0.14±0.05	-7.8±3.36
LNS12	283.4±14.32	0.14±0.02	-17.4±5.23
LNS13	294.1±11.61	0.14±0.04	-20.6±7.46
LNS18	178.5±6.7	0.18±0.09	-19.0±1.40

Other prepared DLNs were easily redistributed to their original volume at nanosized range with accepted PDI (**Table 10**) and higher ZP than corresponding nanosuspensions, probably due to enhanced specific interaction between LOR and the polymeric stabilizers during drying and hence stability (Kim and Lee, 2010).

**Table 10:** Mean particle size (MPS), polydispersity index (PDI), and zeta potential (ZP) for the selected DLNs after reconstitution in water (Alshweiat et al., 2019b, 2018) (Mean ± SD, n=3).

Sample	MPS (nm)	PDI	ZP (mV)
DLN5	406.80±16.32	0.24±0.02	-25.80±5.87
DLN12	353.55±31.75	0.20±0.04	-22.35±5.62
DLN13	441.42±37.90	0.25±0.02	-20.70±4.82
DLN18	220.21±6.23	0.21±0.02	-23.81±4.43

#### 6.5 Characterization of LOR dry nanoparticles

##### 6.5.1 Morphology of DLNs

Raw LOR showed irregular shapes of crystals with a particle size larger than 5 µm with aggregation resulting in a broad range of size distribution. Drug particles in the PMs also showed the crystals of LOR. DLN5, DLN12, and DLN13 were characterized by short rod shape particles in the nanoscale, while Soluplus<sup>®</sup>-containing sample (DLN18) had spherical particles at the nanosized scale embedded within the carriers. The surfaces of DLNs were smooth due to the uniform drug dispersion at the



molecular level (Alshweiat et al., 2018) (**Fig.8**). The SEM images confirmed the high impact of the stabilizer type on the morphology of the nanoparticles as it was expected by the RA part of the QbD (**Fig.5**).

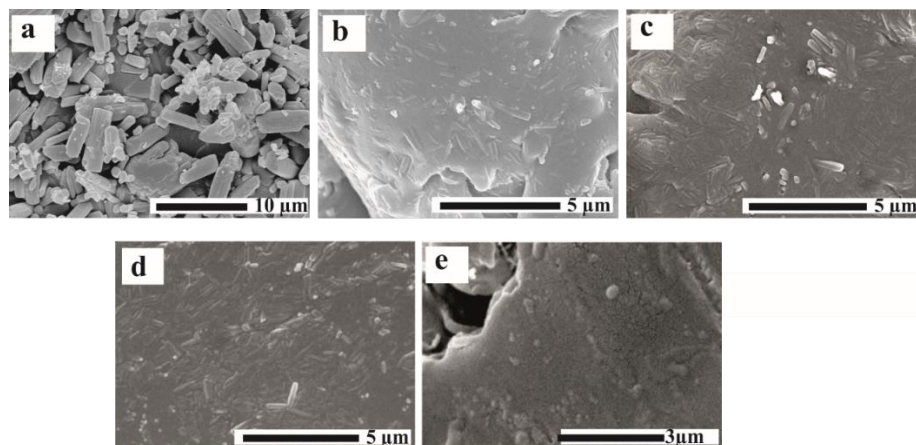


**Figure 8:** SEM images of (a) raw LOR, (b) DLN5, (c) DLN12, (d) DLN13, and (e) DLN18 (Alshweiat et al., 2019b, 2018).

### 6.5.2 Differential scanning calorimetry of DLNs

**Fig.9** shows the DSC thermograms of the raw materials, PMs, and DLNs. Pure LOR exhibited a single sharp endothermic peak at 135.5°C, corresponding to its melting point. F68 also showed a single peak for its melting point at 55 °C. For Soluplus<sup>®</sup> and PVP-K25, peaks corresponding to the evaporation of water appeared in the temperature range of 50–80 °C (Ruan et al., 2005). The absence of LOR peaks in PM1 and PM2 may be ascribed to the effect of F68 as it melted at 55 °C and dissolved LOR during further heating (Ahuja et al., 2007). DLN5, DLN12, and DLN13 showed two broad peaks, one at 55–60 °C and the other at 110 °C. These thermal events could be related to trehalose, to the interactions between the drug, the stabilizer, and trehalose during freeze-drying, to the phenomenon of the drug's dissolving in the stabilizer or the transformation into the amorphous state. Alshweiat et al. (Alshweiat et al., 2018) reported further evaluation of freeze-dried excipients that emphasized the interaction of trehalose with LOR or the stabilizer during the freeze-drying. On the other hand, DLN18 showed thermal events at 90 °C due to the glass transition temperature of amorphous trehalose, at 211°C due to the melting of trehalose, and a broad peak at 270 °C related to trehalose decomposition (Alshweiat et al., 2019b; Chang et al., 2017; Dolenc et al., 2009).

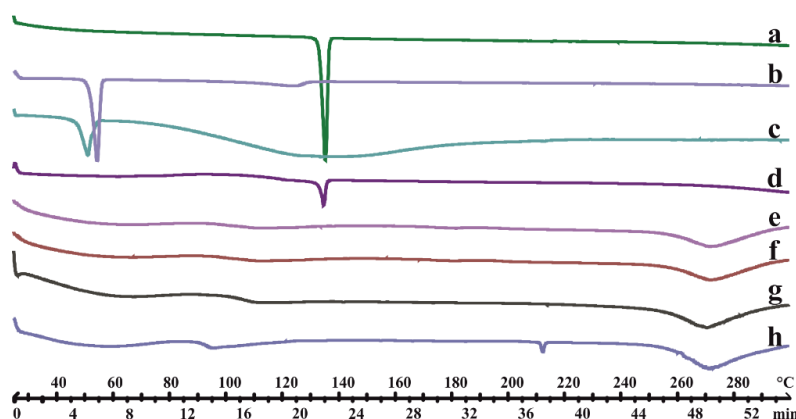


**Figure 9:** DSC thermograms of (a) raw LOR, (b) PM1 (1.25:1 weight ratio of LOR: F68), (c) PM2 (1.25:1:1 weight ratio of LOR:F68:PVP-K25), (d) PM3 (1:2.4 weight ratio of LOR:Soluplus<sup>®</sup>), (e) DLN5, (f) DLN12, (g) DLN13, and (h) DLN18 (Alshweiat et al., 2019b, 2018).

### 6.5.3 Structural analysis of DLNs

The XRPD-diffractogram of LOR displayed intense crystalline  $2\theta$  peaks between  $5^\circ$  and  $30^\circ$ , indicating its crystalline nature. The PMs showed the characteristic crystalline diffraction peaks of LOR. These findings could support the previous assumption related to the absence of LOR peaks in the DSC thermograms of PM1 and PM2. The DLNs showed the halo and the diffused pattern typical of amorphous material (**Fig.10**). The degree of crystalline index confirmed the amorphous form of the LOR in these samples (37, 37, 18.1, and 27% for DLN5, DLN12, DLN13, and DLN18, respectively). These observations support that the crystalline structure vanishes as a result of the precipitation and drying processes (Colombo et al., 2017). Moreover, XRPD diffractograms revealed the conversion of trehalose dihydrate to an amorphous anhydrate form.

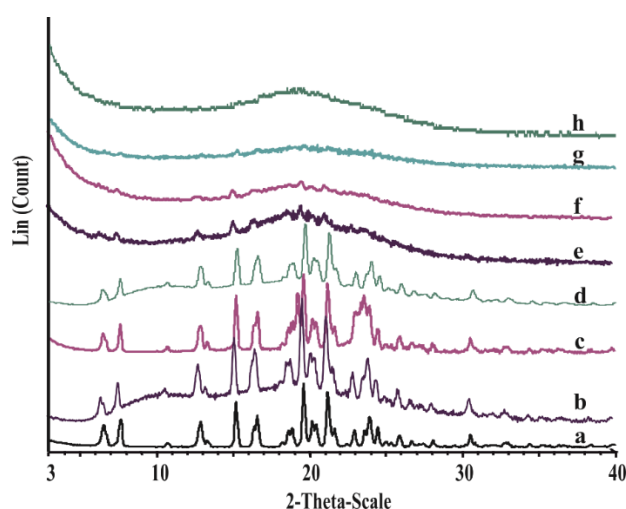


**Figure 10:** XRPD diffractograms of (a) raw LOR, (b) PM1 (1.25:1 weight ratio of LOR: F68), (c) PM2 (1.25:1:1 weight ratio of LOR:F68:PVP-K25), (d) PM3 (1:2.4 weight ratio of LOR:Soluplus<sup>®</sup>), (e) DLN5, (f) DLN12, (g) DLN13, and (h) DLN18 (Alshweiat et al., 2019b, 2018).

#### 6.5.4 Fourier transform infrared spectroscopy of DLNs

The FT-IR spectra of the raw materials and DLNs are presented in **Fig.11**. Pure LOR's FT-IR spectrum is described by bands at approximately  $997\text{ cm}^{-1}$  and  $1,227\text{ cm}^{-1}$  for Aryl C-Cl stretching and C-N stretching of aryl N, respectively. There are two characteristic bands at  $1560$  and  $1703\text{ cm}^{-1}$ , corresponding to C-O bonds of the amide or ester groups. Bands from  $3000$  to  $2850\text{ cm}^{-1}$  were related to the C-H bond.

PMs spectra showed the characteristic peaks of pure LOR, indicating negligible interactions between the API and the excipients. On the other hand, DLN5, DLN12, DLN13, and DLN18 showed significant differences at  $3532$ ,  $2900\text{--}2982$ ,  $1700$ , and  $997\text{--}1171\text{ cm}^{-1}$ . These shifts could be ascribed to the interaction of LOR with the excipients during freeze-drying.

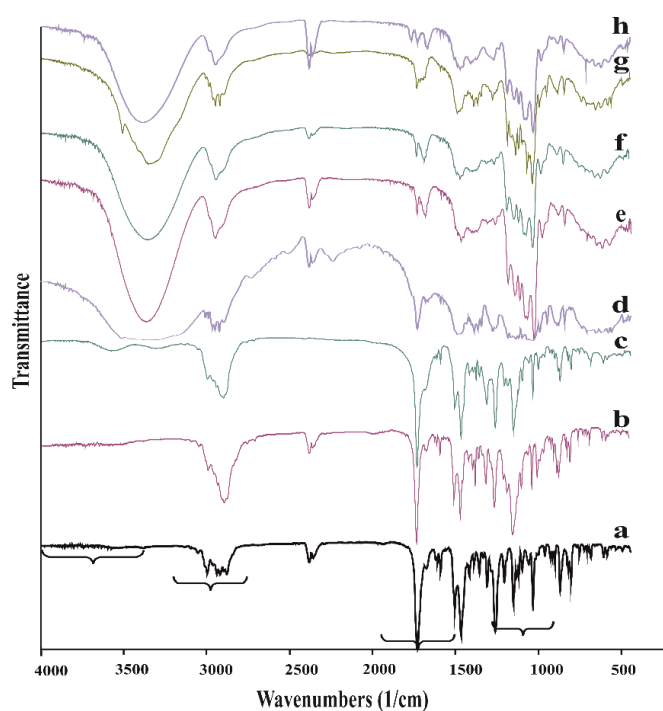


**Figure 11:** FT-IR spectra of (a) raw LOR, (b) PM1 (1.25:1 weight ratio of LOR: F68), (c) PM2 (1.25:1:1 weight ratio of LOR:F68:PVP-K25), (d) PM3 (1:2.4 weight ratio of LOR:Soluplus<sup>®</sup>), (e) DLN5, (f) DLN12, (g) DLN13, and (h) DLN18 (Alshweiat et al., 2019b, 2018).

#### 6.5.5 Effect of drying process on drug-excipients interactions

Using of pre-dispersion directly to prepare the NFs is a simple step. However, the LOR characteristics and interactions with the excipients could be different from the Freeze-dried nanoparticles. Therefore, evaluating the interactions between LOR and the excipient during preparation can be achieved by comparing the samples dried by varying methods.

Vacuum drying for 24 h at 25 °C was applied for the LNS to produce a sample corresponding to DLN5. Both samples contained equal amounts of LOR and F68 and were prepared by the same conditions of the precipitation-assisted ultrasonication method. However, TRE was added to dry one sample by freeze-drying to get DLN5. The XRPD diffractogram and FT-IR spectrum were compared to the raw LOR and the PM1 ones (**Fig.12**). The vacuum dried LNS showed the same characteristic FT-IR bands of raw LOR and PM. On the other hand, DLN5 showed alterations, as has been discussed earlier. Furthermore, the XRPD test confirmed the crystalline state of LOR in the vacuum dried LNS5, while DLN5 showed an amorphous state.

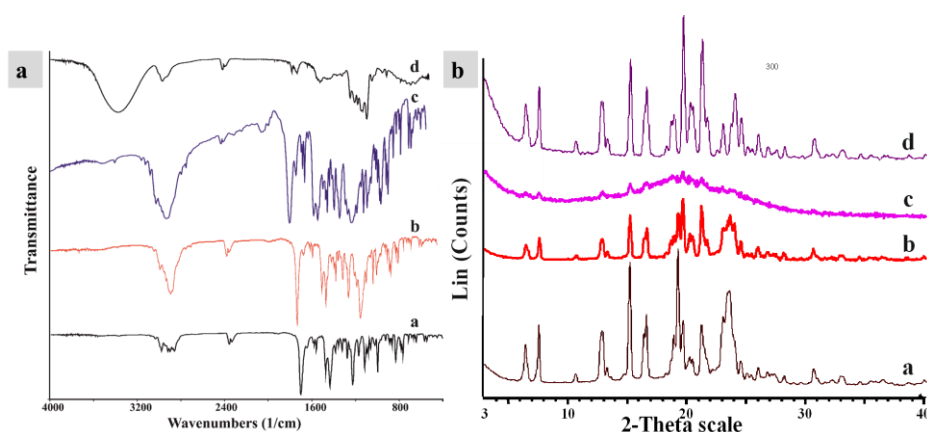


**Figure 12:** (a) FT-IR of (a) raw LOR, (b) PM1 (1.25:1, weight ratio of LOR:F68), (C) DLN5, and (d) vacuum dried LNS5, vs (b) XRPD of (a) raw LOR, (b) PM1 (1.25:1, weight ratio of LOR:F68), (C) DLN5, and (d) vacuum dried LNS5.

The presence of interactions between the components of excipient mixtures during freeze-drying also has been confirmed by freeze-dried excipients. The DSC showed a change in the thermogram of TRE in freeze-dried samples containing PVP-K25, as FD-(PVP-K25/TRE) and FD-(F68/PVP-K25/TRE) revealed the absence of the endothermic peak characteristic of TRE at 210°C (**Fig.13**) (Cardona et al., 1997; Imamura et al., 2008; Taylor, 1998).

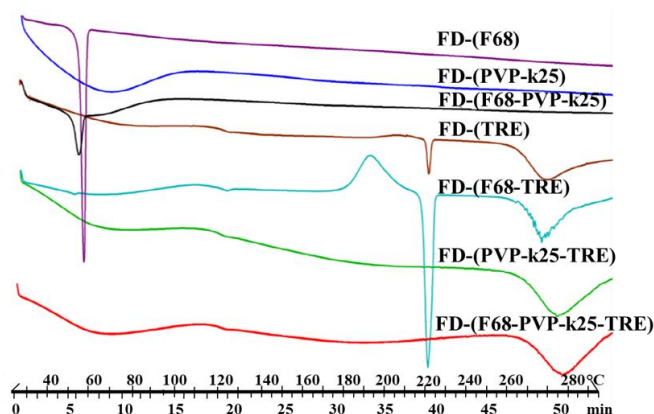


**Figure 13:** DSC thermograms of ultrasonicated, freeze-dried excipients; F68, PVPK25, TRE, F68/PVP-K25, F68/TRE, PVP-K25/TRE, and F68/PVP-K25/TRE (Alshweiat et al., 2018).

FT-IR subtracted curves were generated by subtracting the FT-IR spectra of the excipients, including TRE from the spectra of the corresponding DLN5, DLN12, DLN13, PM1, and PM2 (Fig.14). The peaks of LOR in the subtracted curves of PMs were identical to the peak of pure LOR. However, the subtracted curves of DLNs showed additional peaks at  $3532\text{ cm}^{-1}$  related to N-H and at  $3100\text{ cm}^{-1}$  related to weak stretching OH bonds. Peak weakening and broadening were observed at  $1703$  and  $1500\text{ cm}^{-1}$ . These investigations revealed the presence of intermolecular hydrogen bond and dipole-dipole interactions, although no chemical decompositions were detected (Alshweiat et al., 2018).

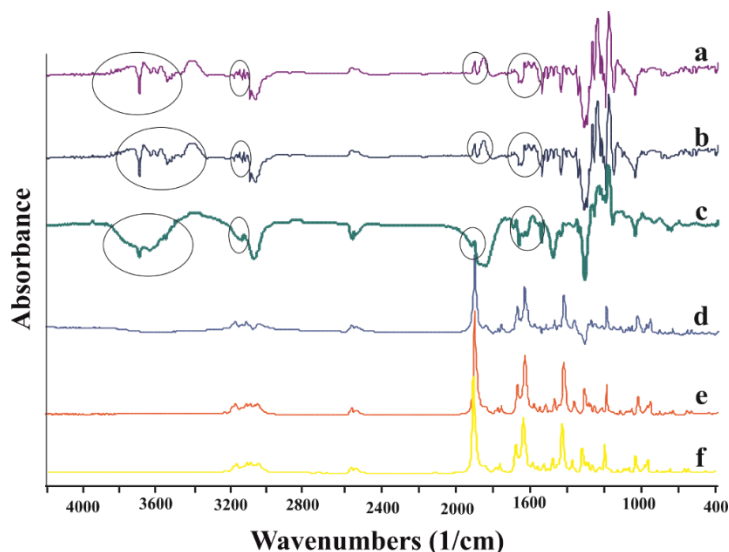


**Figure 14:** FT-IR spectra produced by subtracting the FT-IR spectra of the excipients from the spectra of corresponding DLNs and PMs.(a) DLN5-Excipients, (b) DLN12-Excipients, (c) DLN13-Excipients, (d) PM1-Excipients, (e) PM2-Excipients compared to (f) LOR (Alshweiat et al., 2018).

#### 6.5.6 Solubility and *in vitro* release from DLNs

Compared to pure LOR, DLNs showed enhanced saturation solubility in water and PBS of pH 7.4. The water solubility of nanoparticles was increased by approximately 5.5, 8.6, and 15.4-fold for DLN5, DLN12, and DLN13, respectively. On the other hand, solubility in PBS of pH 7.4 was enhanced by 9.3, 8.0, and 8.6-fold for DLN5, DLN12, and DLN13. This enhancement could be related to the reduction in particle size and the wettability of the polymers. When the particle size was reduced from the micron-range to the nano-range, the overall surface area of all particles increased sharply. Therefore, dissolution based on Noyes–Whitney equation (Noyes and Whitney, 1897). Water solubility was increased by increasing concentrations of PVP-K25. This increment may be attributed to the anti-plasticizing activity of PVP-K25, which could retard the formation of the crystal lattice. For Soluplus<sup>®</sup>-based nanosuspension, DLN18 showed a  $59.39 \pm 5.18\ \mu\text{g mL}^{-1}$  solubility of LOR in PBS (pH 7.4), this means 121-fold enhanced solubility compared to LOR. The factors responsible for

such enhancement could be related to the reduction in particle size and the higher wettability due to the Soluplus® polymers.

**Fig.15** shows the dissolution profiles for LOR, PMs, and DLNs at PBS of pH 7.4. Poor dissolution of LOR results in only 6% of the drug dissolving in 120 min. PM1 and PM2 showed higher dissolving of the drug (20.3 and 17.7%, respectively) due to the increased wettability of the drug powder. DLNs showed higher drug release than pure LOR and PMs as 30 and 42% of the drug was detected to be released in the first 10 min, followed by no further significant dissolution because the sink conditions were not applied. Enhanced drug release can be attributed to particle size reduction, which produces a higher surface area for dissolution, and possibly to better wettability (Jinno et al., 2006).

In a careful estimation, DLN5 showed the highest rate of dissolution, which may be related to F68 that forms micelles and increases dissolution. On the other hand, decreasing concentrations of PVP-K25 were found to improve dissolution due to increased viscosity around the stagnant layer. Additionally, the amorphous form is characterized by better solubility compared to the crystalline form (Lindfors et al., 2007).

Alternatively, about 57% of LOR h released from the s Soluplus®-based dry nanoparticles (DLN18) in the first 15 min and 80% within 2 h. This could be related to the high surface area of the nanoparticles, while the corresponding physical mixture (PM3) showed a release of 4.7 within 2 h.

The differences in dissolution rates between different samples could be related to the stabilizer type and concentration.

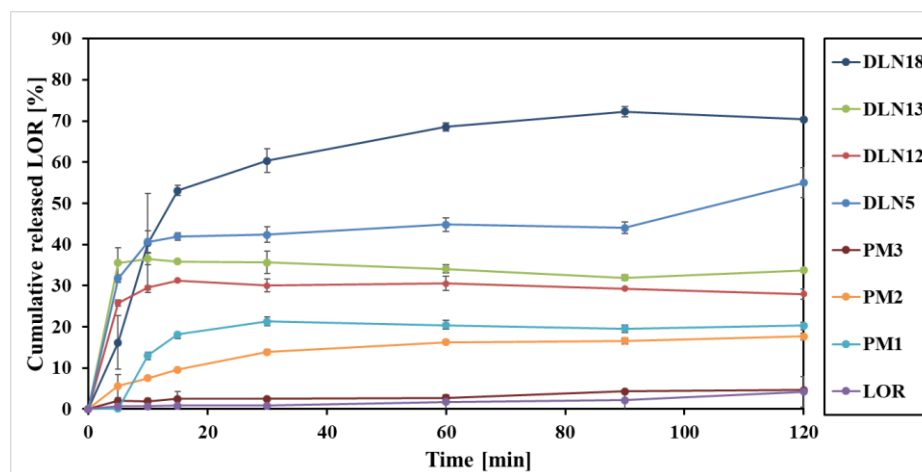


**Figure 15:** Dissolution behaviours of LOR, PM1, PM2, PM3, DLN5, DLN12, DLN13, and DLN18 at PBS, pH 7.4 (Alshweiat et al., 2019b, 2018).

### 6.5.7 *In vitro* dissolution kinetics

The enhancement of the dissolution efficiency at different time points and RD60 can be noticed for the DLNs. At 30 min, the DE value of the drug is only 1.6%. PMs also showed low values in the range

of 2.1–13%, while DLNs showed values in the range of 27–47.0%. Similar increments were observed at 60 and 120 min, the maximum DE was shown by DLN18 at 120 min (67.30%). RD60 of DLNs showed an observed enhancement compared to PMs as well. On the other hand, the MDT values of the DLNs were lower than LOR. However, DLN5, DLN12, and DLN18 showed lower values than DLN18 (**Table 11**). These findings demonstrated the higher and faster dissolution of DLNs compared to the raw LOR (Alshweiat et al., 2019b, 2018).

**Table 11:** %DE, MDT, and RD60 min for LOR and DLNs (Alshweiat et al., 2019b, 2018).

Sample	%DE30	%DE60	%DE120	MDT	RD <sub>60min</sub>
LOR	1.6	1.5	2.0	34.3	-
PM1	13.6	17.6	18.6	6.6	4.2
PM2	8.9	11.8	14.4	16.9	2.9
PM3	2.1	2.4	3.2	32.0	1.6
DLN5	36.7	40.1	43.5	5.0	9.7
DLN12	27.2	28.7	29.0	0.5	6.9
DLN13	32.9	33.9	33.4	1.2	8.2
DLN18	47.0	58.2	67.3	11.2	38.3

## 6.6 Nanosuspension-based nasal formulations

The selection of potential stabilizers for the nanosuspension of the nasal delivery application was based on three preconditions: 1. to have a significant reduction of particle size, 2. it should have a weak effect on drug solubility since that drug solubility in the stabilizer solution plays a significant role in the formation of a stable nanosuspension (Verma et al., 2009), and 3. the stabilizer should be used in a low concentration. Therefore, F68 of 0.2%, w/v was selected to be the stabilizer for the pre-dispersion over Soluplus<sup>®</sup> of 0.6%, w/v concentration, as the solubility of LOR in the 0.6% Soluplus<sup>®</sup> was  $63.39 \pm 27.38 \mu\text{g mL}^{-1}$  compared to  $2.25 \mu\text{g mL}^{-1}$  in 0.2% F68. Besides, the ability of F68 to stabilize the LOR nanosuspension at this low concentration.

Based on the previous experiments for the preparation and characterization of LNS, LNS5 was selected as a base to prepare the pre-dispersion for the nasal formulations. However, the drug content was increased, and suitable dilution of the nanosuspension with 0.2%, w/v F68 was applied to control the final concentration of LOR and HA in the final nasal formulations. Accordingly, material and process parameters were set as 200 mg mL<sup>-1</sup> of LOR concentration of in the solvent phase, 0.2% w/v F68 as an antisolvent phase, 1:40 (mL:mL) of solvent:antisolvent. Moreover, the sonication process was set for sonication time of 30 min, sonication temperature of 4 °C, and sonication power of 50% amplitude.

### 6.6.1 Characterization of the nanoparticles in the nasal formulations

The LOR pre-dispersion exhibited a particle size of  $311.55 \pm 5.16$  nm, polydispersity index of  $0.16 \pm 0.02$ , and zeta potential of  $-22.05 \pm 2.75$  mV, thus homogenous and stable nanosuspension was produced by the antisolvent precipitation assisted ultrasonication method. LOR in the LNS showed saturation solubility of  $8.5 \pm 0.65$   $\mu\text{g mL}^{-1}$  in PBS at pH, 5.6. Though, pure LOR showed solubility of  $1.63 \pm 0.38$   $\mu\text{g mL}^{-1}$ . After three days of storage, the particles of LNS showed a MPS of  $319.45 \pm 4.90$  nm, PDI of  $0.17 \pm 0.02$ , and ZP of  $-18.50 \pm 4.33$ , respectively.

The SEM images (**Fig.16a**) revealed the changes in the surface morphology between LOR and LNS. LOR showed an irregular rod-like crystal shape with aggregation. Conversely, LNS showed a uniform distribution of nanocrystals within the matrix of F68.

The DSC thermograms (**Fig.16b**) depict the reduction of LOR particle size and crystallinity in LNS; LOR showed a single sharp endothermic peak at 135 °C. The LNS showed a peak at 55 °C related to F68 and a reduced intensity and shifted peak toward a lower melting point of LOR.

XRPD (**Fig.16c**) diffractogram of LNS and LOR were similar. Therefore, the reduction of the melting point and intensity of LOR in the sample could be related to the particle size rather than crystallinity reduction (Murdande et al., 2015). Moreover, The FT-IR spectra showed that LNS preserved the characteristic bands of LOR, thus confirmed the compatibility between LOR and F68 (Alshweiat et al., 2018).

In summary, the morphological and structural analyses have demonstrated that LOR was produced in the nano-range as a homogenous nanosuspension while it preserved the crystalline state of the drug (Alshweiat et al., 2020).

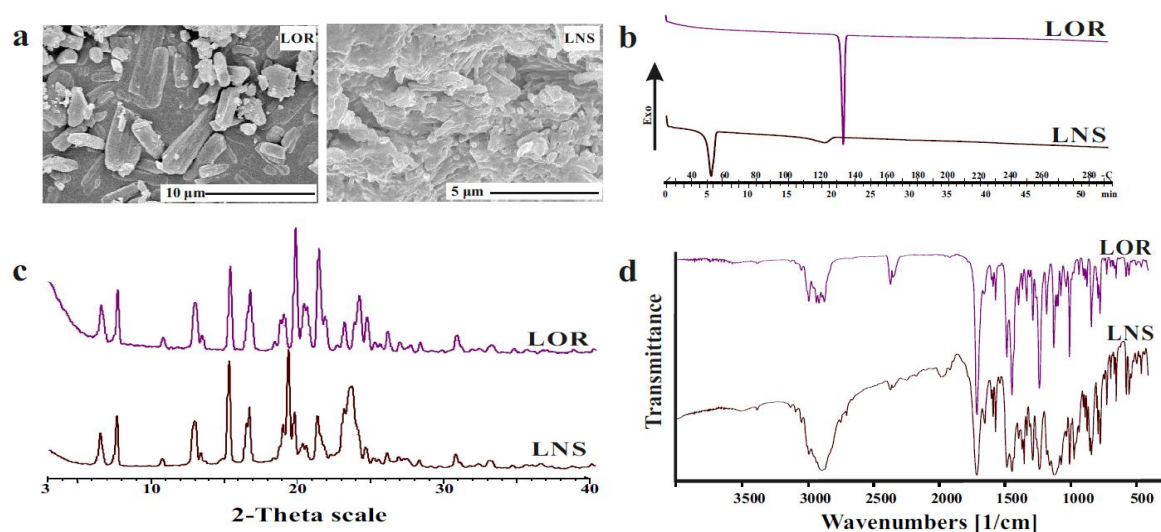


**Figure 16:** LOR and vacuum dried LNS characterization of (a) SEM images, (b) DSC thermograms, (c) XRPD diffractograms, and (d) FTIR spectra (Alshweiat et al., 2020).



### 6.6.2 Characterization of the nasal formulations

The prepared NFs appeared as viscous formulations. The samples showed drug content higher than 90%, particularly  $98.98 \pm 1.2$ ,  $97.66 \pm 4.2$ ,  $95.15 \pm 3.4$ , and  $92.99 \pm 2.8$  for NF1, NF2, NF3, and NF4, respectively. The pH of the samples was in the range of 6.3–6.4, hence within the acceptable range for nasal administration (pH of the nasal mucosa is 4.5– 6.5) (England et al., 1999). LOR is unionized at these pH values. Therefore, dissolution enhancement is not ascribed to the salt form of LOR (Popovi et al., 2009).

The addition HA had significant effects on the particle size and zeta potential of the LOR nanosuspensions in the NFs, as the MPS and ZP were increased by the addition of HA. The MPS of LOR in NF1, NF2, NF3, and NF4 was  $327.2 \pm 8.23$ ,  $437.27 \pm 28.60$ ,  $341.6 \pm 11.84$ , and  $450.63 \pm 24.30$  nm, respectively. Their respective PDI values were  $0.25 \pm 0.04$ ,  $0.31 \pm 0.07$ ,  $0.25 \pm 0.04$ , and  $0.26 \pm 0.03$ , respectively (Alshweiat et al., 2020). This significant increase in particle size could be attributed to the coating of the particles by HA (Shen et al., 2015). Moreover, the presence of HA in the formulation increased the negativity charge. The zeta potential values were  $-55.1 \pm 5.67$ ,  $-50.3 \pm 6.68$ ,  $-45.9 \pm 6.36$ , and  $-52.2 \pm 6.91$  mV for NF1, NF2, NF3, and NF4, respectively (Sharma et al., 2016; Shen et al., 2015).

### 6.6.3 Rheological properties of NFs

The NFs showed a shear thinning-flow (pseudoplastic) (**Fig.17a**). The rheological behaviours of the NFs were similar to the corresponding blank solutions that contained  $1 \text{ mg mL}^{-1}$  and  $5 \text{ mg mL}^{-1}$  of HA in 0.2% w/v F68 noted as blank1 and blank5, respectively. The apparent viscosity of the NFs was decreased by increasing the shear rate, which is typical for sodium hyaluronate solutions (**Fig.17b**) (Krause et al., 2001). However, the reduced particle size of LOR showed higher viscosity than the blank samples. Therefore, the nanosized LOR improved the viscosity of blank solutions. Comparable outcomes are reported by the work of Bartos et al. (Bartos et al., 2015). Apart from this, the viscosity of the formulations was related to the used HA polymer concentration.  $1 \text{ mg mL}^{-1}$  containing NFs (NF1 and NF3) showed lower values than  $5 \text{ mg mL}^{-1}$  containing NFs (NF2 and NF4) (Alshweiat et al., 2020).

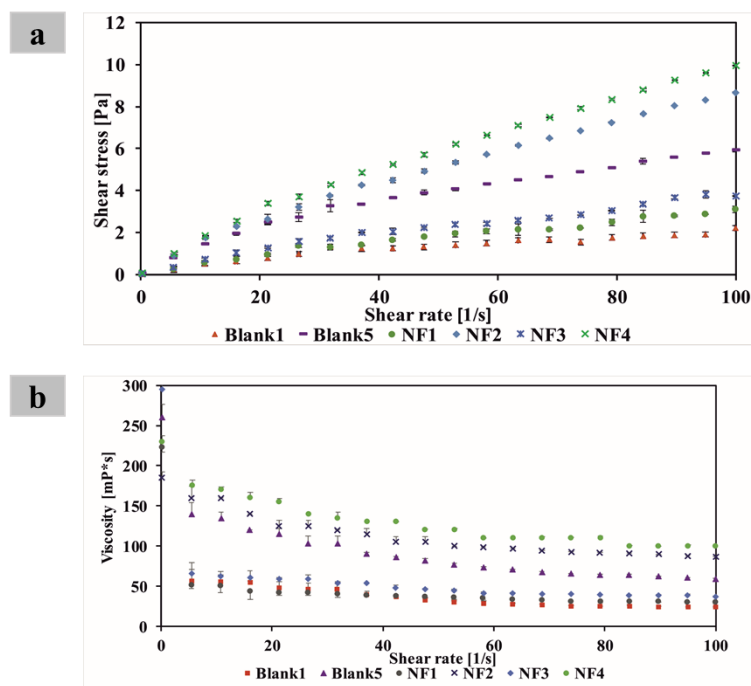


**Figure 17:** (a) The flow curves, and (b) the apparent viscosity of the NFs, blank1, and blank5 samples at 37 °C (Mean  $\pm$  SD, n=3) (Alshweiat et al., 2020).

The viscosity of the NFs was related to the used HA polymer concentration. 1 mg mL<sup>-1</sup> containing NFs (NF1 and NF3) showed lower values than 5 mg mL<sup>-1</sup> containing NFs (NF2 and NF4).

#### 6.6.4 Mucoadhesion of the nasal formulations

Samples with and without mucin were prepared to evaluate the role of LOR nanosuspension in mucoadhesion. The bioadhesive viscosity component, synergism parameter, was calculated from the average viscosity values. The systems of NFs and 5% mucin (NF-M) showed shear-thinning behaviours. The viscosity of the NF-M systems was higher than the corresponding NF (Fig.18) due to the polymer or mucin entanglement, and interactions between the polymer and mucin via the hydrogen bonds (Thirawong et al., 2008).

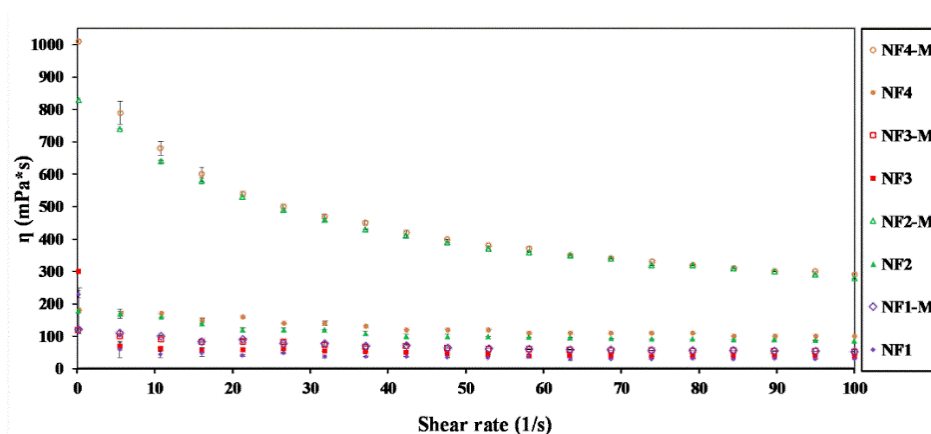


**Figure 18:** The observed viscosity of NFs and the combined NF with mucin (NF-M) at 37 °C (Mean  $\pm$  SD, n=3) (Alshweiat et al., 2020).

The synergism parameters ( $\eta_b$ ) of the NFs were compared to the F68 solution, corresponding REF samples, and the corresponding blanks (**Fig.19**). The blanks showed mucoadhesive properties, depending on the concentration of the sodium hyaluronate. The values of the bioadhesive viscosity were 0.60 and 46.5 mPa\*s for blank1 and blank5, respectively. The negative values  $\eta_b$  of REF1 and REF3 could be related to the insufficient amount of HA to interact with the mucin. The addition of the LNS to the blanks increased the mucoadhesivity of the formulations. This effect could be related to the interactions between the mucin and the dispersed nanosized LOR particles (Alshweiat et al., 2020). The synergism effect was directly linked to the HA and nanosized drug amount. These outcomes could be related to a higher interaction of the HA with the mucin and the nanocrystals. Accordingly, NF4 showed the highest synergism parameter. The  $\eta_b$  was 2.8-fold compared to blank5. The nanosized LOR was in the size of polymeric molecules of HA and mucin chains, hence better interaction among the components and higher mucoadhesivity could be obtained (Horvát et al., 2009).

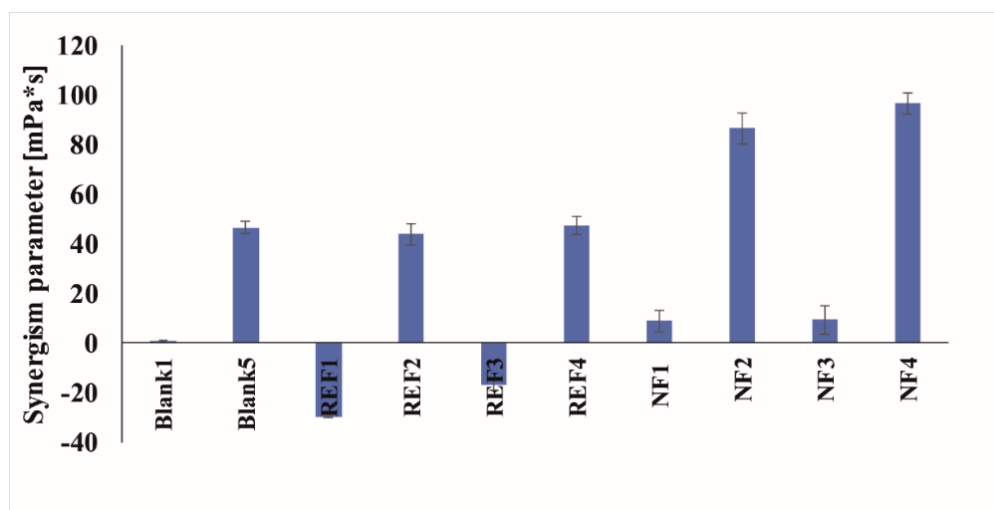


**Figure 19:** Calculated synergism parameters of blanks, REF, and NF samples at a shear rate of 100  $s^{-1}$  and 37 °C (Mean  $\pm$  SD, n=3) (Alshweiat et al., 2020).

NF4 that showed the highest mucoadhesive parameter. Therefore, it was selected for further studies.

#### 6.6.5 Effects of nanosizing on the dissolution, diffusion, and permeability

LOR shows a poor water solubility. Thus, many studies suggested the use of 900 mL of dissolution media or/and the addition of surfactant or co-solvent in the dissolution media to attain sink conditions (Damian et al., 2016; Song and Shin, 2009; Vlaia et al., 2017). In this study, the sink conditions were not applied due to factors related to the limited volume of the nasal delivery, lack of surfactant on the nasal cavity to be simulated by the dissolution media and to evaluate the effect of the particle size reduction on dissolution and diffusion without any interventions from the surfactant. Moreover, the NF4 solubility in the ANF was  $6.43 \pm 1.68 \mu g mL^{-1}$ . Thus, drug content was too high ( $0.14 mg \pm 1.68$ )

to fulfil the sink conditions. NF4 formulation was compared to REF4. NF4 showed an enhanced drug release compared to the reference sample (**Fig.20a**). Approximately 77% of the drug was released from NF4 within the first 15 min compared to 10% from the reference sample (Alshweiat et al., 2020). These differences in dissolution rates could be related to the nanosizing effects, as small particles produced a higher surface area than the microparticles. Thus, dissolution according to the Noyes-Whitney equation. Moreover, the nanosizing of LOR showed a 5.2-fold saturation solubility compared to the raw drug (Agrawal and Patel, 2011).

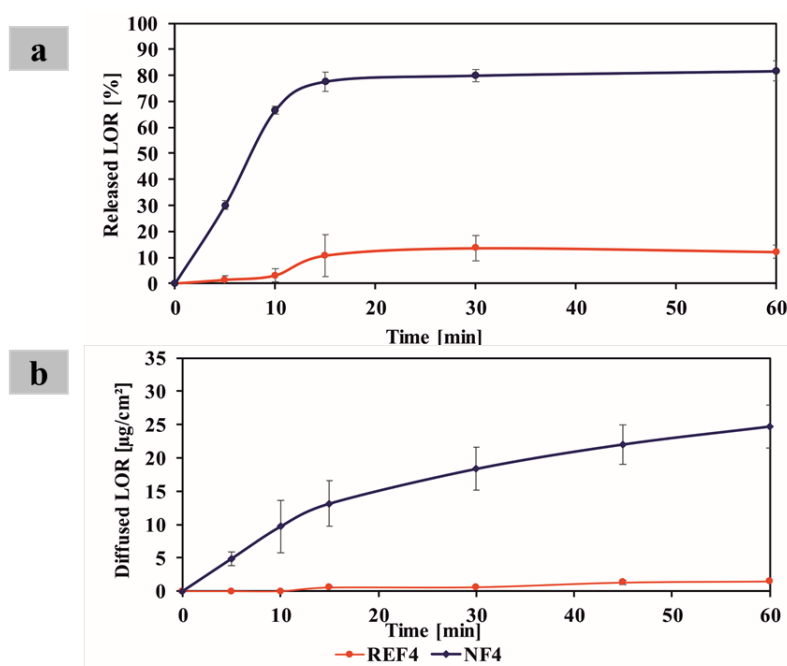


**Figure 20:** (a) Dissolution profile, and (b) In vitro permeability of NF4 and REF4 in ANF media at 37 °C (Mean  $\pm$  SD, n=3) (Alshweiat et al., 2020).

The diffusion indicates the permeation property. In this study, the membrane pore size was 100 nm, so LOR particles were unable to pass directly through the membrane. Consequently, the high surface area achieved by the nanosized particles was the main factor affecting the rate of passive diffusion.

The diffusion from NF4 was faster than REF4 due to the higher dissolution of the drug (**Fig.20b**). LOR diffused immediately from NF4 while it was diffused after 10 min from the REF4. The flux (J) represents the amount of LOR permeated through a 1 cm<sup>2</sup> of the membrane within 1h. NF4 that contained LOR nanoparticles showed a significantly increased J compared to REF4 ( $24.73 \pm 3.2$  and  $1.49 \pm 1.03 \mu\text{g cm}^{-2} \text{h}^{-1}$ , respectively). Therefore, HA containing-formulations allowed the penetration of LOR through the synthetic membrane. However, the flux of the nanosized-based formulation was higher than the reference sample containing the raw LOR. The permeability coefficient (Kp) of NF4 also showed a higher value than REF4. Kp values were 0.082 and 0.017 cm h<sup>-1</sup>, respectively. In

particular,  $11.15 \mu\text{g cm}^{-2}$  of the drug diffused in the first 15 min from the NF4 compared to  $0.56 \mu\text{g cm}^{-2}$  from the REF4. The higher diffusion could be connected to the higher surface area produced by the nanoparticles. The viscosity of the NF4 was at a low level that is suitable for nasal spray (Bartos et al., 2018).

### 6.6.6 *In vivo studies of the selected NF*

Nanosuspension based LOR was designed to improve the drug bioavailability by the intranasal route. Plasma levels after intranasal administration of the nanoparticle formulations were compared with those achieved with a reference sample that contained unprocessed suspended LOR (REF4). Moreover, nasal delivery was compared to the oral one. **Fig.21a** shows the mean LOR plasma concentration-time profiles after intranasal and oral delivery of NF4 and REF4.

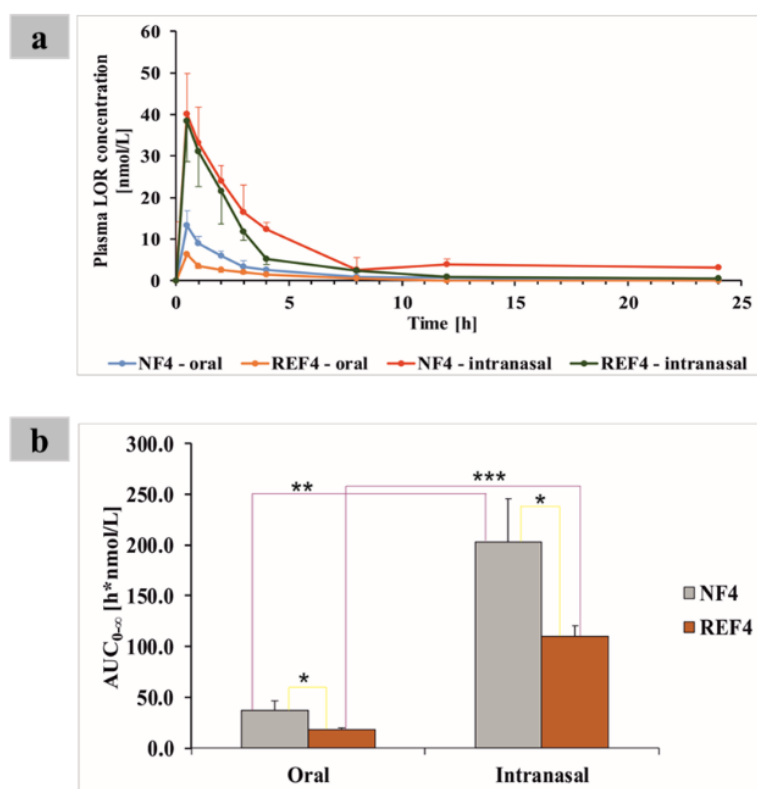


**Figure 21:** (a) Plasma concentration of LOR, and (b)  $AUC_{0-\infty}$  ( $\text{h nmol L}^{-1}$ ) of plasma after nasal and oral administration of NF4 and REF4 (\*,  $P=0.02$ ; \*\*,  $P=0.003$ , \*\*\*,  $P=0.0003$ ) (Mean  $\pm$  SD,  $n=4$ ) (Alshweiat et al., 2020).

LOR belongs to class II of the BCS. Thus it shows good permeability.  $C_{\text{max}}$  after the nasal administration is significantly higher than the oral administration ( $P \leq 0.01$ ). The  $C_{\text{max}}$  was 6.39, 13.29, 38.36, and 39.99 nM for REF4-oral, NF4-oral, REF4-nasal, and NF4-nasal, respectively (**Table 12**). The higher nasal concentrations could be related to higher absorption through the high vascularized

mucosa and bypassing the first-pass metabolism. Moreover, HA could act as a permeation enhancer for LOR through the nasal mucosa (Illum et al., 1994). Apart from this, the plasma concentration of REF4-oral, REF4-nasal, and NF4-oral decreased after 12 h. However, NF4-nasal plasma concentration was 3.85 nmol L<sup>-1</sup> and still detected to 24 h resulting in lower k<sub>e</sub> (Alshweiat et al., 2020).

**Table 12:** Pharmacokinetics parameters of LOR concentration in plasma after administration of NF4 and REF4 using oral and intranasal administration (Mean ± SD, n = 4) (Alshweiat et al., 2020).

	Oral		Intranasal	
	REF4	NF4	REF4	NF4
AUC <sub>0-∞</sub> [h nmol L <sup>-1</sup> ]	17.81±1.96	36.59±9.79	110.35±10.41	202.71±43.31
C <sub>max</sub> [nM]	6.39±2.21	13.29±5.72	38.36±9.78	39.99±14.18
k <sub>e</sub> [h <sup>-1</sup> ]	0.24±0.03	0.24±0.03	0.24±0.09	0.12±0.01

The mucoadhesive properties for the nanosuspension in NF4 were visible as mucoadhesion would improve the drug absorption and could prolong the intimate contact time of the particle on the nasal mucosa by adhering to the surface of the mucus layer. Therefore, NF4 showed extended and elevated plasma concentration of LOR than REF4, considering the exclusion of the mucoadhesive agent consequences as the samples contained the same concentrations of HA (Morimoto et al., 1991). **Fig.20b** shows the AUC<sub>0-∞</sub> values (**Table 12**) for LOR after oral and nasal administration. The relative bioavailability of the intranasal delivered NF4 was 1.84-fold compared to the REF4 and 5.54-fold compared to the oral delivered sample i.e. NF4-oral. These findings provide evidence that nasal administration enhanced the bioavailability of LOR. Moreover, the nanoparticles are practical to improve the delivery of LOR through the nasal route (Alshweiat et al., 2020).

#### 6.6.7 Stability of the selected NF

The selected NF4 sample showed no significant change in terms of physical appearance and viscosity. Furthermore, no particle precipitation occurred over 6 weeks for the samples kept at 4 °C. Though, the samples at 25 °C showed precipitation and phase separation. Thus, the storage of formulations would be more appropriate at refrigerated conditions to ensure the stability of the products. The drug content of NF4 samples after the storage period at 4 °C was 89.48 ± 3.60% (Alshweiat et al., 2020). The mean particle size of LOR nanosuspension in NF4 was 425.50 ± 14.50 nm. Moreover, the NF4 showed a PDI of 0.37 ± 0.05 and zeta potential of - 42.60 ± 7.98 mV. The stability of the formulation could be related to the high zeta potential and the viscosity of the formulation that kept the LOR nanoparticles separated and homogeneously distributed through the matrix (Müller and Jacobs, 2002). Moreover, the reduction of particle size after the storage period compared to the fresh samples could be related to the drug-stabilizer interactions (Md et al., 2018).

## 7. CONCLUSIONS

In this study, a novel combined-method of preparation was used to develop loratadine nasal formulation. The combination of nanosuspension and simple addition of a mucoadhesive agent presented a promising platform for the nasal delivery of loratadine.

- Quality by design (QbD) was implemented to define the QTPP of the final nasal formulation as well as the CQAs, CMPs, and CPPs for the preparation of the LOR nanosuspensions. The RA was used to evaluate the influential effects of the CMPs and CPPs according to the required CQAs.
- Process and material parameters were demonstrated to have a pronounced effect on controlling the properties of the final nanoparticles. The optimized process parameters were set to 30 min time, 4 °C temperature, and 50% power. At fixed amount of drug (100 mg), the nanosuspension showed a MPS range of 256, 253, and 265 nm when 0.2% F68, 0.2% of F68 and 0.2% of PVP-K25, and 0.2% of F68 and 0.4% of PVP-K25, respectively. The PDI was less than 0.25 using the previously mentioned stabilizers. The increase of the amount of the drug to 200 mg produced nanoparticles having a mean particle size of 312, polydispersity of 0.16, and zeta potential of -22.05 mV, thus homogenous and stable nanosuspension. On the other hand, using Soluplus<sup>®</sup> as a stabilizer showed great potential for the preparation of LOR nanosuspensions.
- Nanosuspension has been used as a pre-dispersion for the preparation of nasal formulation as a simple and straightforward strategy. The reduction of particle size presented enhanced properties of the nasal formulation rheology. Moreover, using a mucoadhesive agent is crucial to extend the contact time between the formulation and nasal mucosa. NF4 formulation that contained 2.5 mg mL<sup>-1</sup> of loratadine and 5 mg mL<sup>-1</sup> sodium hyaluronate showed enhanced rheological behaviours, where nanosizing had the main effect in the mucoadhesive properties. NF4 showed enhanced dissolution in an artificial nasal fluid. Besides, higher diffusion and permeability coefficient compared to the unprocessed loratadine.
- The *in vivo* studies showed the superiority of nasal delivery over the oral administration. Moreover, the nanoparticles showed higher AUC<sub>0-∞</sub> compared to the unprocessed LOR.
- Nanosuspension-based nasal formulation (NF4) showed no significant change in terms of physical appearance and viscosity. Furthermore, no particle precipitation occurred over 6 weeks for the samples kept at 4 °C. The NF4 showed a mean particle size of 425.5 ± 14.5, a polydispersity of 0.37 ± 0.05, and zeta potential of -42.6 ± 7.98. The stability of the formulation could be related to the high zeta potential and the viscosity of the formulation that kept the LOR nanoparticles separated and homogeneously distributed through the matrix.

## 8. NOVELTY AND PRACTICAL ASPECTS

The delivery of poorly water-soluble drugs requires the need of high bioavailability to achieve consistent therapeutic outcomes. In industry, the selection of the preparation and the delivery technology is not only driven by therapeutic targets, but also by technical aspects, such as simplicity, scalability, the time required for production, and production costs.

- The novelty and power of the presented work based on its ability to control and compromise different aspects from analyzing the literature to select the route of administration to produce LOR in a new dosage form that has not been studied and developed before.
- Applying QbD rationalized the selection of the methodologies and the route of the administration, significantly improved the targetability of getting optimized formulations in the voice of predefined quality and safety.
- Optimization of critical parameters to produce LOR's nanosuspension is considered a significant step toward extending the application of precipitation-assisted ultrasonication methods to formulate different APIs as nanosuspension-based dosage forms. By these findings, this method can compete with the top-down one in the development of potential products for the market.
- A novel formulation of LOR has been developed based on the nanosuspension of the drug. The prepared nasal formulation showed an improved bioavailability of LOR. Therefore, this formulation could offer new possibilities for the delivery of LOR as a new dosage form.
- A combination of the nanosuspension and the simple addition of a mucoadhesive agent could suggest a promising platform for the nasal delivery of various poorly water-soluble drugs.
- Developing nasal formulation with an improved bioavailability compared to oral delivery could boost the chances for the nasal formulations to enter the market.
- The applicability of nanosuspensions as a nasal delivery system to the systemic circulation is a new approach in pharmaceutical technology.



## REFERENCES

- Abboud, T.K., Zhu, J., Longhitano, M., Minehart, M., Mantilla, M., Chu, G., Kimball, S., Rodriguez, J., Terrasi, J., Gangolli, J., Nelson, D., Choi, Y., 1994. Efficacy and safety of butorphanol nasal spray for the relief of postepisiotomy pain. *Current Therapeutic Research* 55, 500–509. [https://doi.org/10.1016/S0011-393X\(05\)80180-8](https://doi.org/10.1016/S0011-393X(05)80180-8)
- Afridi, S.K., Giffin, N.J., Kaube, H., Goadsby, P.J., 2013. A randomized controlled trial of intranasal ketamine in migraine with prolonged aura. *Neurology* 80, 642–647. <https://doi.org/10.1212/WNL.0b013e3182824e66>
- Agrawal, Y., Patel, V., 2011. Nanosuspension: An approach to enhance solubility of drugs. *Journal of Advanced Pharmaceutical Technology & Research* 2, 81. <https://doi.org/10.4103/2231-4040.82950>
- Ahuja, N., Katare, O.P., Singh, B., 2007. Studies on dissolution enhancement and mathematical modeling of drug release of a poorly water-soluble drug using water-soluble carriers. *European Journal of Pharmaceutics and Biopharmaceutics* 65, 26–38. <https://doi.org/10.1016/j.ejpb.2006.07.007>
- Ali, J., Ali, M., Baboota, S., Sahani, J.K., Ramassamy, C., Dao, L., Bhavna, 2010. Potential of nanoparticulate drug delivery systems by intranasal administration. *Current pharmaceutical design* 16, 1644–1653. <https://doi.org/10.2174/138161210791164108>
- Alpar, H.O., Somavarapu, S., Atuah, K.N., Bramwell, V.W., 2005. Biodegradable mucoadhesive particulates for nasal and pulmonary antigen and DNA delivery. *Advanced Drug Delivery Reviews* 57, 411–430. <https://doi.org/10.1016/j.addr.2004.09.004>
- Alshweiat, A., Ambrus, R., Csoka, I., 2019a. Intranasal Nanoparticulate Systems as Alternative Route of Drug Delivery. *Current Medicinal Chemistry* 26, 6459–6492. <https://doi.org/10.2174/0929867326666190827151741>
- Alshweiat, A., Csóka, I., Tömösi, F., Janáky, T., Kovács, A., Gáspár, R., Sztojkov-Ivanov, A., Ducza, E., Márki, Á., Szabó-Révész, P., Ambrus, R., 2020. Nasal delivery of nanosuspension-based mucoadhesive formulation with improved bioavailability of loratadine: Preparation, characterization, and in vivo evaluation. *International Journal of Pharmaceutics*. 119166. <https://doi.org/10.1016/j.ijpharm.2020.119166>
- Alshweiat, A., Ambrus, R., Katona, G., Csoka, I., 2019b. QbD based control strategy of loratadine nanosuspensions and dry nanoparticles stabilized by Soluplus®. *Farmacia* 67, 729–735. <https://doi.org/10.31925/farmacia.2019.4.23>
- Alshweiat, A., Katona, G., Csóka, I., Ambrus, R., 2018. Design and characterization of loratadine nanosuspension prepared by ultrasonic-assisted precipitation. *European Journal of Pharmaceutical Sciences*. <https://doi.org/10.1016/j.ejps.2018.06.010>
- Ambrus, R., Alshweiat, A., Csóka, I., Ovari, G., Esmail, A., Radacsi, N., 2019. 3D-printed electrospinning setup for the preparation of loratadine nanofibers with enhanced physicochemical properties. *International Journal of Pharmaceutics* 118455. <https://doi.org/10.1016/j.ijpharm.2019.118455>
- Anantachaisilp, S., Smith, S.M., Treetong, A., Pratontep, S., Puttipipatkachorn, S., Ruktanonchai, U.R., 2010. Chemical and structural investigation of lipid nanoparticles: drug–lipid interaction and molecular distribution. *Nanotechnology* 21, 125102–125102. <https://doi.org/10.1088/0957-4484/21/12/125102>
- Anil, P., Pravin, C., Prashant, G., Amol, P., Prakash, B., 2016. Study the Effect of Surfactant Concentration and Ultrasonication Time on Aqueous Solubility, Particle Size and In-vitro Drug Diffusion of Ezogabine Nanosuspension by 3 2 Factorial Designs. *British Biomedical Bulletin* 4, 15–26.
- Baghel, S., Cathcart, H., O'Reilly, N.J., 2016. Polymeric Amorphous Solid Dispersions: A Review of Amorphization, Crystallization, Stabilization, Solid-State Characterization, and Aqueous Solubilization of Biopharmaceutical Classification System Class II Drugs. *Journal of Pharmaceutical Sciences*. <https://doi.org/10.1016/j.xphs.2015.10.008>
- Balakrishnan, A., Rege, B.D., Amidon, G.L., Polli, J.E., 2004. Surfactant-mediated dissolution: contributions of solubility enhancement and relatively low micelle diffusivity. *J Pharm Sci* 93, 2064–2075. <https://doi.org/10.1002/jps.20118>
- Bartos, C., Ambrus, R., Kovács, A., Gáspár, R., Sztojkov-Ivanov, A., Márki, Á., Janáky, T., Tömösi, F., Kecskeméti, G., Szabó-Révész, P., 2018. Investigation of absorption routes of meloxicam and its salt form from intranasal delivery systems. *Molecules* 23, 1–13. <https://doi.org/10.3390/molecules23040784>

- Bartos, C., Ambrus, R., Sipos, P., Budai-Szucs, M., Csányi, E., Gáspár, R., Márki, Á., Seres, A.B., Sztojkov-Ivanov, A., Horváth, T., Szabó-Révész, P., 2015a. Study of sodium hyaluronate-based intranasal formulations containing micro- or nanosized meloxicam particles. *International Journal of Pharmaceutics* 491, 198–207. <https://doi.org/10.1016/j.ijpharm.2015.06.046>
- Bartos, C., Kukovecz, Á., Ambrus, R., Farkas, G., Radacsi, N., Szabó-Révész, P., 2015b. Comparison of static and dynamic sonication as process intensification for particle size reduction using a factorial design. *Chemical Engineering and Processing: Process Intensification* 87, 26–34. <https://doi.org/10.1016/j.cep.2014.10.015>
- Bartzatt, R., 2017. Comparative Analysis of Antihistamines and Nonsteroidal Anti-inflammatory Drugs (NSAIDs): Properties, Structure and Prediction of New Potential Drugs. *Journal of Advances in Medical and Pharmaceutical Sciences* 12, 1–18. <https://doi.org/10.9734/JAMPS/2017/32695>
- Beirowski, J., Inghelbrecht, S., Arien, A., Gieseler, H., 2011. Freeze-Drying of Nanosuspensions, 1: Freezing Rate Versus Formulation Design as Critical Factors to Preserve the Original Particle Size Distribution. *Journal of Pharmaceutical Sciences* 100, 1958–1968. <https://doi.org/10.1002/jps.22425>
- Ben Zirar, S., Astier, A., Muchow, M., Gibaud, S., 2008. Comparison of nanosuspensions and hydroxypropyl- $\beta$ -cyclodextrin complex of melarsoprol: Pharmacokinetics and tissue distribution in mice. *European Journal of Pharmaceutics and Biopharmaceutics* 70, 649–656. <https://doi.org/10.1016/j.ejpb.2008.05.012>
- Bernocchi, B., Carpentier, R., Lantier, I., Ducournau, C., Dimier-Poisson, I., Betbeder, D., 2016. Mechanisms allowing protein delivery in nasal mucosa using NPL nanoparticles. *Journal of Controlled Release* 232, 42–50. <https://doi.org/10.1016/j.jconrel.2016.04.014>
- Berger, W.E., White, M.V., Rhinitis Study Group, 2003. Efficacy of azelastine nasal spray in patients with an unsatisfactory response to loratadine. *Ann. Allergy Asthma Immunol.* 91, 205–211. [https://doi.org/10.1016/S1081-1206\(10\)62179-5](https://doi.org/10.1016/S1081-1206(10)62179-5)
- Bhavna, Md, S., Ali, M., Ali, R., Bhatnagar, A., Baboota, S., Ali, J., 2014. Donepezil nanosuspension intended for nose to brain targeting: In vitro and in vivo safety evaluation. *International Journal of Biological Macromolecules* 67, 418–425. <https://doi.org/10.1016/j.ijbiomac.2014.03.022>
- Blaiss, M.S., Hammerby, E., Robinson, S., Kennedy-Martin, T., Buchs, S., 2018. The burden of allergic rhinitis and allergic rhinoconjunctivitis on adolescents: A literature review. *Ann. Allergy Asthma Immunol.* 121, 43-52.e3. <https://doi.org/10.1016/j.anai.2018.03.028>
- Brooking, J., Davis, S.S., Illum, L., 2001. Transport of nanoparticles across the rat nasal mucosa. *Journal of Drug Targeting* 9, 267–279. <https://doi.org/10.3109/10611860108997935>
- Buwalda, S.J., Vermonden, T., Hennink, W.E., 2017. Hydrogels for Therapeutic Delivery: Current Developments and Future Directions. *Biomacromolecules* 18, 316–330. <https://doi.org/10.1021/acs.biomac.6b01604>
- Chang, R., Fu, Q., Li, Y., Wang, M., Du, W., Chang, C., Zeng, A., 2017. Crystallization and relaxation dynamics of amorphous loratadine under different quench-cooling temperatures. *crystal engineering communication* 19, 335–345. <https://doi.org/10.1039/C6CE01645F>
- Chaturvedi, M., Kumar, M., Pathak, K., 2011. A review on mucoadhesive polymer used in nasal drug delivery system. *Journal of Advanced Pharmaceutical Technology & Research* 2, 215–222. <https://doi.org/10.4103/2231-4040.90876>
- Chaubal, M. V., Popescu, C., 2008. Conversion of nanosuspensions into dry powders by spray drying: A case study. *Pharmaceutical Research* 25, 2302–2308. <https://doi.org/10.1007/s11095-008-9625-0>
- Chavanpatil, M.D., Khair, A., Gerard, B., Bachmeier, C., Miller, D.W., Shekhar, M.P. V., Panyam, J., 2007. Surfactant–Polymer Nanoparticles Overcome P-Glycoprotein-Mediated Drug Efflux. *Molecular Pharmaceutics* 4, 730–738. <https://doi.org/10.1021/mp070024d>
- Chen, H., Khemtong, C., Yang, X., Chang, X., Gao, J., 2011. Nanonization strategies for poorly water-soluble drugs. *Drug Discovery Today* 16, 354–360. <https://doi.org/10.1016/j.drudis.2010.02.009>
- Chogale, M.M., Ghodake, V.N., Patravale, V.B., 2016. Performance Parameters and Characterizations of Nanocrystals: A Brief Review. *Pharmaceutics* 8, 26. <https://doi.org/10.3390/pharmaceutics8030026>
- Colombo, M., Orthmann, S., Bellini, M., Staufenbiel, S., Bodmeier, R., 2017. Influence of Drug Brittleness, Nanomilling Time, and Freeze-Drying on the Crystallinity of Poorly Water-Soluble Drugs and Its Implications for Solubility Enhancement. *An Official Journal of the American Association of Pharmaceutical Scientists* 18. <https://doi.org/10.1208/s12249-017-0722-4>

- Corrigan, M., Wilson, S.S., Hampton, J., 2015. Safety and efficacy of intranasally administered medications in the emergency department and prehospital settings. *American Journal of Health-System Pharmacy* 72, 1544–1554. <https://doi.org/10.2146/ajhp140630>
- Costa, P., & Lobo, J.M.S., 2001. Modelling and Comparison of Dissolution Profiles. *European Journal of Pharmaceutical Science* 13, 123–133. [https://doi.org/10.1016/S0928-0987\(01\)00095-1](https://doi.org/10.1016/S0928-0987(01)00095-1)
- Costantino, H.R., Illum, L., Brandt, G., Johnson, P.H., Quay, S.C., 2007. Intranasal delivery: Physicochemical and therapeutic aspects. *International Journal of Pharmaceutics* 337, 1–24. <https://doi.org/10.1016/j.ijpharm.2007.03.025>
- Csóka, I., Pallagi, E., Paál, T.L., 2018. Extension of quality-by-design concept to the early development phase of pharmaceutical R&D processes. *Drug Discovery Today*. <https://doi.org/10.1016/j.drudis.2018.03.012>
- Cui, F., Qian, F., Yin, C., 2006. Preparation and characterization of mucoadhesive polymer-coated nanoparticles. *International Journal of Pharmaceutics* 316, 154–161. <https://doi.org/10.1016/j.ijpharm.2006.02.031>
- Dagenais, C., Avdeef, A., Tsinman, O., Dudley, A., Beliveau, R., 2009. P-glycoprotein deficient mouse in situ blood-brain barrier permeability and its prediction using an in combo PAMPA model. *European Journal of Pharmaceutical Sciences* 38, 121–137. <https://doi.org/10.1016/j.ejps.2009.06.009>
- Davis, M.E., Brewster, M.E., 2004. Cyclodextrin-based pharmaceuticals: past, present and future. *Nature Reviews Drug Discovery* 3, 1023–1035. <https://doi.org/10.1038/nrd1576>
- Devarakonda, B., Hill, R.A., De Villiers, M.M., 2004. The effect of PAMAM dendrimer generation size and surface functional group on the aqueous solubility of nifedipine. *International Journal of Pharmaceutics* 284, 133–140. <https://doi.org/10.1016/j.ijpharm.2004.07.006>
- Djupesland, P.G., 2013. Nasal drug delivery devices: Characteristics and performance in a clinical perspective—a review. *Drug Delivery and Translational Research* 3, 42–62. <https://doi.org/10.1007/s13346-012-0108-9>
- Dodick, D., Brandes, J., Elkind, A., Mathew, N., Rodichok, L., 2005. Speed of onset, efficacy and tolerability of zolmitriptan nasal spray in the acute treatment of migraine: A randomised, double-blind, placebo-controlled study. *CNS Drugs* 19, 125–136. <https://doi.org/10.2165/00023210-200519020-00003>
- Dolenc, A., Kristl, J., Baumgartner, S., Planinšek, O., 2009. Advantages of celecoxib nanosuspension formulation and transformation into tablets. *International Journal of Pharmaceutics*. 376, 204–212. <https://doi.org/10.1016/j.ijpharm.2009.04.038>
- El-Nemr, A., Bhide, M., Khalifa, Y., Al-Mizyen, E., Gillott, C., Lower, A.M., Al-Shawaf, T., Grudzinskas, J.G., 2002. Clinical evaluation of three different gonadotrophin-releasing hormone analogues in an IVF programme: A prospective study. *European Journal of Obstetrics Gynecology and Reproductive Biology* 103, 140–145. [https://doi.org/10.1016/S0301-2115\(01\)00297-4](https://doi.org/10.1016/S0301-2115(01)00297-4)
- EMA, 2006. Reflection Paper on Nanotechnology-Based Medicinal Products for Human Use 4. Available from [https://etp-nanomedicine.eu/wp-content/uploads/2018/10/reflection-paper-nanotechnology-based-medicinal-products-human-use\\_en-1.pdf](https://etp-nanomedicine.eu/wp-content/uploads/2018/10/reflection-paper-nanotechnology-based-medicinal-products-human-use_en-1.pdf) (accessed 2.2.2020).
- England, R.J.A., Homer, J.J., Knight, L.C., Ell, S.R., 1999. Nasal pH measurement: A reliable and repeatable parameter. *Clinical Otolaryngology and Allied Sciences* 24, 67–68. <https://doi.org/10.1046/j.1365-2273.1999.00223.x>
- EMA, 2001. Available from <https://doi.org/10.1136/bmj.333.7574.873-a> (accessed 2.2.2020).
- Fahr, A., Liu, X., 2007. Drug delivery strategies for poorly water-soluble drugs. *Expert Opinion on Drug Delivery* 4, 403–416. <https://doi.org/10.1517/17425247.4.4.403>
- FDA, 1998. Guidance for Industry Metered Dose Inhaler (MDI) and Dry Powder Inhaler (DPI) Drug Products 1–65. Available from <https://www.fda.gov/media/70851/download> (accessed 2.2.2020).
- FDA, 2019a. FDA Organization [WWW Document]. FDA. Available from <http://www.fda.gov/about-fda/fda-organization> (accessed 1.7.20).
- FDA, 2019b. Considering Whether an FDA-Regulated Product Involves the Application of Nanotechnology. Available from <http://www.fda.gov/regulatory-information/search-fda-guidance-documents/considering-whether-fda-regulated-product-involves-application-nanotechnology> (accessed 2.2.20).
- Fenske, D.B., Chonn, A., Cullis, P.R., 2008. Liposomal nanomedicines: an emerging field. *Toxicologic pathology* 36, 21–9. <https://doi.org/10.1177/0192623307310960>

- Ganta, S., Paxton, J.W., Baguley, B.C., Garg, S., 2009. Formulation and pharmacokinetic evaluation of an asulacrine nanocrystalline suspension for intravenous delivery. *International Journal of Pharmaceutics* 367, 179–186. <https://doi.org/10.1016/j.ijpharm.2008.09.022>
- Gao, L., Liu, G., Ma, J., Wang, X., Zhou, L., Li, X., Wang, F., 2013. Application of Drug Nanocrystal Technologies on Oral Drug Delivery of Poorly Soluble Drugs. *Pharm Res* 30, 307–324. <https://doi.org/10.1007/s11095-012-0889-z>
- Gao, X., Tao, W., Lu, W., Zhang, Q., Zhang, Y., Jiang, X., Fu, S., 2006. Lectin-conjugated PEG-PLA nanoparticles: Preparation and brain delivery after intranasal administration. *Biomaterials* 27, 3482–3490. <https://doi.org/10.1016/j.biomaterials.2006.01.038>
- Gao, Y., Li, Z., Sun, M., Li, H., Guo, C., Cui, J., Li, A., Cao, F., Xi, Y., Lou, H., Zhai, G., 2010. Preparation, characterization, pharmacokinetics, and tissue distribution of curcumin nanosuspension with TPGS as stabilizer. *Drug development and industrial pharmacy* 36, 1225–1234. <https://doi.org/10.3109/03639041003695139>
- Gawel, M., Aschoff, J., May, A., Charlesworth, B.R., 2005. Zolmitriptan 5 mg nasal spray: Efficacy and onset of action in the acute treatment of migraine - Results from phase 1 of the REALIZE study. *Headache* 45, 7–16. <https://doi.org/10.1111/j.1526-4610.2005.05004.x>
- George, M., Ghosh, I., 2013. Identifying the correlation between drug/stabilizer properties and critical quality attributes (CQAs) of nanosuspension formulation prepared by wet media milling technology. *European Journal of Pharmaceutical Sciences* 48, 142–152. <https://doi.org/10.1016/j.ejps.2012.10.004>
- Ghadiri, M., M. Young, P., Traini, D., 2019. Strategies to Enhance Drug Absorption via Nasal and Pulmonary Routes. *Pharmaceutics* 11, 113. <https://doi.org/doi:10.3390/pharmaceutics11030113>
- Gieszinger, P., Csóka, I., Pallagi, E., Katona, G., Jójárt-Laczkovich, O., Szabó-Révész, P., Ambrus, R., 2017. Preliminary study of nanonized lamotrigine containing products for nasal powder formulation. *Drug Des Devel Ther* 11, 2453–2466. <https://doi.org/10.2147/DDDT.S138559>
- Gigliobianco, M.R., Casadidio, C., Censi, R., Di Martino, P., 2018. Nanocrystals of Poorly Soluble Drugs: Drug Bioavailability and Physicochemical Stability. *Pharmaceutics* 10, 34. <https://doi.org/10.3390/pharmaceutics10030134>
- Giroux, M., Hwang, P., Prasad, A., 2005. Controlled Particle Dispersion<sup>TM</sup>: Applying Vortical Flow to Optimize Nasal Drug Deposition 5, 5.
- Gizurarson, S., 2015. The effect of cilia and the mucociliary clearance on successful drug delivery. *Biological & Pharmaceutical Bulletin* 38, 497–506. <https://doi.org/10.1248/bpb.b14-00398>
- Gorain, B., Choudhury, H., Kundu, A., Sarkar, L., Karmakar, S., Jaisankar, P., Pal, T.K., 2014. Nanoemulsion strategy for olmesartan medoxomil improves oral absorption and extended antihypertensive activity in hypertensive rats. *Colloids Surf B Biointerfaces* 115, 286–294. <https://doi.org/10.1016/j.colsurfb.2013.12.016>
- Gratton, S.E.A., Ropp, P.A., Pohlhaus, P.D., Luft, J.C., Madden, V.J., Napier, M.E., DeSimone, J.M., 2008. The effect of particle design on cellular internalization pathways. *Proceedings of the National Academy of Sciences* 105, 11613–11618. <https://doi.org/10.1073/pnas.0801763105>
- Graudins, A., Meek, R., Egerton-Warburton, D., Oakley, E., Seith, R., 2015. The PICHFORK (Pain in Children Fentanyl or Ketamine) Trial: A randomized controlled trial comparing intranasal ketamine and fentanyl for the relief of moderate to severe pain in children with limb injuries. *Annals of Emergency Medicine* 65, 248-254.e1. <https://doi.org/10.1016/j.annemergmed.2014.09.024>
- Gursoy, R.N., Benita, S., 2004. Self-emulsifying drug delivery systems (SEDDS) for improved oral delivery of lipophilic drugs. *Biomedicine and Pharmacotherapy* 58, 173–182. <https://doi.org/10.1016/j.biopha.2004.02.001>
- Hao, J., Zhao, J., Zhang, S., Tong, T., Zhuang, Q., Jin, K., Chen, W., Tang, H., 2016. Fabrication of an ionic-sensitive in situ gel loaded with resveratrol nanosuspensions intended for direct nose-to-brain delivery. *Colloids and Surfaces B: Biointerfaces* 147, 376–386. <https://doi.org/10.1016/j.colsurfb.2016.08.011>
- Han, M.Z.I.K., Aus, D.R., Filipovi, P., 2004. Classification of Loratadine Based on the Biopharmaceutics Drug Classification Concept and Possible in Vitro – in Vivo Correlation. *Biol. Pharm. Bull* 27, 1630–1635. <https://doi.org/10.1248/bpb.27.1630>
- Hassan, E.E., Gallo, J.M., 1990. A Simple Rheological Method for the in Vitro Assessment of Mucin-Polymer Bioadhesive Bond Strength. *Pharmaceutical Research: An Official Journal of the American Association of Pharmaceutical Scientists* 7, 491–495. <https://doi.org/10.1023/A:1015812615635>

- He, C.X., He, Z.G., Gao, J.Q., 2010. Microemulsions as drug delivery systems to improve the solubility and the bioavailability of poorly water-soluble drugs. *Expert Opinion on Drug Delivery* 7, 445–460. <https://doi.org/10.1517/17425241003596337>
- Hecq, J., Deleers, M., Fanara, D., Vranckx, H., Amighi, K., 2005. Preparation and characterization of nanocrystals for solubility and dissolution rate enhancement of nifedipine. *International Journal of Pharmaceutics* 299, 167–177. <https://doi.org/10.1016/j.ijpharm.2005.05.014>
- Hellings, P.W., Dobbels, F., Denhaerynck, K., Piessens, M., Ceuppens, J.L., De Geest, S., 2012. Explorative study on patient's perceived knowledge level, expectations, preferences and fear of side effects for treatment for allergic rhinitis. *Clinical and Translational Allergy* 2, 9–9. <https://doi.org/10.1186/2045-7022-2-9>
- Hoekman, J.D., Ho, R.J.Y., 2011. Enhanced Analgesic Responses After Preferential Delivery of Morphine and Fentanyl to the Olfactory Epithelium in Rats. *Anesthesia & Analgesia* 113, 641–651. <https://doi.org/10.1213/ANE.0b013e3182239b8c>
- Homayouni, A., Sadeghi, F., Varshosaz, J., Afrasiabi Garekani, H., Nokhodchi, A., 2014. Promising dissolution enhancement effect of soluplus on crystallized celecoxib obtained through antisolvent precipitation and high pressure homogenization techniques. *Colloids Surf B Biointerfaces* 122, 591–600. <https://doi.org/10.1016/j.colsurfb.2014.07.037>
- Horak, F., Zieglmayer, U.P., 2009. Azelastine nasal spray for the treatment of allergic and nonallergic rhinitis. *Expert Rev Clin Immunol* 5, 659–669. <https://doi.org/10.1586/eci.09.38>
- Horvát, S., Fehér, A., Wolburg, H., Sipos, P., Veszeka, S., Tóth, A., Kis, L., Kurunczi, A., Balogh, G., Kürti, L., Eros, I., Szabó-Révész, P., Deli, M.A., 2009. Sodium hyaluronate as a mucoadhesive component in nasal formulation enhances delivery of molecules to brain tissue. *European Journal of Pharmaceutics and Biopharmaceutics*. <https://doi.org/10.1016/j.ejpb.2008.10.009>
- Illum, L., 2012. Nasal drug delivery — Recent developments and future prospects. *Journal of Controlled Release, Drug Delivery Research in Europe* 161, 254–263. <https://doi.org/10.1016/j.jconrel.2012.01.024>
- Illum, L., Farraj, N.F., Fisher, A.N., Gill, I., Miglietta, M., Benedetti, L.M., 1994. Hyaluronic acid ester microspheres as a nasal delivery system for insulin. *Journal of Controlled Release* 29, 133–141. [https://doi.org/10.1016/0168-3659\(94\)90129-5](https://doi.org/10.1016/0168-3659(94)90129-5)
- Issa, M.M., Köping-Höggård, M., Artursson, P., 2005. Chitosan and the mucosal delivery of biotechnology drugs. *Drug Discovery Today: Technologies* 2, 1–6. <https://doi.org/10.1016/j.ddtec.2005.05.008>
- Jinno, J., Kamada, N., Miyake, M., Yamada, K., Mukai, T., Odomi, M., Toguchi, H., Liversidge, G.G., Higaki, K., Kimura, T., 2006. Effect of particle size reduction on dissolution and oral absorption of a poorly water-soluble drug, cilostazol, in beagle dogs. *Journal of Controlled Release* 111, 56–64. <https://doi.org/10.1016/j.jconrel.2005.11.013>
- Junghanns, J.U.A.H., Müller, R.H., 2008. Nanocrystal technology, drug delivery and clinical applications. *International Journal of Nanomedicine* 3, 295–309. <https://doi.org/10.2147/IJN.S595>
- Kaliner, M.A., Berger, W.E., Ratner, P.H., Siegel, C.J., 2011. The efficacy of intranasal antihistamines in the treatment of allergic rhinitis. *Annals of Allergy, Asthma & Immunology* 106, S6–S11. <https://doi.org/10.1016/j.anai.2010.08.010>
- Kapoor, M., Winter, T., Lis, L., Georg, G.I., Siegel, R.A., 2014. Rapid delivery of diazepam from supersaturated solutions prepared using prodrug/enzyme mixtures: toward intranasal treatment of seizure emergencies. *The Official Journal of the American Association of Pharmaceutical Scientists* 16, 577–85. <https://doi.org/10.1208/s12248-014-9596-5>
- Kansara, H., Panola, R., Mishra, A., 2015. Techniques used to Enhance Bioavailability of BCS Class II Drugs: A Review. *International Journal of Drug Development and Research* 7, 82–93.
- Kato, Y., Hosokawa, T., Hayakawa, E., Ito, K., 1992. Influence of liposomes on tryptic digestion of insulin. *Biological & Pharmaceutical Bulletin* 16, 457–461. <https://doi.org/10.1248/cpb.37.3229>
- Khan, K.A., 1975. The concept of dissolution efficiency. *Journal of Pharmacy and Pharmacology* 27, 48–49. <https://doi.org/10.1111/j.2042-7158.1975.tb09378.x>
- Kim, S., Lee, J., 2010. Effective polymeric dispersants for vacuum, convection and freeze drying of drug nanosuspensions. *International Journal of Pharmaceutics* 397, 218–224. <https://doi.org/10.1016/j.ijpharm.2010.07.010>
- Kipp, J., Wong, J., Doty, M., Rebbeck, C., 2003. Microprecipitation method for preparing submicron suspensions. US Patent 6607784.

- Kola Srinivas, N.S., Verma, R., Pai Kulyadi, G., Kumar, L., 2016. A quality by design approach on polymeric nanocarrier delivery of gefitinib: formulation, in vitro, and in vivo characterization. *International Journal of Nanomedicine* 12, 15–28. <https://doi.org/10.2147/IJN.S122729>
- Kraft, W.K., Steiger, B., Beussink, D., Quiring, J.N., Fitzgerald, N., Greenberg, H.E., Waldman, S. a, 2004. The pharmacokinetics of nebulized nanocrystal budesonide suspension in healthy volunteers. *Journal of clinical pharmacology* 44, 67–72. <https://doi.org/10.1177/0091270003261490>
- Krause, W.E., Bellomo, E.G., Colby, R.H., 2001. Rheology of sodium hyaluronate under physiological conditions. *Biomacromolecules* 2, 65–69. <https://doi.org/10.1021/bm0055798>
- Kumar, S., Burgess, D.J., 2014. Wet milling induced physical and chemical instabilities of naproxen nanocrystalline suspensions. *International Journal of Pharmaceutics* 466, 23–232. <https://doi.org/10.1016/j.ijpharm.2014.03.021>
- Kürti, L., Gáspár, R., Márki, Á., Kápolna, E., Bocsik, A., Veszelka, S., Bartos, C., Ambrus, R., Vastag, M., Deli, M.A., Szabó-Révész, P., 2013. In vitro and in vivo characterization of meloxicam nanoparticles designed for nasal administration. *European Journal of Pharmaceutical Sciences* 50, 86–92. <https://doi.org/10.1016/j.ejps.2013.03.012>
- Kushwaha, S.K.S., Keshari, R.K., Rai, A.K., 2011. Advances in nasal trans-mucosal drug delivery. *Journal of Applied Pharmaceutical Science* 1, 21–28.
- LaForce, C.F., Corren, J., Wheeler, W.J., Berger, W.E., Rhinitis Study Group, 2004. Efficacy of azelastine nasal spray in seasonal allergic rhinitis patients who remain symptomatic after treatment with fexofenadine. *Ann. Allergy Asthma Immunol.* 93, 154–159. [https://doi.org/10.1016/S1081-1206\(10\)61468-8](https://doi.org/10.1016/S1081-1206(10)61468-8)
- Leuner, C., Dressman, J., 2000. Improving drug solubility for oral delivery using solid dispersions. *European journal of pharmaceutics and biopharmaceutics: official journal of Arbeitsgemeinschaft für Pharmazeutische Verfahrenstechnik e.V* 50, 47–60. [https://doi.org/10.1016/S0939-6411\(00\)00076-X](https://doi.org/10.1016/S0939-6411(00)00076-X)
- Li, B. V, Jin, F., Lee, S.L., Bai, T., Chowdhury, B., Caramenico, H.T., Conner, D.P., 2013. Bioequivalence for Locally Acting Nasal Spray and Nasal Aerosol Products: Standard Development and Generic Approval. an official journal of the American Association of Pharmaceutical Scientists 15, 875–83. <https://doi.org/10.1208/s12248-013-9494-2>
- Lindfors, L., Skantze, P., Skantze, U., Westergren, J., Olsson, U., 2007. Amorphous drug nanosuspensions. 3. Particle dissolution and crystal growth. *Langmuir* 23, 9866–9874. <https://doi.org/10.1021/la700811b>
- Lipinski, C., 2002. Poor aqueous solubility - An industry wide problem in drug discovery. *American Pharmaceutical Review* 5, 82–85.
- Lipinski, C.A.; L., F.; Dominy, B.W.; Feeney, P.J., 1997. Experimental and computational approaches to estimate solubility and permeability in drug discovery and development setting. *Advanced Drug Delivery Reviews* 23, 3–25. <https://doi.org/10.1016/j.addr.2012.09.019>
- Liu, F., Park, J.Y., Zhang, Y., Conwell, C., Liu, Y., Bathula, S.R., Huang, L., 2010. Targeted Cancer Therapy With Novel High Drug-Loading Nanocrystals. *Journal of Pharmaceutical Sciences* 99, 3542–3551. <https://doi.org/10.1002/jps.22112>
- Lockman, P.R., Koziara, J.M., Mumper, R.J., Allen, D.D., 2004. Nanoparticle Surface Charges Alter Blood–Brain Barrier Integrity and Permeability. *Journal of Drug Targeting* 12, 635–641. <https://doi.org/10.1080/10611860400015936>
- Loftsson, T., Brewster, M.E., Másson, M., 2004. Role of cyclodextrins in improving oral drug delivery. *American Journal of Drug Delivery* 2, 261–275. <https://doi.org/10.2165/00137696-200402040-00006>
- Lonare, A.A., Patel, S.R., 2013. Antisolvent Crystallization of Poorly Water Soluble Drugs. *International Journal of Chemical Engineering and Applications* 4, 337–341. <https://doi.org/10.7763/IJCEA.2013.V4.321>
- McEwen, J., 2000. Clinical pharmacology of piroxicam-[beta]-cyclodextrin. Implications for innovative patient care. *clinical drug investigation* 19, 27–31.
- Md, S., Kit, B.C.M., Jagdish, S., David, D.J.P., Pandey, M., Chatterjee, L.A., 2018. Development and in vitro evaluation of a zerumbone loaded nanosuspension drug delivery system. *Crystals* 8, 1–13. <https://doi.org/10.3390/cryst8070286>
- Meltzer, E., Weiler, J., Dockhorn, R., Widlitz, M., Freitag, J., 1994. Azelastine nasal spray in the management of seasonal allergic rhinitis. *Ann Allergy* 72, 354–359.
- Menzel, C., Jelkmann, M., Laffleur, F., Bernkop-Schnürch, A., 2017. Nasal drug delivery: Design of a novel mucoadhesive and in situ gelling polymer. *International Journal of Pharmaceutics* 517, 196–202. <https://doi.org/10.1016/j.ijpharm.2016.11.055>

- Meredith, M.E., Salameh, T.S., Banks, W.A., 2015. Intranasal Delivery of Proteins and Peptides in the Treatment of Neurodegenerative Diseases. *An Official Journal of the American Association of Pharmaceutical Scientists* 17, 780–787. <https://doi.org/10.1208/s12248-015-9719-7>
- Milhem, O.M., Myles, C., McKeown, N.B., Attwood, D., D’Emanuele, A., 2000. Polyamidoamine Starburst® dendrimers as solubility enhancers. *International Journal of Pharmaceutics* 197, 239–241. [https://doi.org/10.1016/S0378-5173\(99\)00463-9](https://doi.org/10.1016/S0378-5173(99)00463-9)
- Mirza, A.Z., Siddiqui, F.A., 2014. Nanomedicine and drug delivery: a mini review. *International Nano Letters* 4, 94. <https://doi.org/10.1007/s40089-014-0094-7>
- Moore, K., Haroz, R., 2017. When Hydromorphone Is Not Working, Try Loratadine: An Emergency Department Case of Loratadine as Abortive Therapy for Severe Pegfilgrastim-Induced Bone Pain. *Journal of Emergency Medicine* 52, e29–e31. <https://doi.org/10.1016/j.jemermed.2016.08.018>
- Morimoto, K., Yamaguchi, H., Iwakura, Y., Morisaka, K., Ohashi, Y., Nakai, Y., 1991. Effects of viscous hyaluronate-sodium solutions on the nasal absorption of vasopressin and an analogue. *Pharmaceutical Research* 8, 471–474. <https://doi.org/10.1023/a:1015894910416>
- Möschwitzer, J., Achleitner, G., Pomper, H., Müller, R.H., 2004. Development of an intravenously injectable chemically stable aqueous omeprazole formulation using nanosuspension technology. *European Journal of Pharmaceutics and Biopharmaceutics* 58, 615–619. <https://doi.org/10.1016/j.ejpb.2004.03.022>
- Möschwitzer, J., Andreas, L., 2006. Method for carefully producing ultrafine particle suspensions and ultrafine particles and use thereof. CA2604770.
- Möschwitzer, J., Müller, R.H., 2006. New method for the effective production of ultrafine drug nanocrystals. *Journal of Nanoscience and Nanotechnology* 6, 3145–3153. <https://doi.org/10.1166/jnn.2006.480>
- Müller, R., Becker, R., Kruss, B., Peters, K., 1999. Pharmaceutical nanosuspensions for medicament administration as systems with increased saturation solubility and rate of solution. US Patent 5,858,410. [https://doi.org/10.1074/JBC.274.42.30033.\(51\)](https://doi.org/10.1074/JBC.274.42.30033.(51))
- Müller, R.H., Jacobs, C., Kayser, O., 2001. Nanosuspensions as particulate drug formulations in therapy. *Advanced Drug Delivery Reviews* 47, 3–19. [https://doi.org/10.1016/S0169-409X\(00\)00118-6](https://doi.org/10.1016/S0169-409X(00)00118-6)
- Muller, R.H., Keck, C.M., 2004. Challenges and solutions for the delivery of biotech drugs - A review of drug nanocrystal technology and lipid nanoparticles. *Journal of Biotechnology* 113, 151–170. <https://doi.org/10.1016/j.jbiotec.2004.06.007>
- Müller, R.H., Möschwitzer, J.P., 2005. Method and apparatus for the production of ultrafine particles and coating of such particles. DE 10 2005 053 862.2 Application.
- Müller, R.H., Peters, K., 1998. Nanosuspensions for the formulation of poorly soluble drugs. I. Preparation by a size-reduction technique. *International Journal of Pharmaceutics* 160, 229–237. [https://doi.org/10.1016/S0378-5173\(97\)00311-6](https://doi.org/10.1016/S0378-5173(97)00311-6)
- Munjaj, S., Gautam, A., Offman, E., Brand-Schieber, E., Allenby, K., Fisher, D.M., 2016. A Randomized Trial Comparing the Pharmacokinetics, Safety, and Tolerability of DFN-02, an Intranasal Sumatriptan Spray Containing a Permeation Enhancer, With Intranasal and Subcutaneous Sumatriptan in Healthy Adults. *Headache: The Journal of Head and Face Pain* 56, 1455–1465. <https://doi.org/10.1111/head.12905>
- Murdande, S.B., Shah, D.A., Dave, R.H., 2015. Impact of Nanosizing on Solubility and Dissolution Rate of Poorly Soluble Pharmaceutical. *Journal of Pharmaceutical Sciences* 104, 2094–2102. <https://doi.org/10.1002/jps.24426>
- Nagy, Z.K., Balogh, A., Vajna, B., Farkas, A., Patyi, G., Kramarics, Á., Marosi, G., 2012. Comparison of Electrospun and Extruded Soluplus®-Based Solid Dosage Forms of Improved Dissolution. *Journal of Pharmaceutical Sciences* 101, 322–332. <https://doi.org/10.1002/jps.22731>
- Nave, R., Schmitt, H., Popper, L., 2013. Faster absorption and higher systemic bioavailability of intranasal fentanyl spray compared to oral transmucosal fentanyl citrate in healthy subjects. *Drug delivery* 7544, 216–223. <https://doi.org/10.3109/10717544.2012.762435>
- Nekkanti, V., Pillai, R., Venkateshwarlu, V., Harisudhan, T., 2009. Development and characterization of solid oral dosage form incorporating candesartan nanoparticles. *Pharmaceutical development and technology* 14, 290–298. <https://doi.org/10.1080/10837450802585278>
- Neves, J. das, Sarmiento, B., 2014. *Mucosal Delivery of Biopharmaceuticals: Biology, Challenges and Strategies*. Springer Science & Business Media.
- Noyes, A.A., Whitney, W.R., 1897. The rate of solution of solid substances in their own solutions. *Journal of the American Chemical Society* 19, 930–934. <https://doi.org/10.1021/ja02086a003>

- Nozaki, A., Ando, T., Akazawa, S., Satoh, T., Sagara, I., Horie, I., Imaizumi, M., Usa, T., Yanagisawa, R.T., Kawakami, A., 2016. Quality of life in the patients with central diabetes insipidus assessed by Nagasaki Diabetes Insipidus Questionnaire. *Endocrine* 51, 140–147. <https://doi.org/10.1007/s12020-015-0637-3>
- Obeidat, W.M., Sallam, A.-S.A., 2014. Evaluation of Tadalafil Nanosuspensions and Their PEG Solid Dispersion Matrices for Enhancing Its Dissolution Properties. *An Official Journal of the American Association of Pharmaceutical Scientists* 15, 364–374. <https://doi.org/10.1208/s12249-013-0070-y>
- Ohwaki, T., Ando, H., Kakimoto, F., Uesugi, K., Watanabe, S., Miyake, Y., Kayano, M., 1987. Effects of dose, pH, and osmolarity on nasal absorption of secretin in rats. II: Histological aspects of the nasal mucosa in relation to the absorption variation due to the effects of pH and osmolarity. *Journal of Pharmaceutical Sciences* 76, 695–698. <https://doi.org/10.1002/jps.2600760905>
- Pallagi, E., Ambrus, R., Szabó-Révész, P., Csóka, I., 2015. Adaptation of the quality by design concept in early pharmaceutical development of an intranasal nanosized formulation. *International Journal of Pharmaceutics* 491, 384–392. <https://doi.org/10.1016/j.ijpharm.2015.06.018>
- Patel, D.A., Patel, M.R., Patel, K.R., Patel, N.M., 2012. Buccal mucosa as a route for systemic drug delivery: A review. *International Journal of Drug Development and Research* 4, 99–116. <https://doi.org/10.1016/j.jconrel.2010.11.003>
- Patravale, V.B., Date, A. a, Kulkarni, R.M., 2004. Nanosuspensions: a promising drug delivery strategy. *The Journal of pharmacy and pharmacology* 56, 827–840. <https://doi.org/10.1211/0022357023691>
- Patton, J.S., 2004. The Lungs as a Portal of Entry for Systemic Drug Delivery. *Proceedings of the American Thoracic Society* 1, 338–344. <https://doi.org/10.1513/pats.200409-049TA>
- Pavis, H., Wilcock, A., Edgecombe, J., Carr, D., Manderson, C., Church, A., Fisher, A., 2002. Pilot study of nasal morphine-chitosan for the relief of breakthrough pain in patients with cancer. *Journal of Pain and Symptom Management* 24, 598–602. [https://doi.org/10.1016/S0885-3924\(02\)00522-5](https://doi.org/10.1016/S0885-3924(02)00522-5)
- Pawar, D., Goyal, A.K., Mangal, S., Mishra, N., Vaidya, B., Tiwari, S., Jain, A.K., Vyas, S.P., 2010. Evaluation of Mucoadhesive PLGA Microparticles for Nasal Immunization. *An Official Journal of the American Association of Pharmaceutical Scientists* 12, 130–137. <https://doi.org/10.1208/s12248-009-9169-1>
- Peterson, B., Weyers, M., Steenekamp, J.H., Steyn, J.D., Gouws, C., Hamman, J.H., 2019. Drug Bioavailability Enhancing Agents of Natural Origin (Bioenhancers) that Modulate Drug Membrane Permeation and Pre-Systemic Metabolism. *Pharmaceutics* 11. <https://doi.org/10.3390/pharmaceutics11010033>
- Pinna, N., 2005. X-Ray Diffraction from Nanocrystals, in: Stribeck, N., Smarsly, B. (Eds.), *Scattering Methods and the Properties of Polymer Materials*, Progress in Colloid and Polymer Science. Springer, Berlin, Heidelberg, pp. 29–32. <https://doi.org/10.1007/b107348>
- Pistolis, G., Malliaris, A., Tsiourvas, D., Paleos, C.M., 1999. Poly ( propyleneimine ) Dendrimers as pH-Sensitive Controlled-Release Systems. *A European Journal* 5, 1440–1444.
- Ponchel, G., Montisci, M.-J., Dembri, A., Durrer, C., Duchêne, D., 1997. Mucoadhesion of colloidal particulate systems in the gastro-intestinal tract. *European Journal of Pharmaceutics and Biopharmaceutics* 44, 25–31. [https://doi.org/10.1016/S0939-6411\(97\)00098-2](https://doi.org/10.1016/S0939-6411(97)00098-2)
- Popovi, G., Ćakar, M., Agbaba, D., 2009. Acid – base equilibria and solubility of loratadine and desloratadine in water and micellar media  $\checkmark$ . *Journal of Pharmaceutical and Biomedical Analysis* 49, 42–47. <https://doi.org/10.1016/j.jpba.2008.09.043>
- Prabhu, V., Uzzaman, S., Grace, V.M.B., Guruvayoorappan, C., 2011. Nanoparticles in Drug Delivery and Cancer Therapy: The Giant Rats Tail. *Journal of Cancer Therapy* 02, 325–334. <https://doi.org/10.4236/jct.2011.23045>
- Pu, X., Sun, J., Wang, Yan, Wang, Yongjun, Liu, X., Zhang, P., Tang, X., Pan, W., Han, J., He, Z., 2009. Development of a chemically stable 10-hydroxycamptothecin nanosuspensions. *International Journal of Pharmaceutics* 379, 167–173. <https://doi.org/10.1016/j.ijpharm.2009.05.062>
- Rahman, Md.A., Hussain, A., Hussain, Md.S., Mirza, Mohd.A., Iqbal, Z., 2013. Role of excipients in successful development of self-emulsifying/microemulsifying drug delivery system (SEDDS/SMEDDS). *Drug Development and Industrial Pharmacy* 39, 1–19. <https://doi.org/10.3109/03639045.2012.660949>
- Randall, K.L., Hawkins, C.A., 2018. Antihistamines and allergy. *Aust Prescr* 41, 41–45. <https://doi.org/10.18773/austprescr.2018.013>
- Rangel-Yagui, C. de O., Pessoa, A., Tavares, L.C., 2005. Micellar solubilization of drugs. *Journal of Pharmacy and Pharmaceutical Sciences* 8, 147–163.



- Rassu, G., Ferraro, L., Pavan, B., Giunchedi, P., Gavini, E., Dalpiaz, A., 2018. The Role of Combined Penetration Enhancers in Nasal Microspheres on In Vivo Drug Bioavailability. *Pharmaceutics* 10. <https://doi.org/10.3390/pharmaceutics10040206>
- Rogers, T.L., Gillespie, I.B., Hitt, J.E., Fransen, K.L., Crowl, C.A., Tucker, C.J., Kupperblatt, G.B., Becker, J.N., Wilson, D.L., Todd, C., Broomall, C.F., Evans, J.C., Elder, E.J., 2004. Development and characterization of a scalable controlled precipitation process to enhance the dissolution of poorly water-soluble drugs. *Pharmaceutical Research* 21, 2048–2057. <https://doi.org/10.1023/B:PHAM.0000048196.61887.e5>
- Rolf, P., 2006. Nanocrystals for use in topical cosmetic formulations and method of production thereof. US86623306P.
- Rosenwasser, L.J., 2002. Treatment of allergic rhinitis. *The American Journal of Medicine* 113, 17–24. [https://doi.org/10.1016/S0002-9343\(02\)01433-X](https://doi.org/10.1016/S0002-9343(02)01433-X)
- Ruan, L.P., Yu, B.Y., Fu, G.M., Zhu, D.N., 2005. Improving the solubility of ampelopsin by solid dispersions and inclusion complexes. *Journal of Pharmaceutical and Biomedical Analysis* 38, 457–464. <https://doi.org/10.1016/j.jpba.2005.01.030>
- Saindane, N.S., Pagar, K.P., Vavia, P.R., 2013. Nanosuspension based in situ gelling nasal spray of carvedilol: development, in vitro and in vivo characterization. *Official Journal of the American Association of Pharmaceutical Scientists* 14, 189–199. <https://doi.org/10.1208/s12249-012-9896-y>
- Salazar, J., Müller, R.H., Möschwitzer, J.P., 2013. Performance Comparison of two Novel Combinative Particle-Size-Reduction Technologies. *Journal of Pharmaceutical Sciences*. <https://doi.org/10.1002/jps.23475>
- Sangshetti, J.N., Deshpande, M., Zaheer, Z., Shinde, D.B., Arote, R., 2014. Quality by design approach: Regulatory need. *Arabian Journal of Chemistry*. <https://doi.org/10.1016/j.arabjc.2014.01.025>
- Satturwar, P., Eddine, M.N., Ravenelle, F., Leroux, J.-C., 2007. pH-responsive polymeric micelles of poly(ethylene glycol)-b-poly(alkyl(meth)acrylate-co-methacrylic acid): Influence of the copolymer composition on self-assembling properties and release of candesartan cilexetil. *European Journal of Pharmaceutics and Biopharmaceutics, Drug delivery: a Canadian perspective* 65, 379–387. <https://doi.org/10.1016/j.ejpb.2006.09.012>
- Serajuddin, A.T.M., 2007. Salt formation to improve drug solubility. *Advanced Drug Delivery Reviews* 59, 603–616. <https://doi.org/10.1016/j.addr.2007.05.010>
- Shah, L., Yadav, S., Amiji, M., 2013. Nanotechnology for CNS delivery of bio-therapeutic agents. *Drug delivery and translational research* 3, 336–51. <https://doi.org/10.1007/s13346-013-0133-3>
- Sharma, S., Singh, J., Verma, A., Teja, B.V., Shukla, R.P., Singh, S.K., Sharma, V., Konwar, R., Mishra, P.R., 2016. Hyaluronic acid anchored paclitaxel nanocrystals improves chemotherapeutic efficacy and inhibits lung metastasis in tumor-bearing rat model. *Royal Society of Chemistry Advances* 6, 73083–73095. <https://doi.org/10.1039/C6RA11260A>
- Shen, H., Shi, S., Zhang, Z., Gong, T., Sun, X., 2015. Coating Solid Lipid Nanoparticles with Hyaluronic Acid Enhances Antitumor Activity against Melanoma Stem-like Cells. *Theranostics* 5, 755–771. <https://doi.org/10.7150/thno.10804>
- Shin, S., Song, I., Um, S., 2015. Role of Physicochemical Properties in Nanoparticle Toxicity. *Nanomaterials* 5, 1351–1365. <https://doi.org/10.3390/nano5031351>
- Shrestha, H., Bala, R., Arora, S., 2014. Lipid-Based Drug Delivery Systems. *Journal of pharmaceutics* 2014, 801820. <https://doi.org/10.1155/2014/801820>
- Shrewsbury, S.B., Bosco, A.P., Uster, P.S., 2009. Pharmacokinetics of a novel submicron budesonide dispersion for nebulized delivery in asthma. *International Journal of Pharmaceutics* 365, 12–17. <https://doi.org/10.1016/j.ijpharm.2008.08.012>
- Sigfridsson, K., Forssén, S., Holländer, P., Skantze, U., de Verdier, J., 2007. A formulation comparison, using a solution and different nanosuspensions of a poorly soluble compound. *European Journal of Pharmaceutics and Biopharmaceutics* 67, 540–547. <https://doi.org/10.1016/j.ejpb.2007.02.008>
- Soares, S., Sousa, J., Pais, A., Vitorino, C., 2018. Nanomedicine: Principles, Properties, and Regulatory Issues. *Front. Chem.* 6. <https://doi.org/10.3389/fchem.2018.00360>
- Song, J.H., Shin, S.C., 2009. Development of the loratadine gel for enhanced transdermal delivery. *Drug Development and Industrial Pharmacy* 35, 897–903. <https://doi.org/10.1080/03639040802680289>

- Sonvico, F., Clementino, A., Buttini, F., Colombo, G., Pescina, S., Guterres, S.S., Pohlmann, A.R., Nicoli, S., 2018. Surface-modified nanocarriers for nose-to-brain delivery: From bioadhesion to targeting. *Pharmaceutics* 10, 1–34. <https://doi.org/10.3390/pharmaceutics10010034>
- Steenblik, J., Goodman, M., Davis, V., Gee, C., Hopkins, C.L., Stephen, R., Madsen, T., 2012. Intranasal sufentanil for the treatment of acute pain in a winter resort clinic. *American Journal of Emergency Medicine* 30, 1817–1821. <https://doi.org/10.1016/j.ajem.2012.02.019>
- Talegaonkar, S., Azeem, A., Ahmad, F.J., Khar, R.K., Pathan, S. a, Khan, Z.I., 2008. Microemulsions: a novel approach to enhanced drug delivery. *Recent patents on drug delivery & formulation* 2, 238–257. <https://doi.org/10.2174/187221108786241679>
- Tanner, T., Marks, R., 2008. Delivering drugs by the transdermal route: review and comment. *Skin Research and Technology* 14, 249–260. <https://doi.org/10.1111/j.1600-0846.2008.00316.x>
- Thirawong, N., Kennedy, R.A., Sriamornsak, P., 2008. Viscometric study of pectin-mucin interaction and its mucoadhesive bond strength. *Carbohydrate Polymers* 71, 170–179. <https://doi.org/10.1016/j.carbpol.2007.05.026>
- Tuomela, A., Hirvonen, J., Peltonen, L., 2016. Stabilizing agents for drug nanocrystals: Effect on bioavailability. *Pharmaceutics* 8. <https://doi.org/10.3390/pharmaceutics8020016>
- Van Eerdenbrugh, B., Van den Mooter, G., Augustijns, P., 2008. Top-down production of drug nanocrystals: Nanosuspension stabilization, miniaturization and transformation into solid products. *International Journal of Pharmaceutics* 364, 64–75. <https://doi.org/10.1016/j.ijpharm.2008.07.023>
- Venishetty, V.K., Chede, R., Komuravelli, R., Adepu, L., Sistla, R., Diwan, P.V., 2012. Design and evaluation of polymer coated carvedilol loaded solid lipid nanoparticles to improve the oral bioavailability: a novel strategy to avoid intraduodenal administration. *Colloids Surf B Biointerfaces* 95, 1–9. <https://doi.org/10.1016/j.colsurfb.2012.01.001>
- Verma, S., Lan, Y., Gokhale, R., Burgess, D.J., 2009. Quality by design approach to understand the process of nanosuspension preparation. *International Journal of Pharmaceutics* 377, 185–198. <https://doi.org/10.1016/j.ijpharm.2009.05.006>
- Viçosa, A., Letourneau, J.J., Espitalier, F., Inês Ré, M., 2012. An innovative antisolvent precipitation process as a promising technique to prepare ultrafine rifampicin particles. *Journal of Crystal Growth* 342, 80–87. <https://doi.org/10.1016/j.jcrysgro.2011.09.012>
- Vlaia, L., Coneac, G., Olariu, I., Ț, A.N.A.M.M.U., Lupuliasa, D., Vlaia, V.Ț.I.U., 2017. Loratadine-loaded microemulsions for topical application . Formulation , physicochemical characterization and in vitro drug release evaluation. *FARMACIA* 65,851–861.
- Vyas, T.K., Shahiwala, A., Marathe, S., Misra, A., 2005. Intranasal drug delivery for brain targeting. *Current Drug Delivery* 2, 165–75. <https://doi.org/10.2174/1567201053586047>
- Warnken, Z.N., Smyth, H.D., Watts, A.B., Weitman, S., Kuhn, J.G., Williams III, R.O., 2016. Formulation and device design to increase nose to brain drug delivery. *Journal of Drug Delivery Science and Technology* 35, 213–222.
- Winner, P., Rothner, A.D., Wooten, J.D., Webster, C., Ames, M., 2006. Sumatriptan nasal spray in adolescent migraineurs: A randomized, double-blind, placebo-controlled, acute study. *Headache* 46, 212–222. <https://doi.org/10.1111/j.1526-4610.2006.00339.x>
- Wong, B.S., Yoong, S.L., Jagusiak, A., Panczyk, T., Ho, H.K., Ang, W.H., Pastorin, G., 2013. Carbon nanotubes for delivery of small molecule drugs. *Advanced Drug Delivery Reviews, Carbon Nanotubes in Medicine and Biology: Therapy and Diagnostics & Safety and Toxicology* 65, 1964–2015. <https://doi.org/10.1016/j.addr.2013.08.005>
- Wu, L., Zhang, J., Watanabe, W., 2011. Physical and chemical stability of drug nanoparticles. *Advanced Drug Delivery Reviews* 63, 456–469. <https://doi.org/10.1016/j.addr.2011.02.001>
- Wu, W., Nancollas, G.H., 1998. A new understanding of the relationship between solubility and particle size. *Journal of Solution Chemistry* 27, 521–531. <https://doi.org/10.1023/A:1022678505433>
- Xi, J., Wang, Z., Nevorski, D., White, T., Zhou, Y., 2016. Nasal and Olfactory Deposition with Normal and Bidirectional Intranasal Delivery Techniques: In Vitro Tests and Numerical Simulations. *Journal of Aerosol Medicine and Pulmonary Drug Delivery* 30, 118–131. <https://doi.org/10.1089/jamp.2016.1295>
- Xie, H., Li, L., Sun, Y., Wang, Y., Gao, S., Tian, Y., Ma, X., Guo, C., Bo, F., Zhang, L., 2019. An Available Strategy for Nasal Brain Transport of Nanocomposite Based on PAMAM Dendrimers via In Situ Gel. *Nanomaterials (Basel)* 9. <https://doi.org/10.3390/nano9020147>

- Yanez, A., Dimitroff, A., Bremner, P., Rhee, C.-S., Luscombe, G., Prillaman, B.A., Johnson, N., 2016. A patient preference study that evaluated fluticasone furoate and mometasone furoate nasal sprays for allergic rhinitis. *Allergy Rhinology* 7, 1–6. <https://doi.org/10.2500/ar.2016.7.0185>
- Yang, H., Teng, F., Wang, P., Tian, B., Lin, X., Hu, X., Zhang, L., Zhang, K., Zhang, Y., Tang, X., 2014. Investigation of a nanosuspension stabilized by Soluplus® to improve bioavailability. *International Journal of Pharmaceutics* 477, 88–95. <https://doi.org/10.1016/j.ijpharm.2014.10.025>
- Yang, W., Peters, J.I., Williams, R.O., 2008. Inhaled nanoparticles-A current review. *International Journal of Pharmaceutics* 356, 239–247. <https://doi.org/10.1016/j.ijpharm.2008.02.011>
- Yu, L.X., 2008. Pharmaceutical quality by design: Product and process development, understanding, and control. *Pharmaceutical Research* 25, 781–791. <https://doi.org/10.1007/s11095-007-9511-1>
- Zaman, M., Chandrudu, S., Toth, I., 2013. Strategies for intranasal delivery of vaccines. *Drug Delivery and Translational Research* 3, 100–109. <https://doi.org/10.1007/s13346-012-0085-z>
- Zhang, L., Gu, F., Chan, J., Wang, A., Langer, R., Farokhzad, O., 2008. Nanoparticles in Medicine: Therapeutic Applications and Developments. *Clinical Pharmacology and Therapeutics* 83, 761–769. <https://doi.org/10.1038/sj.clpt.6100400>
- Zhang, Y., Jiang, T., Zhang, Q., Wang, S., 2010. Inclusion of telmisartan in mesocellular foam nanoparticles: drug loading and release property. *European Journal of Pharmaceutics and Biopharmaceutics* 76, 17–23. <https://doi.org/10.1016/j.ejpb.2010.05.010>
- Zhong, H., Hu, Y., Hu, H., Ouyang, D., 2018. A Comprehensive Map of FDA-Approved Pharmaceutical Products. *Pharmaceutics* 10, 263. <https://doi.org/10.3390/pharmaceutics10040263>

## ACKNOWLEDGEMENTS

My sincere thanks to the head of the department and my associate supervisor **Dr. Ildikó Csóka** for her support and advice during the preparation of this project.

I would like to express my deepest gratitude to my principal supervisor **Dr. Rita Ambrus** for giving me the opportunity to pursue my PhD under her supervision and constant support.

I would like to thank Prof. **Dr. Piroska Szabó-Révész** for her kindness and support during my work.

I would like to thank **Dr. Norbert Radacsi** from University of Edinburgh for sharing me his knowledge about the nanofibers, for the successful collaboration, and guidance.

I would also thank the **laboratory technicians**, particularly, Piroska Lakatosné and Erika Feczóné for their care and help that made the hard things easier.

Then I would like to thank all my colleagues and friends for their moral and scientific support.

I would like to acknowledge the **Hashemite University** of Jordan for believing in my capabilities and supporting my decisions.

I would acknowledge the financial support of the **Stepindium Hangaricum Programme, Ministry of Human Capacities, Hungary**, grant number 20391-3/2018/FEKUSTRAT, and **Gedeon Richter Ltd** –GINOP project (2.2.1-15-2016-00007) and GINOP-2.3.2-15-2016-00060-Development and targeting new active pharmaceutical ingredients by means of new drug-carrier systems.

My last words are dedicated to my family. Thanks for your support and encouragement during these years. I know how hard it was to be away, but you have been with me during all the moments of sadness or joy.